

Regulation of Metabotropic Glutamate Receptor subtype 7a by PDZ-domain protein PICK1

Dissertation

zur Erlangung des Doktorgrades der
Naturwissenschaften vorgelegt beim Fachbereich
Biochemie, Chemie und Pharmazie der Johann
Wolfgang Goethe-Universität in Frankfurt am Main

von

Chuansheng Zhang

aus Anhui (China)

Frankfurt 2007

Die vorliegende Arbeit wurde in der Abteilung Neurochemie am Max-Planck Institut für Hirnforschung in Frankfurt am Main unter Anleitung von Prof. Heinrich Betz durchgeführt und vom Fachbereich Biochemie, Chemie und Pharmazie der Johann Wolfgang Goethe-Universität in Frankfurt am Main als Dissertation angenommen.

Dekan: Prof. Harald Schwalbe

Gutachter: Prof. Ernst Bamberg

Prof. Heinrich Betz

Datum der Disputation:

Summary

Metabotropic glutamate receptor subtype 7 (mGluR7) belongs to the family of G-protein coupled receptors. mGluR7 is widely distributed in the brain and primarily localized at presynaptic terminals, where it is thought to regulate neurotransmitter release and synaptic plasticity. Studies have shown that the intracellular C-terminal tail of mGluR7 binds a variety of proteins in addition to trimeric G-proteins. These newly identified protein interactions are believed to play a key role in the synaptic targeting and G-protein dependent signaling of mGluR7. Protein interacting with C kinase 1 (PICK1), a PDZ-domain protein, is a strong interaction partner of mGluR7a. In order to investigate the role of PICK1 in the synaptic trafficking and signaling of mGluR7a, a knock-in mouse line in which the interaction of mGluR7a and PICK1 is disrupted was generated. Analysis of the mutant mice by immunocytochemistry and immunoelectron microscopy showed that the synaptic targeting and clustering of mGluR7a was not altered, indicating that PICK1 is not required for mGluR7a receptor membrane trafficking and synaptic localization. However, when the spontaneous synaptic activity of cerebellar granule cell cultures prepared from both wild-type and knock-in mice was monitored, and L-AP4 (400 μ m) was found to decrease the frequency, but not the amplitude, of spontaneous excitatory currents in wild-type neurons, while no effect of L-AP4 on spontaneous synaptic activity was observed in knock-in neurons. This indicates that PICK1 binding to the C-terminal region of mGluR7a plays an essential role in mGluR7a mediated G-protein signaling. We examined the threshold sensitivity for the convulsant pentetrazole (PTZ) in knock-in mice. It was found that mGluR7a knock-in mice had a greater sensitivity to PTZ than wild-type mice. Moreover, the surface parietal cortex EEG recordings of the mutant mice revealed spontaneous synchronous oscillation, or "spike-and-wave discharges" (SWD), which displayed similar characteristics to absence-like seizures. It was also observed that the knock-in mice responded to pharmacology as human absence epilepsy. These data suggests that the knock-in mice displayed the phenotype of absence-like epilepsy. Furthermore, the behavioral analysis of the mGluR7a knock-in mice showed no deficits in motor coordination, pain sensation, anxiety as well as spatial learning and memory, thus the interaction of mGluR7a and PICK1 appears not to contribute to these physiological processes. Taken together, our data provides evidence for an important role of PICK1 in G-protein dependent signaling of mGluR7a, whereas PICK1 is not required for synaptic targeting and clustering of mGluR7a. Our results also provide an animal model of absence-like epilepsy generated by disruption of a single mGluR7a-PDZ interaction, thus creating a novel therapeutic target against this neurological disease.

ABBREVIATIONS

AA	amino acid
Amp	ampicillin
AMPA	Alpha-amino-3-hydroxy-5-methyl-4-isoxazolepropionic Acid
ATP	Adenosin-5'-triphosphate
bp	base pair
BAC	bacterial artificial chromosome
BSA	bovine serum albumine
cAMP	Cyclic Adenosin-5'-monophosphate
cDNA	complementary deoxyribonucleic acid
CIAP	calf intestinal alkaline phosphatase
CNS	central nervous system
Da	dalton
DAB	3', 3'-Diaminobenzidine
DAT	Dopamine Transporter
DIV	Days in vitro
DMEM	dulbecco's modified essential medium
DMSO	dimethylsulfoxide
DNA	desoxyribonucleic acid
dNTP	deoxyribonucleoside-5'-triphosphate
DTT	1,4-Dithio-DL-threitol
<i>E.coli</i>	<i>Escherichia coli</i>
EEG	electroencephalogram
EDTA	ethylenediamine tetra acetic acid
EGTA	ethylene glycol-bis(β -aminoethyl ether)-N,N,N',N'-tetraacetic acid
EPSP	Excitatory Postsynaptic Potential
EtOH	ethanol
FCS	fetal calf serum
g	gram
GRIP	glutamate receptor interacting protein
GPCR	G-protein coupled receptor
h	hour
HEPES	2-[4-(2-hydroxyethyl)-1-piperazine]ethanesulfonic acid
HPLC	high performance liquid chromatography
HRP	horseradish peroxidase β -d-thiogalactopiranoside
iGluR	ionotropic Glutamate Receptor
L	liter
L-AP4	L (+)-2-amino-4-phosphonobutyric acid
LB	Luria-Bertani
Ig	immunoglobulin
IgG	immunoglobuline G
LTD	Long-term depression
LTP	Long-term potentiation

mEPSCs	miniature excitatory postsynaptic currents
mRNA	messenger ribonucleic acid
min	minute
mg	milligram
mGluR	metabotropic glutamate receptor
NaOAc	sodium acetate
NMDA	N-Methyl-D-Aspartate
PAGE	polyacrylamide gel electrophoresis
PBS	phosphate buffered saline
PCR	polymerase chain reaction
PDZ	PSD-95/Discs-large/ZO-1
PFA	paraformaldehyde
PICK1	Protein Interacting with C Kinase 1
PKA	cAMP-dependent protein kinase A
PKC	Protein Kinase C
PLC	Phospholipase C
PolyA	polyadenylation signal
RNA	ribonucleic acid
rpm	revolutions per minute
R/T	room temperature
SDS	sodium dodecyl sulphate
SWD	spike-wave discharge
Taq	Thermus aquaticus DNA polymerase
TE	Tris-EDTA buffer
TEMED	N,N,N',N'-tetramethylethylenediamin
Tris	tris-hydroxymethyl-aminomethane
UV	ultraviolet
v/v	volume to volume
w/v	weight to volume

Contents

1. Introduction	5
1.1. Synapses and synaptic transmission.....	5
1.2. Glutamate.....	7
1.3. Glutamate receptors.....	7
1.3.1. Ionotropic glutamate receptors.....	7
1.3.1.1. AMPA receptors.....	8
1.3.1.2. NMDA receptors.....	9
1.3.1.3. Kainate receptors.....	10
1.3.2. Metabotropic glutamate receptors (mGluRs)	11
1.4. Metabotropic glutamate receptor subtype 7 (mGluR7)	15
1.4.1. Splice variants of mGluR7 receptors.....	15
1.4.2. Localization of mGluR7 mRNA and protein in the mammalian CNS.....	17
1.4.3. mGluR7 and its implicatons for signal transduction and synaptic transmission.....	18
1.4.4. The role of mGluR7 in epilepsy and seizures.....	19
1.4.5. mGluR7 interacts with PICK1 (<u>P</u> rotein <u>I</u> nteracting with <u>C</u> <u>K</u> inase1).....	20
1.5. Aim of this thesis.....	23
2. Material and Methods	24
2.1. Materials.....	24
2.1.1. Organism.....	24
2.1.2. Chemicals.....	24
2.1.3. Medium and antibiotics for Bacterial culture.....	25
2.1.4. Medium and supplements for Embryonic stem (ES) cells and mouse	

embryonic fibroblast (MEF) feeder cells.....	26
2.1.5. Medium and supplements for primary culture of Hippocampal neurons.....	27
2.1.6. General buffers and solutions.....	27
2.1.7. Plasmids and BAC clones.....	30
2.1.8. Oligonucleotides.....	31
2.1.9. Antibodies.....	32
2.1.10. Commercial Kits for molecular biology.....	33
2.2. Methods.....	34
2.2.1. Biochemistry and molecular biology methods.....	34
2.2.2. Cell biology methods.....	43
2.2.3. Immunocytochemistry, imunohistochemistry and immunoelectron microscopy methods.....	46
2.2.4. Electrophysiology methods.....	49
2.2.5. Animal behavioral assay methods.....	51
3. Results.....	53
3.1. Generation of mGluR7a knock-in mice.....	53
3.1.1. Gene targeting strategy.....	55
3.1.2. Assembly of gene targeting vector.....	56
3.1.3. Electroporation of ES cells and identification of homologous recombination events.....	59
3.1.4. Cre recombinase mediated deletion of the Neo resistance cassette in ES cells.....	61
3.1.5. Production of chimeric mice by blastocyst injection of ES cell.....	63
3.1.6. Germline transmission of the mutation and generation of homozygous mutant mice	64

3.2. Biochemical, anatomical and electrophysiological characterization of homozygous KI mice	67
3.2.1. Expression of mGluR7a in homozygous KI mice.....	68
3.2.2. Reduced mGluR7a–PICK1 interaction in homozygous KI mice.....	69
3.2.3. Homozygous KI mice show normal gross brain anatomy and mGluR7a distribution.....	70
3.2.4. Synaptic targeting and localization of mGluR7a in homozygous KI neurons.....	71
3.2.5. Ultrastructural localization of mGluR7a by immunoelectron microscopy.....	73
3.2.6. Loss of mGluR7a mediated presynaptic inhibition in homozygous KI mice.....	74
3.2.7. Increased susceptibility of the mGluR7 KI mice to convulsant drugs.....	76
3.2.8. mGluR7a KI mice develop spontaneous absence-like seizures.....	79
3.3. Behavioral analysis of mGluR7a KI mice.....	81
3.3.1. Open field	81
3.3.2. Tail flick test.....	82
3.3.3. Acoustic startle response and prepulse inhibition.....	83
3.3.4. Elevated plus-maze.....	85
3.3.5. Barnes maze.....	86
4. Discussion.....	87
4.1. Knock-in approach and the role of proteins interacting with C-terminal region of mGluR7.....	88
4.2. The role of PICK1 in the presynaptic targeting and localization of mGluR7a.....	89

4.3. Requirement of PICK1 in the mGluR7a receptor signaling and control of synaptic transmission	91
4.4. Involvement of mGluR7a-PICK1 signaling pathway in anxiety.....	92
4.5. mGluR7a knock-in mice – an animal model for absence epilepsy?.....	93
4.6. The interaction of PICK1 with mGluR7a and mGluR7b.....	94
4.7. Perspectives	95
5. Bibliography.....	97
6. Appendices.....	107
7. Zusammenfassung.....	111
ACKNOWLEDGEMENT.....	115
CURRICULUM VITA.....	116

1. Introduction

1.1. Synapses and synaptic transmission

The information processing capacity of the central nervous system (CNS) is achieved by synapses, which are very important structures for communication between nerve cells and their target cells (neurons, muscle or gland cells). Two distinct types of synapses are identified: electrical synapses and chemical synapses (Gundelfinger and tom Dieck, 2000). Electrical synapses are formed by gap junctions and conduct electrical activity directly from one cell to another, they are rarely found in the vertebrate nervous system. The vast majority of the synapses in the vertebrate brains are chemical synapses, which need particular molecules to transmit the signals. The chemical synapse is a specialized junctional complex consisting of: a presynaptic ending that contains neurotransmitters, mitochondria and other cell organelles; a synaptic cleft or space between the presynaptic and postsynaptic endings and a postsynaptic apparatus that contains receptor sites for neurotransmitters (Figure 1A). Based on electron microscopic investigations by Gray (Gray, 1959) and Hamlyn (Hamlyn, 1962), two types of chemical synapse are distinguished in the central nervous system. Type I junction is a type of synapse usually occurring between an axon and a dendritic spine or dendritic shaft. It is generally thought that this type of synapses involve axons that contain predominantly spherical vesicles and contain a thickened postsynaptic density (PSD), which renders the synapse asymmetrical (Figure 1B). In contrast, the type II synapses display the less identifiable postsynaptic density and the narrow cleft which does not contain a dense plaque, thus the overall configuration is symmetrical. In terms of physiological typing, neurobiological studies have revealed that type I synapse is excitatory, whereas the type II is inhibitory.

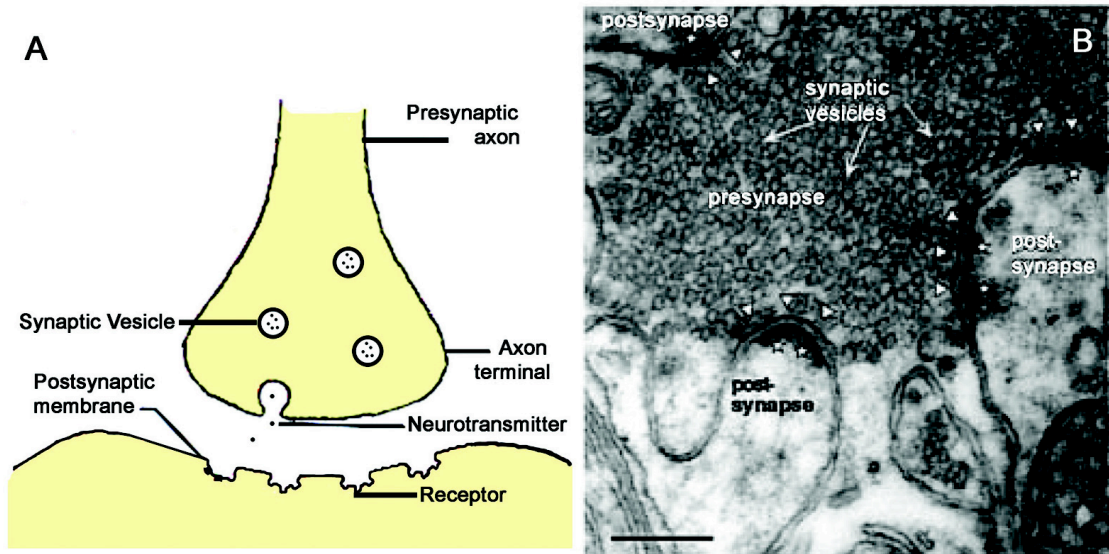


Figure 1. Illustration of a typical chemical synapse and ultrastructural features of the synapse. **A.** The image illustrates a chemical synapse, the major pre- and post-synaptic elements are indicated. Synapses allow nerve cells to communicate with target cells, converting electrical impulses into chemical signals. **B.** Electron photomicrograph of a mossy fiber terminal in the rat hippocampus making contact with multiple postsynaptic neurons (Adapted from Gundelfinger and tom Dieck, 2000). Note the presynaptic terminal is stuffed with synaptic vesicles. The postsynaptic side is characterized by an even more prominent electron-dense structure, the postsynaptic density (*PSD*). *Scale bars:* 300 nm.

Synaptic transmission is a process that allows nerve impulses are propagated from a neuron to a target cell at synapses by the release of neurotransmitters. As a nerve impulse, or action potential, reaches the end of a presynaptic axon, molecules of neurotransmitter are quickly and efficiently released into the synaptic cleft. These neurotransmitter then are recognized by selective receptors on the postsynaptic cell so that they can open nearby ion channels in the post-synaptic cell membrane, causing ions to rush in or out and changing the transmembrane potential of the postsynaptic cell and initiate another action potential. After binding to the receptors, the neurotransmitter must be inactivated or removed rapidly from synaptic cleft so that the receptor sites of the postsynaptic cell will not be continually occupied and therefore avoids constant stimulation of the postsynaptic cell.

For the removing of transmitters from synaptic cleft, neurons adopt special proteins called transporters to clear many transmitters by being taken up into the presynaptic

terminals. This process is known as reuptake, reuptake system regulates synaptic activity precisely and also allows the terminal to recycle transmitter molecules.

1.2. Glutamate

The amino acid glutamate is considered the primary excitatory neurotransmitter in the mammalian central nervous system. In addition to acting as a key molecule in cellular metabolism, the role of glutamate as neurotransmitter is now well established, and excitatory processes mediated by glutamate are involved in most higher brain functions, including cognition, memory and learning. The glutamate that is present in the brain is mainly synthesized by astrocytes (Hertz et al., 1999), and glutamate released from synaptic vesicles is the major source of extracellular glutamate under normal physiological conditions. Glutamate is stored intracellularly and activates glutamate receptors only when actively released from nerve terminals. Studies have shown that the efflux of cytosolic glutamate from neurons and astrocytes also can lead to an increase of glutamate levels in the cerebrospinal fluid and thereby cause disorders of nervous systems (Anderson and Swanson, 2000). In the synaptic cleft, glutamate mediates neurotransmission by binding to glutamate receptors. Several subtypes of glutamate receptors have been identified: ionotropic glutamate receptors (NMDA, AMPA and Kainate receptors) and metabotropic glutamate receptors (Figure 2). Since the maintenance of low extracellular concentrations of glutamate is essential for brain function, neurons and glial cells possess specialized glutamate uptake systems, e.g. glutamate transporter proteins that remove excess glutamate (Shigeri et al., 2004).

1.3. Glutamate receptors

1.3.1. Ionotropic glutamate receptors

The ionotropic glutamate receptors are ligand-gated ion channels that mediate the majority of excitatory neurotransmission in the vertebrate central nervous system. These receptors are crucially involved in development and in different forms of synaptic plasticity, which may underlie learning and memory formation (Hollmann and Heinemann, 1994; McBain and Mayer, 1994). Based on electrophysiological

studies, three distinct classes of ionotropic glutamate receptors have been identified and named after the agonists NMDA (N-methyl-D-aspartate), AMPA (alpha-amino-3-hydroxy-5-methyl-4-isoxazolepropionate) and Kainate. The activation of ionotropic glutamate receptors increases transmembrane sodium and calcium fluxes, and thereby produce depolarization of the neuronal membrane (Myers et al., 1999).

1.3.1.1. AMPA receptors

AMPA receptors are the glutamate gated channels which are responsible for most fast excitatory response in the central nervous system. Increasing evidence suggests that AMPA receptors are tetrameric structures that combine homologous subunits GluR1 to GluR4 in different stoichiometries. Most AMPA receptors are either homo-tetramers of GluR1 or GluR4, or symmetric "dimer of dimers" of GluR2/3 and either GluR1 or GluR4 (Wisden and Seeburg, 1993).

AMPA receptors are mainly Na⁺ permeable, but also flux Ca²⁺. Some subgroups of AMPA receptors lack Ca²⁺ permeability, which is due to posttranscriptional RNA editing of one of the AMPA receptor subunit. In the GluR2 mRNA, a single base pair is altered so that the codon encodes an arginine (R) instead of a glutamine (Q) in the pore-forming region. The editing of this 'Q/R' site abolishes the Ca²⁺ permeability of the AMPA receptor channel (Seeburg, 2002).

AMPA receptors have a crucial role on the regulation of synaptic efficacy and postsynaptic excitability. The trafficking, density and degradation of AMPA receptors are therefore tightly regulated in neurons. For the delivery of AMPA receptors into synapses, two distinct pathways seem to exist (Borgdorff and Choquet, 2002). Multiple studies have shown GluR2-GluR3 oligomers are constitutively inserted into synapses (Passafaro et al., 2001; Shi et al., 2001), while GluR1-GluR2 and GluR4- containing receptors are delivered to synaptic sites in an activity dependent manner (Zhu et al., 2000). The two pathways that control the synaptic trafficking of AMPA receptors work together to maintain the synaptic strength and plasticity.

1.3.1.2. NMDA receptors

NMDA receptors are heteromeric proteins composed of NR1, NR2 and/or NR3 subunits (Schorge and Colquhoun, 2003). The NR1 subunit is encoded by a single gene that give rise to at least eight different splice variants (a-h), while the NR2 subunits are the products of four different genes, NR2A-NR2D (McBain and Mayer, 1994). More recently, NR3 subunits have been cloned and studied in heterologous expression systems, but their functions and distribution in the brain still need further characterization (Nishi et al., 2001; Yamakura et al., 2005).

The NMDA receptor channel is permeable to various mono and divalent cations (Na^+ , K^+ , Ca^{2+} , Ba^{2+} , etc.); however, at resting membrane potential, the NMDA receptor channel is blocked by Mg^{2+} ions, membrane depolarization is required to remove the Mg^{2+} blockage to allow activation of channel upon agonist binding (Mayer et al., 1984; Nowak et al., 1984; Danysz and Parsons, 1998). The NMDA receptor has distinct binding sites for different endogenous ligands that regulate ion channel opening: glutamate, glycine, polyamine, Mg^{2+} and Zn^{2+} . For efficient opening of the channel, binding of both glutamate and the co-agonist glycine is required (Johnson and Ascher, 1987). Additionally, the NMDA receptor channel is modulated by various compounds. For instance, Zn^{2+} blocks the NMDA current in a non-competitive and voltage-independent manner (Berger and Rebernik, 1999), whereas polyamine potentiate or inhibit glutamate responses (Kashiwagi et al., 1997; Herin and Aizenman, 2004).

NMDA receptors play a key role in a wide range of physiological and pathologic processes. It has been shown that activation of the NMDA receptor is linked to long-term potentiation (LTP) and depression (LTD), as well as neuronal development (Dingledine et al., 1999). On the other hand, overactivation of the NMDA receptor is thought to account for different pathological processes, such as ischemia-induced excitotoxicity (Lee et al., 1999) and seizures (Loscher, 1998).

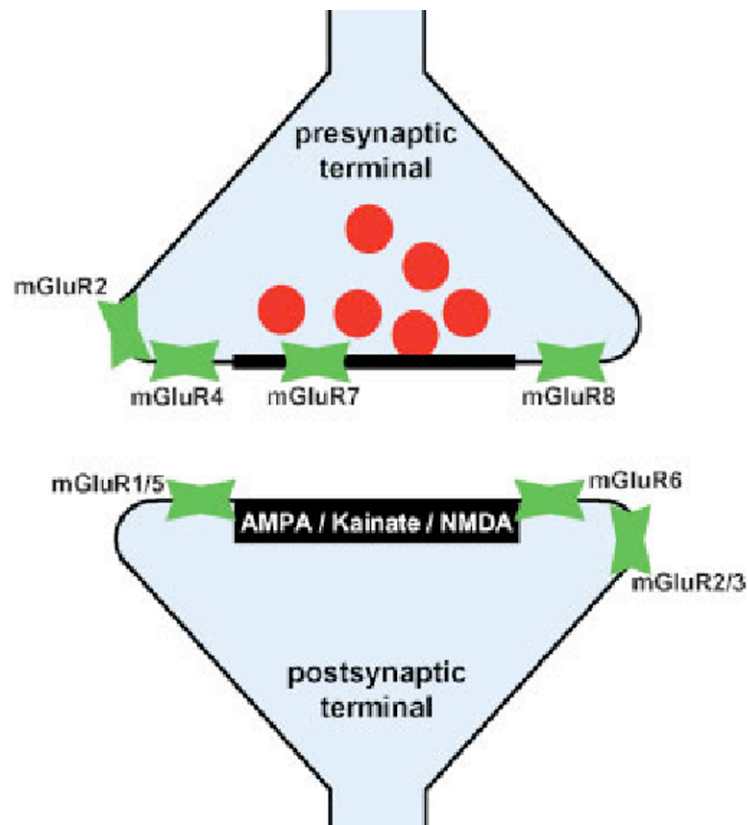


Figure 2. The general synaptic localization of glutamate receptors at a typical excitatory synapse (Adapted from Enz 2007). The ionotropic glutamate receptors subtypes (NMDA, Kainate and AMPA receptors), mainly function to mediate fast synaptic transmission, but also mediate the changes required for neuronal plasticity. The metabotropic glutamate receptors have a diverse synaptic localization, mGluR1 and mGluR5 (group I) are mostly localized postsynaptically, mGluR4, mGluR7 and mGluR8 (group III) at the presynapse, while mGluR2 and mGluR3 (group II) do not show any preference. mGluR6 is only expressed in retinal bipolar cells postsynaptic to photoreceptors. Vesicles containing the neurotransmitter glutamate are shown in red, and the active zone is indicated by black boxes at the presynaptic terminal.

1.3.1.3. Kainate receptors

Kainate receptors and AMPA receptors are often called `non-NMDA receptors`. Due to limited data on pharmacology and electrophysiology, kainate receptors are not as well understood as the other ionotropic glutamate receptors. So far, five kainate receptor subunits have been cloned, they are GluR5, GluR6, GluR7, KA1

and KA2 (Hollmann and Heinemann, 1994). All these subunit share a conserved transmembrane topology with AMPA and NMDA receptor subunits. GluR5, 6 and 7 can form homomeric and heteromeric receptors; however, KA1 and KA2 only assemble into functional receptors in combination with one of the GluR5, 6 or 7 subunits (Sommer et al., 1992; Madden, 2002). Kainate receptors have been found to be present at both pre-and postsynaptically. The activation of presynaptic kainate receptors modulates transmitter release and synaptic transmission, whereas postsynaptic receptors are involved in synaptic plasticity particularly at mossy fibre synapses in the hippocampus (Lerma, 2003).

1.3.2. Metabotropic glutamate receptors (mGluRs)

Studies in the 1980s have shown that glutamate receptor activation can lead to phosphoinositide hydrolysis through GTP-binding proteins (Sugiyama et al., 1987). Subsequent analysis revealed that there is a large family of glutamate receptors, termed metabotropic glutamate receptors (mGluRs), which couple to second messenger systems via G-proteins. Like all family C GPCR members, mGluRs have a long extracellular N-terminus that is crucial for ligand binding and activation. In 1991, two groups isolated and cloned cDNA encoding the first mGluR (Houamed et al., 1991; Masu et al., 1991), now named mGluR1a. To date, eight mGluRs family members have been cloned, classified into three groups (Table 1) based on sequence homology and pharmacology. mGluRs of the same group display about 70% sequence identity, whereas between groups this percentage decreases to about 45% (Conn and Pin, 1997). mGluRs belong to the G-protein coupled receptor (GPCR) superfamily, which can be divided in three subgroups (Pierce et al., 2002). Family 1 GPCRs share homology with the rhodopsin, including acetylcholine, catecholamine, glycoprotein and certain peptide receptors. Family 2 receptors share homology with secretin receptors that includes receptors for polypeptide hormones and a group of *Drosophila* proteins that regulate stress responses and longevity. The mGluRs belong to family 3 GPCRs, which also includes the gamma-aminobutyric acid type B (GABA_B) receptors, the parathyroid hormone receptors and Ca²⁺-sensing receptors, as well as putative taste, olfactory, and pheromone receptors. Unlike family 1 and 2 GPCRs, whose ligand binding sites include portions of the transmembrane domain regions, the ligand binding site of family 3

GPCRs is located within a large N-terminal domain of approximately 500 amino acids.

The discovery of mGluRs dramatically expanded the understanding of glutamatergic neurotransmission in the mammalian CNS. It is believed that activation of mGluRs can modulate or fine-tune neuronal activity in glutamatergic circuits (Conn and Pin, 1997). Many studies have shown that mGluRs are ubiquitously distributed in the brain and participate in a wide variety of functions of the CNS (Swanson et al., 2005). Generally, mGluRs play important roles in regulating neuronal cell excitability and synaptic transmission. Activation of mGluRs modulates various voltage-sensitive ion channels, and may also stimulate intracellular signaling cascades which affect synaptic transmission, synaptic integration, and plasticity (Conn, 2003).

Group I mGluRs (mGluR1/5) are predominantly located at the periphery of the postsynaptic density (Baude et al., 1993; Lujan et al., 1997), and they are expressed in many different brain regions. Activation of group I mGluRs results in phosphoinositide hydrolysis, calcium release and protein kinase C activation, and also causes postsynaptic depolarization and spike frequency adaptation in a number of brain regions, such as hippocampus, cortex, striatum and hypothalamic nuclei (Keele et al., 1997; Schrader and Tasker, 1997). Different types of K^+ channels are major down-stream targets of group I mGluRs. Inhibition of K^+ channels following activation of group I mGluRs leads to an increase in neuronal excitability. Voltage-gated calcium channels (VGCCs) may also be modulated by group I mGluRs (Sahara and Westbrook, 1993; Sung et al., 2001). It has been reported that group I mGluRs can use distinct signal transduction pathways to modulate calcium channels (Lester and Jahr, 1990; McCool et al., 1998). Proper function of group I mGluR requires special scaffolding proteins, termed Homer proteins. Homer proteins interact with group I mGluRs via the C-terminal tails and constitute components of postsynaptic densities (PSD) (Xiao et al., 2001). Homer proteins also link mGluRs to intracellular calcium stores via IP3 receptors and other scaffolding proteins such as Shank. Published data suggests that Homer proteins are involved in the physical coupling, synaptic targeting, and/or clustering of group I mGluRs, thereby regulating diverse functions of these receptors (Brakeman et al., 1997).

Table 1. Classification of mGluRs

Receptor family	Coupling	Transduction	Group/subtype-selective pharmacological agents
Group I			
mGluR1	Gq-coupled (Excitatory)	↑PLC ↑Ca	Agonists: DHPG, 1S, 3R-ACPD, quisqualate Antagonist: LY393675 allosteric antagonist: LY367385
mGluR5	Gq-coupled (Excitatory)	↑PLC ↑Ca	agonists: DHPG, 1S,3R-ACPD, quisqualate, CHPG allosteric antagonist: MPEP
Group II			
mGluR2	Gi/Go-coupled (Inhibitory)	adenylate cyclase (AC)	Agonists: DCG-IV, LY354730, 1S, 3R-ACPD Antagonist: LY341495
mGluR3	Gi/Go-coupled (Inhibitory)	adenylate cyclase (AC)	Agonists: DCG-IV, LY354730, 1S, 3R ACPD Antagonist: LY341495
Group III			
mGluR4	Gi/Go-coupled (Inhibitory)	adenylate cyclase (AC)	Agonists: L-AP4, L-SOP Antagonist: MSOP, MAP4
mGluR6	Gi/Go-coupled (Inhibitory)	adenylate cyclase (AC)	Agonists: L-AP4, L-SOP Antagonist: MSOP, MAP4
mGluR7	Gi/Go-coupled (Inhibitory)	adenylate cyclase (AC)	Agonists: L-AP4, L-SOP Antagonist: MSOP, MAP4
mGluR8	Gi/Go-coupled (Inhibitory)	adenylate cyclase (AC)	Agonists: L-AP4, L-SOP, 3,4-DCPG Antagonist: MSOP, MAP4

Modified from Swanson et al., 2005

Group II mGluRs (mGluR2/3) are widely distributed throughout the CNS (Sato et al., 2004), mGluR2 is found at the periphery of the presynaptic terminal, while

mGluR3 is more diversely localized, at both pre- and postsynaptic sites, and on certain glial cells where its functional role is unclear (Aronica et al., 2005). Presynaptic group II mGluRs decrease the probability of synaptic vesicle release through a negative feedback mechanism (Gereau and Conn, 1994); in addition, postsynaptic functions have also been found at multiple synapses within the CNS (Heinbockel and Pape, 2000; Otani et al., 2002). Voltage-dependent Ca^{2+} channels are likely to be involved in the presynaptic inhibition mediated by group II mGluRs. Additionally, it has been suggested that K^+ channels mediate some of the effects induced by activation of group II mGluRs (Anwyl, 1999). mGluR2 knockout mice have been generated and used to show that mGluR2 is a presynaptic modulatory receptor in the hippocampus (Yokoi et al., 1996). In mGluR2-deficient mice, long-term depression induced by low-frequency stimulation of the mossy fiber CA3 synapses is abolished, thus illustrating an important role of mGluR2 in the modulation of neuronal excitability. However, these knockout mice otherwise appear to be normal, with no alterations in basal synaptic transmission, suggesting that mGluR2 do not play a prominent role in the acute regulation of excitatory synaptic transmission (Yokoi et al., 1996). In addition, it has been shown that LTD can be induced by activation of group II mGluRs (Kahn et al., 2001; Kawasaki et al., 2004). Notably, group II mGluRs induce LTD presynaptically in the basolateral amygdala (BLA), the nucleus accumbens (Robbe et al., 2002) and the striatum (Lovinger and McCool, 1995). In contrast, stimulation of thalamic inputs to the lateral nucleus of the amygdala induces a group II mGluR mediated postsynaptic LTD (Heinbockel and Pape, 2000). Furthermore, in the dentate gyrus and the medial region of the prefrontal cortex, group II mGluRs induce postsynaptic LTD that is PKA and PKC-dependent (Otani et al., 2002; Kawasaki et al., 2004).

Group III mGluRs (mGluR4, 6, 7, 8) inhibit cAMP production and modulate ion channels (Gereau and Conn, 1994). In contrast to other group mGluRs, group III mGluRs are primarily located at presynaptic active zones of the axon terminal where they inhibit transmitter release (Shigemoto et al., 1996; Lujan et al., 1997). Unfortunately, only a limited number of pharmacological tools with mGluR subtype selectivity exists to examine the functional significance of individual group III receptors. L-AP4 is the most commonly used selective group III agonist; it has a high affinity for mGluR4/6/8 and a low affinity for mGluR7 (O'Hara et al., 1993; Cartmell and Schoepp, 2000). More recently, 3, 4-DCPG and AMN082 have been

described relatively specific agonists of mGluR8 and mGluR7, respectively (Linden et al., 2003b; Mitsukawa et al., 2005).

Recently, the functions of distinct group III mGluR subtypes have been studied with knockout mouse models. These studies suggest that mGluR6 plays an important role in processing of visual sensory information (Masu et al., 1995). mGluR6 is highly localized to dendrites of retinal ON bipolar cells, with very low expression in brain tissues. mGluR4 was found localized at both presynaptic and postsynaptic sites of different neurons, with high expression in cerebellum. mGluR4 knockout mice show deficits in motor-learning tests, and in electrophysiological studies, paired-pulse facilitation and post-tetanic potentiation were impaired in contrast to wild-type mice; additionally, the knockout mice were resistant to absence seizures induced by GABA_A receptor antagonists (Pekhletski et al., 1996; Snead et al., 2000). mGluR8 is localized largely presynaptically on glutamatergic synapses, and highly expressed in forebrain regions. mGluR8 knockout mice show increased anxiety-like behavior and increased body weight (Linden et al., 2002; Linden et al., 2003a). mGluR7 is widely distributed in the brain, considered to be one of the most important mGluR subtypes in shaping synaptic responses at glutamatergic and GABAergic synapses (Callaerts-Vegh et al., 2006), and will be discussed in great details in the subsequent section.

1.4. Metabotropic glutamate receptor subtype 7 (mGluR7)

1.4.1. Splice variants of mGluR7 receptors

mGluR7 has two distinct splice variants and usually named mGluR7a and mGluR7b (Figure 3). mGluR7a is considered the major isoform of mGluR7, and extensive studies were thus dedicated to mGluR7a. Later on, mGluR7b was isolated from a human brain cDNA library and found to be conserved among other species, such as mouse and rat (Flor et al., 1997). The full length cDNAs of human mGluR7a and mGluR7b differ at the 3' end of the coding region by an out-of-frame insertion of 92 nucleotides resulting in two putative proteins of 915 and 922 amino acids length. In mGluR7b, the last 15 amino acids of human mGluR7a are replaced

by a novel sequence of 23 amino acids which have no sequence similarity to the C-terminus of other mGluRs. Immunohistochemical studies in rat brain have shown that, at the protein level, mGluR7b is much less abundant than mGluR7a (Kinoshita et al., 1998). Pharmacological assays suggest CHO cells stably transfected with the cloned human mGluR7b cDNA exhibited L-AP4 induced depression of forskolin-stimulated cAMP accumulation (Flor et al., 1997) and human mGluR7a and mGluR7b shows an identical rank order of potency and similar EC50 values for both L-SOP and L-AP4.

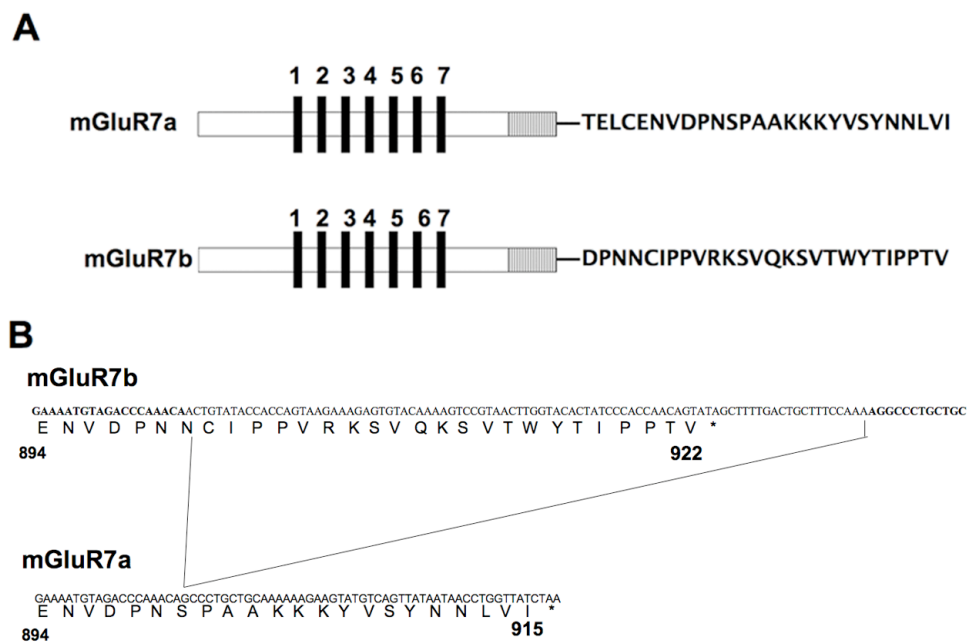


Figure 3. Two splice variants of mouse mGluR7 (mGluR7a and mGluR7b). **A.** Schematic representation of the two mouse mGluR7 splice variants, mGluR7a and mGluR7b. Seven transmembrane regions are indicated by numbered black boxes, the splice-specific regions are located in the C-terminus, note the different sequence for the last 26 amino acids of mGluR7a and mGluR7b. **B.** Alignment of the C-terminal end of the mouse mGluR7a and mGluR7b cDNA sequences and the deduced amino acid sequences in single letter code (modified from Flor et al., 1997). Out-of-frame insertion of 92 nucleotides into mGluR7a C-tail results in putative proteins of mGluR7b.

Kinases, phosphatases and structural proteins have been shown to associate with mGluR7b and to regulate mGluR7 mediated neurotransmission (Enz and Croci, 2003). Compared with mGluR7a, mGluR7b shares some of the known interacting proteins in the intracellular C-terminal region.

Recently, it was reported that three putative novel isoforms of mGluR7 were identified based on splicing events involving the 3' end of the mGluR7 coding sequence (Schulz et al., 2002). The new isoforms might be expressed in non-neuronal tissues. However, these results were never confirmed by in-situ hybridization, immunohistochemistry or functional analysis. Additional data are needed to confirm the existence of these novel isoforms of mGluR7.

1.4.2. Localization of mGluR7 mRNA and protein in the mammalian CNS

Both in situ hybridization and immunocytochemistry have been performed to disclose the distribution of mGluR7 mRNAs and proteins in the mammalian CNS. Due to the antibody quality, more data are available for mGluR7a, while mGluR7b is less well explored. Quite a few studies showed that mGluR7a immunoreactivity is widely distributed throughout the adult rat and/or mouse brain (Kinzie et al., 1997; Bradley et al., 1998; Kinoshita et al., 1998; Kosinski et al., 1999). mGluR7a protein levels are particularly high in sensory areas, such as piriform cortex and entorhinal cortex, superior colliculus, dorsal cochlear nucleus, olfactory bulbs, and high in the hippocampus, thalamic reticular nucleus, corpus striatum, globus pallidus, and facial nerve. In contrast, mGluR7a immunostaining was rarely detected in medial septal nucleus, ventromedial nucleus, ventral tegmental area, oculomotor nucleus, and cerebellar nuclei (Kinoshita et al., 1998).

In neocortical regions, mGluR7a antibody staining shows a diffuse distribution. In cortex, it was intense in layer I, moderate in layers II, III, and V, and weak in layers IV and VI. In the amygdala, intense to moderate mGluR7a was seen in the periamygdaloid cortical regions. The amygdala-hippocampal area also displayed intense to moderate mGluR7a distribution. In the CA1 region of hippocampus, mGluR7a signals were intense in the stratum oriens and stratum radiatum and moderate in the stratum lacunosum-moleculare; no mGluR7a staining was seen in

the stratum pyramidale. In CA3, mGluR7a staining was intense in stratum lacunosum-moleculare, moderate in the stratum radiatum and stratum oriens, and weak in the stratum lucidum; In the dentate gyrus, mGluR7a was intense in the molecular layer; no mGluR7a, however, was seen in the granule cell layer (Kinoshita et al., 1998).

1.4.3. mGluR7 and its implications for signal transduction and synaptic transmission

As all group III mGluRs, mGluR7 has been shown to modulate second messenger systems and ion channels. mGluR7 inhibits forskolin-stimulated adenylate cyclase activity in various cell lines and brain slices (Okamoto et al., 1994; Wu et al., 1998). This effect is pertussis toxin (PTX)-sensitive, implying an interaction with $G_{i/o}$ proteins. In different brain tissues, selective group III mGluR agonists decrease Ca^{2+} currents via the inhibition of L-type, and P/Q-type voltage-sensitive Ca^{2+} channels (Trombley and Westbrook, 1992; Herrero et al., 1996; Takahashi et al., 1996). This decrease in Ca^{2+} current is PTX-sensitive and involves protein kinase C. The group III mGluRs selective agonist L-AP4 has also been shown to couple mGluR7 to recombinant G-protein inwardly rectifying potassium channels (GIRK) in *Xenopus oocytes* (Saugstad et al., 1996). The localization of mGluR7 at presynaptic nerve terminals, combined with its negative coupling to adenylate cyclase and voltage-sensitive Ca^{2+} channels, suggests a role for mGluR7 as an autoreceptor that inhibits neurotransmitter release. Different studies have demonstrated that group III agonists decrease synaptic transmission at glutamatergic synapses located in the hippocampus, olfactory bulb, cerebellum, and the thalamus (Schoppa and Westbrook, 1997; Perroy et al., 2000; Panatier et al., 2004).

More recently, the functional role of mGluR7 has been further investigated, and new data suggest that mGluR7 may play an important role in regulating synaptic transmission and plasticity.

Bough et al. (2004) studied the function of mGluR7 by performing experiments in hippocampal slices prepared from mGluR4/8 double knockout mice. In the medial

perforant path (MPP), L-AP4 (600 μ M) reversibly reduced the fEPSP slope equally in slices taken from either wild-type or mGluR4/8 double knockout mice. In the lateral perforant path (LPP) of animals, L-AP4 (600 μ M) suppressed fEPSPs by $40 \pm 3\%$ in slices taken from wild-type mice, however, L-AP4 only slightly inhibited responses in mGluR4/8 double knockout animals. This suggests that mGluR7-mediated presynaptic inhibition is functionally limited to the MPP, but not the LPP, which is consistent with the notion that a reduction of mGluR7 function may contribute to epileptogenesis (Bough et al., 2004). In the other elegant work, Pelkey et al. (2005) investigated the mossy fiber synaptic transmission and found that the bidirectional plasticity of mossy fiber–stratum lucidum feedforward inhibition was controlled by mGluR7. Their experiments on the mice brain slices have shown that the presynaptically located mGluR7, whose activation and surface expression governs the direction of plasticity, is a metaplastic switch at MF (hippocampal mossy fiber)-SLIN (CA3 stratum lucidum interneurons) synapses. In naive slices, mGluR7 activation during high-frequency stimulation generates MF-SLIN long-term depression (LTD), depressing presynaptic release through a PKC-dependent mechanism. Moreover, following agonist exposure, mGluR7 undergoes internalization, unmasking the ability of MF-SLIN synapses to undergo presynaptic potentiation in response to the high frequency stimulation that induces LTD in naive slices. Thus, selective mGluR7 targeting to MF terminals contacting SLINs and not principal cells provides cell target–specific plasticity and bidirectional control of feedforward inhibition (Pelkey et al., 2005).

1.4.4. The role of mGluR7 in epilepsy and seizures

Epilepsy is a chronic neurological disorder characterized by large populations of neurons in selected portions of the CNS showing increased activity and beginning to fire in periodic, synchronous discharges. The defining phenotypic feature of epileptic syndromes is the seizure. Seizure phenotypes are quite diverse, ranging from electrographic seizures with no obvious behavioral symptoms, to generalized seizures with severe motor convulsions and impaired consciousness (Doherty and Dingledine, 2002). Increasing evidences suggest that mGluRs are linked to the etiology and therapy of epilepsy (Ghuri et al., 1996; Klapstein et al., 1999; Barton

and Shannon, 2005), however, only the potential role of mGluR7 in epilepsy and seizure generation will be discussed here.

The first evidence for a role of mGluR7 in seizures came from in vivo studies. The agonist L-AP4 for mGluR7, when focally injected into the hippocampus, effectively suppressed amygdala-kindled seizures (Abdul-Ghani et al., 1997). On the other hand, the group III mGluR agonist also increases the latency to pentylenetetrazol (PTZ)-induced seizures in mice (Thomsen and Dalby, 1998). Additional support for a role of mGluR7 in epilepsy came from mGluR7 knockout mice.

mGluR7 knockout mice were first described by Masugi et al. (Masugi et al., 1999). These mice develop seizures after 12 weeks of age, especially when placed in a novel environment. Sansig et al. confirmed (Sansig et al., 2001b) that tonic-clonic seizures are triggered in adult (>12 weeks) mGluR7-deficient mice when the animals are exposed to new bedding. In another set of experiments, the authors could show that homozygous mutant mice, but not heterozygous mice or wild-type mice had a lowered threshold for bicuculline-induced seizures (Sansig et al., 2001b). However, these mice did not display spontaneous seizures, suggesting mGluR7 gene ablation result in an increased susceptibility to sensory and chemoconvulsant-induced seizures.

1.4.5. mGluR7 interacts with PICK1 (Protein Interacting with C Kinase 1)

The identification of specific proteins that interact with the C-terminal domain of mGluR7 receptors has been investigated during the last decade in different labs, and considerable progress has been made towards understanding the mechanisms that underlie the regulation, signal transduction pathways and targeting of mGluR7 receptors (Dev et al., 2001). Yeast two-hybrid screens using the C-terminal tail of mGluR7 as “bait” revealed a direct interaction of mGluR7 with PICK1 (Boudin et al., 2000; Dev et al., 2000; El Far et al., 2000). PICK1 has originally been described as a PDZ (PSD-95/Dlg1/ZO-1) domain-containing protein that interacts with and is phosphorylated by PKC α (Staudinger et al., 1995; Staudinger et al., 1997). The previous work in our lab has shown that the protein kinase C substrate PICK1 interacts with the major cytoplasmic domain of mGluR7a. PICK1 binding is

mediated by the extreme C-terminus of the receptor, the replacement of the last three amino acids leucine, valine and isoleucine of mGluR7a by alanines decreased the intensity of the interaction. Similarly, the integrity of the PICK1 PDZ domain proved crucial for this interaction. Substitution of residues K27 and D28 in the carboxylate binding loop of PICK1 by alanines prevented its interaction with mGluR7a (Boudin et al., 2000; Dev et al., 2000; El Far et al., 2000). It is relatively clear that the interaction of mGluR7a with PICK1 is based on a conventional PDZ domain–C-terminal peptide interaction (Figure 4). Based on binding specificities and sequence homologies, PDZ domains are classified into three types. Type I sequences select for peptides with the C-terminal consensus motif [-S/T-X-Φ (X: unspecified amino acid; Φ: hydrophobic amino acid)] (Songyang et al., 1997), whilst type II PDZ domain, specific for -X-Φ-X-Φ sequences, is characterized by hydrophobic residues at both the -2 position of the peptide ligand and the αB1 position of the PDZ domain. As for type III PDZ domain, it is specific for a different -X-D/E-X-Φ pattern, and prefers negatively charged amino acids at the -2 position (Stricker et al., 1997). When considering these characteristics and comparing the primary sequence of the PICK1 PDZ domain with those of different members of types I, II and III PDZ motifs, it is difficult to classify the PICK1 PDZ domain into particular subtypes. Since PDZ domain of PICK1 could mediate interactions with PKCα through type I peptide ligand (DSSL) and with GluR2 through type II peptide ligand (SVKI), it could be therefore proposed that this PDZ region specifies a new type of PDZ domains.

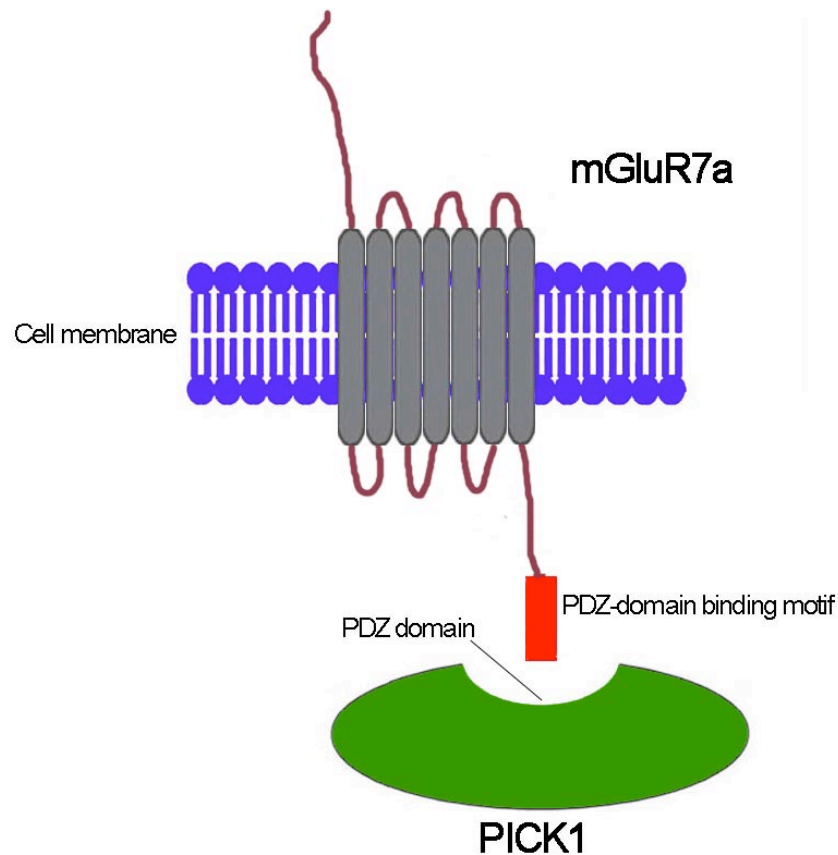


Figure 4. The specific interaction between mGluR7a and PICK1. PICK1 is a single PDZ-domain containing protein, the interaction of mGluR7a cytoplasmic domain with PICK1 is based on a conventional PDZ domain–C-terminal peptide interaction, the PDZ-domain binding motif is located in extreme C-terminal region of mGluR7a.

In addition to binding $\text{PKC}\alpha$, PICK1 serves as a scaffolding protein for presynaptic mGluRs. Strong evidence exists that the interaction with PICK1 is crucial for the clustering of mGluR7 at presynaptic release sites. Boudin et al. (2000) reported, in transfected hippocampal neurons, both wild-type and C-terminally mutated mGluR7 lacking the last three amino acids required for PICK1 binding were targeted equally well to axons; however, only the wild-type, and not the mutant receptor was clustered presynaptically. Both the coiled-coil regions of PICK1 and the PDZ motifs were found to be important for the presynaptic enrichment of PICK1, as mutation of the PDZ domain and deletion of the coiled-coil regions abolished co-clustering of PICK1 with mGluR7 in transfected hippocampal cultures (Boudin et al., 2000).

Perroy et al. (2002) have investigated the functional consequences of the mGluR7a-PICK1 interaction in cultured cerebellar granule neurons and found that PICK1 is required for the specific inhibition of P/Q-type Ca^{2+} channels (Perroy et al., 2002). Furthermore, they could show that activation of mGluR7a receptor inhibits synaptic transmission and that this effect requires the presence of PICK1. Therefore, they concluded that PICK1 plays an essential role in mGluR7a receptor signaling rather than merely receptor clustering (Perroy et al., 2002).

1.5. Aim of this thesis

As outlined above, the goals of our laboratory are to elucidate the biochemical and physiological functions of protein-protein interaction of Group III mGluRs in the mammalian CNS. To this end, intracellular binding partners to group III mGluRs were identified and related signalling processes at central synapses were investigated at different levels. My thesis project focused on the protein interaction between mGluR7 and the PDZ-domain protein PICK1, which was identified by Yeast Two-Hybrid analysis. Preliminary data has indicated that PICK1 might be a potential mGluR7 clustering molecule or alternatively alter signal transduction through a protein kinase C dependent pathway. However, the precise physiological roles of mGluR7-PICK1 interaction are still poorly understood, and no detailed functional analysis has been performed so far because of the lack of suitable *in vitro* assays. The best insights into the physiological functions of this protein interaction could be provided by genetic approaches. Gene targeting technology allows to introduce any kind of specific mutation into the genome of the mouse by homologous recombination in embryonic stem cells (ES cells). The aim of this thesis was the generation of a mouse strain which carries a mutation and disrupts the specific interaction between mGluR7a and PICK1. The generated mice provide an animal model to study how the intracellular binding proteins regulate the function of mGluR7; moreover, the control of synaptic trafficking and targeting of mGluR7 by PDZ protein will be investigated in more detail, and mGluR7 mediated synaptic transmission mechanism will be further studied using this mutant mouse, it will also provide a tool to dissect the molecular mechanism of excitatory neurotransmission of group III mGluRs in the brain.

2. Material and Methods

2.1. Materials

2.1.1. Organism

Mouse

MTK-neo CD1 transgenic mice were used for preparation of mouse embryonic fibroblast (MEF) feeder cells.

The C57BL6 mouse line was used for backcrossing and maintaining the mGluR7 Knock-in mouse line.

Bacterial strain

E. coli XL-1 blue, Genotype: *recA1 endA1 gyrA96 thi-1 hsdR17. supE44 relA1 lac[F' proAB lacI. q. Z M15 Tn10(Tet. R.)]*

E. coli DH5 α , genotype: *supE44 deltalacU169 (phi80 lacZ deltaM15) hsdR17 recA1 endA1 gyrA96 thi-1 relA1*

ES cell

The SV129/Ola ES cell line (E14) was used to generate the mutant mouse model described in this thesis.

2.1.2. Chemicals

All the chemicals, unless otherwise stated, were purchased from the following firms: Roche Diagnostic (Heidelberg, Germany), Fluka (Taufkirchen, Germany), Invitrogen (Karlsruhe, Germany), Merck Biosciences (Schwalbach, Germany), Sigma –Aldrich-Chemie (Taufkirchen, Germany) and Roth Carl (Karlsruhe, Germany). Water used to make solutions was prepared with a Milli-Q-Water-System (Millipore, Schwalbach, Germany). Restriction enzymes were purchased from Roche Diagnostic (Heidelberg, Germany), or New England Biolabs (Frankfurt, Germany).

2.1.3. Medium and antibiotics for Bacterial culture

LB-Medium (Luria-Bertrani)

Bacto-trypton 10 g/l

Yeast-extract 5 g/l

NaCl 10 g/l

pH 7.5

LB-Agar

Bacto-trypton 10 g/l

Yeast-extract 5 g/l

NaCl 10 g/l

Agar 15 g/l

pH 7.5

Antibiotics (diluted 1:1000 in medium upon use)

Ampicillin Stock 100mg/ml in H₂O

Kanamycinsulfate Stock 50mg/ml in H₂O

Chloroamphenicol stock 20mg/ml in methanol

2.1.4. Medium and supplements for Embryonic stem (ES) cells and mouse embryonic fibroblast (MEF) feeder cells

ES-Medium

Dulbecco's Modified Eagles Medium, high glucose

L-Glutamin 2 mM

Penicillin 100 U/ml

Streptomycin 100 µg/ml

Non-essential amino acids 0.1 mM

Mercapto-ethanol 0. 1mM

Heat inactivated ES-tested Fetal Bovine Serum 20%(v/v)

Leukemia Inhibitory Factor (LIF) 1000 IU/ml

The medium was sterilized through filtration with a 0.22 µm Bottle Top Filter (Becton Dickinson) and used for no longer than 2 weeks.

ES-medium for double selection

ES-medium

Geneticin (G-418) 0.2 mg/ml

2-Deoxy-2-Fluoro-β- D-arabinofuranosyl-5-iodouracil (FIAU) 0.2 µM

MEF-medium

DMEM

Heat Inactivated Fetal Bovine Serum 10% (v/v)

Penicillin 100 U/ml

Streptomycin 100 µg/ml

L-Glutamin 2 mM

ES-freezing medium

ES-medium

Dimethyl-sulfoxide(DMSO)

10% (v/v)

MEF-freezing Medium

MEF-medium

DMSO 10% (v/v)

2.1.5. Medium and supplements for primary culture of Hippocampal neurons

Hippocampal medium

L-Glutamin 2 mM

Penicillin 50 U/ml

Streptomycin 50 µg/ml

0.23mM sodium pyruvate

2% B27

Neurobasal medium

2.1.6. General buffers and solutions

10X PBS

1.3M NaCl

70mM Na₂HPO₄

30mM NaH₂PO₄, pH 7.2

Buffer P1 (resuspension buffer)

Tris/HCl 50 mM

EDTA 10 mM

RNase A 100 µg/ml

pH 8.0

Buffer P2 (lysis buffer)

NaOH 200 mM

SDS 1% (w/v)

Buffer P3 (neutralization buffer)

Potassium--acetate 3M, pH 5.5

1X MOPS

0.418% MOPS

2mM Na-Acetate

1mM EDTA pH8.0

20xSSC

NaCl 3 M

Na-Citrate 0.3 M

pH 7.0

Separating gel

Acrylamide/bisacrylamide 7.5-15% (v/v)

Tris/HCl 0.375 M

SDS 0.1% (v/v)

10% Ammonium-persulfate (APS, w/v) 4 µl/ml

N,N,N',N'-Tetramethyl-ethylenamin (TEMED) 0.72 µl/ml

pH 8.8

Stacking gel

Acrylamide/bisacrylamide 7.5-15% (v/v)

Tris/HCl 0.125 M

SDS 0.1% (v/v)

APS 6 µl/ml

TEMED 0.72 µl/ml

10 x Running Buffer

Tris/HCl 0.25 M

Glycin 1.92 M

SDS 1% (v/v)

Transfer Buffer (western-blot)

Tris-HCl 200 mM

Glycine 1,54 M

SDS 0.8% (w/v)

Methanol 20% (v/v)

Poinceau Solution

Poinceau S 0.3% (w/v)

Trichloroacetic Acid 3% (w/v)

4x Sample buffer for non-reducing conditions:

4ml 10% SDS
16.ml 1M Tris pH6.8
2ml glycerol
1.9ml H2O
0.1% bromophenol blue

4x Sample buffer for reducing conditions:

50µl β-mercaptoethanol /ml 4x sample buffer

2.1.7. Plasmids and BAC clones

Cloning vector	pBluescript II SK(+)	Stratagene
	pBluescript II SK(-)	Stratagene
	pEasy-Flox	Werner Müller, Institute of Genetics, University of Köln
Cre-recombinase expression vector	pPGKcrebpA	Werner Müller, Institute of Genetics, University of Köln
mGluR7 gene containing clone	BAC RP23-391F16	BACPAC resources center, Children's Hospital Oakland, USA

2.1.8. Oligonucleotides

All oligonucleotides were ordered from MWG Biotech and dissolved in HPLC water.

Name	Sequence (5'—3')	Special features
Primer1	GCCAAAGTGTATGTGTATTCCTC	BAC clone identification
Primer2	TCCATCACAACACCTACCATGTAC	
Primer3	GTATGTCAGTTATAATAACGCAGCTGCCTAACCTGTTCC ATCCC	Site-directed Mutagenesis
Primer4	GGGATGGAACAGGTTAGGCAGCTGCGTTATTATAACTG ACATAC	
Primer5	GCCTTATCCAGGGATCCACCC	Short arm amplification
Primer6	GCAGGATCCATTTATTTTGTCTGGCTGAG	
Primer7	CTGAAGTGTGGACACTATGCCCTC	ES clone screening
Primer8	GCTACTTCCATTTGTCACGTCCTGC	
Primer9	GCAGAGTTGGGAGTGAGACAGCTCAG	External probe amplification
Primer10	CTACATGTATGAATATGTACCATATGG	
Primer11	GAATTCCAATGACACAGGACATC	Internal probe amplification
Primer12	GATAGAGCGTGGATGATTTCCAG	
Primer13	GCCATTGTCAAGTACACATGACAAAGAG	ES clone characterization
Primer14	CCGGGGGATCCACTAGATAACTTCGTA	
Primer15	CCTGTAGATGCACTCAGCCAGACA	ES clone characterization
Primer16	TTCCATGGGATGGAACAGGTTAGGC	
Primer17	CCACCCTGAACTCAATGTCCAGAAAC	RT-PCR

Primer18	GAGAAGCTCCTCCAGAGATAGGAAGC	
Primer19	CCACCCTGAACTCAATGTCCAGAAAC	Northern probe amplification
Primer20	TTAGATAACCAGGTTATTATAACTGACATAC	
Primer21	CCAGTGTGATTGTTTCAGACATCGGAAAG	Mice genotyping
Primer22	CCAGCCCTAAGCTGCAAAGGTGATCTGG	

2.1.9. Antibodies

Primary antibodies

Name	species	Western blot	Immunostaining	supplier
mGlu7, C-terminal	Rabbit polyclonal	1:4000	1:200	Upstate, NY, USA
mGluR4, N-terminal	Rabbit polyclonal	1:2000	-	Upstate NY, USA
PICK1	Rabbit polyclonal	1:1000	-	Richard Huganir
PICK1	Goat Polyclonal	1:500	-	Santa Cruz Biotechnology, Inc.
Synapsin	Mouse monoclonal	-	1:400	Synaptic systems
β -tubulin	Mouse monoclonal	1:2000	-	Sigma

Secondary antibodies

Name	dilution	supplier
HRP α Mouse	1:5000	Promega, Madison USA
HRP α Rabbit	1:5000	Promega, Madison USA
Alexa 488 α Rabbit	1:500-1:1000	Molecular probes, Eugene, USA
Alexa 546 α Mouse	1:500-1:1000	Molecular probes, Eugene, USA
Alexa 546 α Ginny- Pig	1:500-1:1000	Molecular probes, Eugene, USA

2.1.10. Commercial Kits for molecular biology

For standard molecular biology experiments, commercial kits were employed and all the protocols were performed according to the manufacturer's instructions

Qiagen Plasmid Kits (Mini, Midi, Maxi)	Qiagen
Qiaquick Gel Extraction kit	Qiagen
Qiaquick PCR Purification Kit	Qiagen
ABI PRISM dye Terminator cycle sequencing Ready Reaction Kit	Perkin Elmer Applied Biosystems
QuickChange Site-Directed mutagenesis Kit	Stratagene
QuickHyb Rapid hybridization Solution	Stratagene
Advantage GC cDNA PCR Kit	Clontech
Prime-a -Gene Labeling System Kit	Promega
ThermoScript RT-PCR system	Invitrogen

2.2. Methods

2.2.1. Biochemistry and molecular biology methods

2.2.1.1. Preparation of DNA

Small scale preparation of Plasmid DNA by alkaline lysis

Cultures of 2 ml LB-medium containing selection antibiotics were prepared from a single colony and incubated overnight at 37 °C. Bacteria were pelleted at 8000 rpm for 1 min, resuspended in 100 µl of Buffer 1, and lysed by adding 200 µl of Buffer 2. After incubation for 5 min at room temperature, 150 µl of Buffer 3 were added to the lysate, gently mixed, incubated at 4 °C for 10 min and centrifuged at 13000 rpm for 5 min. The supernatant was transferred to another tube and the DNA was precipitated with 2 volumes of ethanol, pelleted by centrifugation for 15 min at 13000 rpm, washed once with 70% ethanol and then resuspended in TE buffer.

Mini, Midi and Maxi preparations of plasmid DNA with Qiagen Kits

Qiagen Plasmid Purification kits were used for preparation of plasmid DNA according to the scale of bacterial culture. All the protocols were performed by following the manufacture's instructions.

DNA isolation from BAC clone

BAC DNA cultures (500ml) was incubated overnight at 37°C with antibiotics. The cells were pelleted at 3000 rpm for 15 min at 4°C and then resuspended in 15 ml of GTE (0.9% glucose, 25 mM Tris, pH 8, 10 mM EDTA, 0.1 mg/ml RNaseA). After 5 min at R/T, 15 ml of fresh SDS/NaOH (1% SDS and 200 mM NaOH) were added,

the cell lysate were mixed gently and then 20 ml of ice-cold KAc (3M potassium acetate made up in 2M acetic acid) were added immediately. The samples were mixed very gently, placed on ice for 20 minutes, and then centrifuged at 3000 rpm for 30 min at 4°C, the supernatant was transferred to clean tubes, the DNA was precipitated with 0.7 volumes of Isopropanol and the pellet was washed once with 70% ethanol. The pellet was dissolved in 1ml TE. The resuspended pellet was treated two times with phenol/chloroform, then 200ul 3M NaOAc and 0.7 volumes Isopropanol were added to precipitate the DNA, the DNA was washed with 70% EtOH; finally, 500ul TE was used to resuspend the DNA.

Preparation of Genomic DNA from ES Cells in 24-well tissue culture plates

Medium were removed from each well containing nearly confluent ES cells, cells were rinsed once with PBS, then 400µl lysis buffer (150mM NaCl, 2mM EDTA, 1% SDS, 20mM Tris-HCl, pH 8.0) were loaded to each well, the dish was incubated for 1h at 37°C, all the lysate were transferred to 1.5 ml eppendorf tubes, 100µl saturated NaCl were added to each tube and shaken vigorously. The tubes were centrifuged at 3000g for 15min, the supernatant containing DNA were transferred to a fresh tube and added 2 volumes of ethanol at room temperature, the tube was inverted several times until the DNA precipitate and then DNA was removed with a glass rod, the DNA pellet was washed in 70% ethanol and resuspended in 80µl TE and dissolved overnight at room temperature.

Preparation of Genomic DNA from mouse tails

Mouse tails were incubated with 500µl lysis buffer (Tris/HCl 100 mM, pH 8.5, EDTA 5mM pH 8.0, NaCl 200 mM, 0.5% SDS (v/v), proteinase K 0.2mg/ml) overnight at 55°C on shaker. After centrifugation for 30 min, supernatant was collected into a new 1.5ml tube, 500µl each of phenol and chloroform were added to the tubes. the samples were mixed by inversion and spun for 10 min. Upper layer was transferred into a new 1.5ml tube, 600µl Isopropanol was added, then mixed and span for 5

min. The pellet was washed with 500µl 70% EtOH, and was allowed to air dry and finally dissolved in 100µl TE.

2.2.1.2. Total brain RNA preparation and RT-PCR

The TRIzol Reagent (Invitrogen) was used to prepare the total RNA from mouse brain tissue, the frozen mouse brain tissue were placed in TRIzol Reagent (1 ml of TRIzol Reagent per 50-100 mg of tissue) and the tissue was homogenized at moderate speed, the homogenized samples were incubated for 5 min at R/T, then 0.2 ml of chloroform per ml of TRIzol Reagent were added, and incubated for 2-3 min at R/T, the 500 µl (up to 750 µl) homogenates aliquots were transferred to a new tube and were centrifuged for 15 min at 12,000 rpm at 4 °C. The upper colorless aqueous phase remaining the RNA were collected into a fresh tube. RNA was precipitated with 0.5 ml Isopropanol per ml of TRIzol Reagent by centrifugation at 12,000 rpm for 10 min at 4 °C. The supernatant was removed carefully, and the pellet was washed with 1 ml 75% ethanol, the RNA pellet was air-dried for 10 min and dissolved in 50 µl RNase-free water.

Reverse transcription reaction was performed with the ThermoScript RT-PCR system (Invitrogen). All procedures followed the manufacturer's instructions. Briefly, 2 µg total RNA were added to 200 ng gene specific primers and 10mM dNTP mix, incubated at 65 °C for 10min, chilled on ice for 1 min. Then the reaction mixture (1X cDNA synthesis buffer, 100mM DTT, RNaseOUT, DEPC-H₂O, ThermoScript RT), was added and incubated at 50 °C for 60 min, the reaction was terminated by incubating at 85 °C for 5 min, then 2 units of RNase H were added and incubated at 37 °C for 20 min. the cDNA synthesis reactions was used immediately for PCR.

2.2.1.3. Site-directed mutagenesis

Mutations were introduced using the QuickChange Site-Directed Mutagenesis Kits (Stratagene). This method is highly effective and simple for introducing site-directed mutations into plasmids without subcloning. Pfu DNA polymerase, two

synthetic oligonucleotide primers containing the desired mutation, and supercoiled double-stranded DNA vector were employed for the basic procedure. After amplification of the mutant DNA, the product was treated with Dpn I, and the mutation-containing synthesized DNA was selected by transforming to competent XL1-Blue cells. The reactions for amplification of mutant DNA were prepared as following:

DNA template plasmid 20 ng

10x pfu DNA polymerase buffer 5.0 μ l

125ng primer1 0.5 μ l

125ng primer2 0.5 μ l

10mM dNTP 1.0 μ l

Pfu DNA polymerase (2.5 units) 1.0 μ l

H₂O up to 50 μ l

PCR conditions

95 °C 30 seconds, then 18 cycles of : 95 °C 30 sec, 55°C 1 min, 68°C 2 min/kb of plasmid length.

After cooling down the PCR reaction, 1 μ l Dpn I (10 unit) was added to PCR reaction and incubated at 37 °C for 1 hr. Then 2 μ l of digested PCR reaction were added to 100 μ l highly competent XL1-Blue cells for normal transformation. Colonies were screened and the mutation was characterized and verified by DNA sequencing.

2.2.1.4. DNA sequencing

Plasmid DNA and PCR products purified with Qiagen kits were used for sequencing reactions. Typical reaction mixtures included:

Sequencing Mix (Amersham Bioscience) 4 μ l

Sequencing primers 5 pmol

DNA template (10 ng DNA for per 100bp in length)

H₂O to 10 μ l

Sequencing PCR reaction:

95°C 20 sec

50°C 15sec

60°C 60sec

25 cycles for PCR product, 35 cycles for plasmid DNA, then holding at 4°C.

Sequencing reaction products were purified with AutoSeqG-50 columns (Amersham Bioscience) and processed by MegaBACE sequencer.

2.2.1.5. Polymerase chain reaction

Advantage GC cDNA PCR kit (Clontech) was used for screening recombinant ES clones. The user's manual of the kit was followed for the experiment. Short (20-30 mers) oligonucleotide primers were designed to have a G/C between 50-60%. Standard PCR reactions were performed using the Taq DNA Polymerase with cell lysate (template DNA), 1 pmol of each Primer, 0.2 mM dNTP mix and 5 μ l GC melt in 1xPCR buffer.

Standard PCR conditions were as follows:

First cycle 94 °C, 5 min

Subsequent

30 cycles 94 °C, 1 min

68 °C 3 min

Final Cycle 68 °C 10 min

Genotyping of mice and other normal PCR in this thesis work were performed using the Taq DNA Polymerase (Invitrogen), with 5 μ l of template DNA (50-100 ng), 1 pmol of each primer, 1.5 mM MgCl₂, 0.2 mM dNTP mix and 1 u Taq DNA Polymerase in 1x PCR Buffer, using the following conditions:

First cycle 95 °C, 5 min

Subsequent

35 cycles 95 °C, 1 min

60 °C, 1 min

72°C 2 min

Final Cycle 72 °C 10 min

All reactions were performed in a Gene Amp PCR System 9600 (Perkin Elmer).

2.2.1.6. Enzymatic treatment of DNA

Cleavage of plasmid DNA: Approximate 2-6 μ g of DNA was incubated in 30 μ l of the appropriate buffer with 5 to 10 U restriction enzyme for 1 to 2 h at an appropriate temperature. Digestion of genomic DNA was performed with a final concentration of restriction enzyme of 10 u/ μ g DNA.

Dephosphorylation of DNA fragments: For the dephosphorylation of DNA fragments, 10 x buffer, H₂O and 1 U (1 μ l) of calf intestine alkaline phosphatase (CIP) were directly added to the restriction enzyme reaction, incubated for 30 min at 37°C and heat-inactivated at 75°C for 15 min. Subsequently the dephosphorylated DNA fragments were purified from the reaction mix. Ligation of DNA fragments: A 20 μ l reaction containing purified linearized vector (approximate 0.1 μ g) and DNA fragments (“insert”) in an 1:3 ratio, 1 μ l of T4 DNA ligase (NEB), ligation buffer (10 x T4 DNA ligase buffer, NEB) were incubated overnight at 16°C. The reaction was then used to transform competent bacterial cells.

2.2.1.7. Random-labelling of DNA probe

DNA probes were radioactively labeled with α -[P³²]-dCTP using the Prime-a- Gene-labeling System kit (Promega). 50 ng of DNA template diluted in 45 μ l of dH₂O were denatured and labeled by following the kit's instructions. After adding 5 μ l of α -[P³²]-dCTP, the reaction was incubated for 60 min at 37 °C.

2.2.1.8. Southern blot analysis of genomic DNA

10 μ g of genomic DNA were fully cut overnight with restriction enzyme in a final volume of 50 μ l. The samples were separated on 0.8% 1xTAE agarose gel at 1,5 V/cm for 7 h. The gel was treated sequentially with denaturation solution (NaCl, 1.5 M, NaOH 0.5 M) and neutralisation solution (NaCl 1.5 M, Tris/HCl 1 M, pH 7.4) and then transferred overnight on a Nylon membrane (Hybond N⁺, Amersham Pharmacia Biotech) in 20 x SSC. After transfer, the membrane was rinsed in 6 x SSC, DNA was crosslinked to the membrane by UV irradiation (Stratagene, UV crosslinker) and stored at room temperature.

Hybridization reactions were performed with QuikHyb Hybridization Solution (Stratagene) in an oven equilibrated to the appropriate temperature. The pre-hybridization and hybridization procedures were done following the user's manual from Stratagene. Blots were exposed at -70 °C using Kodak Biomax MR films with intensifying screens.

2.2.1.9. Northern blot analysis

A 1% agarose gel was prepared in DEPC treated water. After cooling for about 10 min, MOPS were added to 1x and 0.6% formaldehyde was added in a fume hood. 30 μ g of total RNA was mixed with sample buffer and incubated at 65°C for 5 min, then 1 μ l of 1 mg/ml ethidium bromide was added, and samples were loaded on

gel. Electrophoresis in 1x MOPS buffer was performed for about 2-3 h. The gel was soaked in 200 ml RNase-free water for 10-15 min and then for 15 min in 50 mM NaOH-1.5M NaCl, then the gel was neutralized by soaking in 0.5M Tris-HCl (pH 7.4)-1.5 M NaCl for 30 min. RNA was transferred overnight to a nylon membrane (pre-soaked in 1x MOPS buffer) with a 20x SSC. After transfer, the membrane was rinsed in 6x DEPC-treated SSC and then treated by UV crosslinker (Stratagene) for 2 minutes. Labeling of the probes and hybridization procedures were performed as for Southern blot analysis.

2.2.1.10. Preparation of competent bacteria for electroporation

20 ml LB-medium were incubated overnight at 37 °C with a single colony of XL1-Blue cells. 10 ml of the cultures were then transferred to 400 ml of pre-warmed LB-Medium and incubated at 37 °C with shaking, until the OD₆₀₀ reached 0.5. Bacteria were harvested by centrifugation (6000 rpm, 20 min) and from here, all the steps were performed on ice using prechilled solutions and glassware. The cell pellet was subjected to three successive washes by resuspension in ddH₂O. Subsequently, the pellet was washed once with 10% (v/v) glycerol, and finally resuspended in 5 ml of 10% glycerol. 100 µl aliquots of the bacteria were frozen in liquid nitrogen and stored at -70 °C.

2.2.1.11. Electroporation of Competent Bacterial Cells

Competent bacterial cells were thawed on ice, 2 µl of ligation reaction were added and the samples were transferred to a prechilled electroporation cuvette (2mm electroporation cuvette, Eurogentech). The cuvette was then placed in the electroporation chamber (Biorad Gene Pulser) and electroporated using the following settings: 25 µF, 2.5 kV, 200 Ohm. Then the bacteria were transferred immediately to 1 ml of LB-medium and incubated at 37 °C for 1 h. Cells were pelleted and plated on LB-agar plates containing the appropriate antibiotic, and incubated overnight at 37 °C.

2.2.1.12. SDS-Polyacrylamide gel electrophoresis (SDS-PAGE)

Separation of proteins was carried out by SDS-PAGE. Protein samples were treated with SDS-sample Buffer before loading onto the gel; 8 µl of See Blue Plus2 marker (Invitrogen) were used as molecules weight standard. The gel was run in Running Buffer at 20 mA until the blue dye had reached the bottom of the gel. Thereafter, the gel was stained with Coomassie blue or transferred to a nitrocellulose membrane.

2.2.1.13. Western blot and Immunodetection of proteins

Proteins were transferred to nitrocellulose membranes (Schleicher & Schull) for 2 h at 100 V. After transfer, the membrane was stained for 5 min in Ponceau Solution to visualize the transferred protein bands. The membrane was incubated for at least 1h in blocking buffer (PBS containing 5% nonfat dry milk) at room temperature, rinsed in PBS/ 0.02% (v/v) Tween-20 and incubated overnight at 4 °C with the primary antibody diluted in blocking buffer. After 5 washes with 1xPBS/0.02% (v/v) Tween-20 for 5 min each, the membrane was incubated with the secondary antibody diluted in blocking buffer for 1 h at room temperature. The blot was washed 4 times in 1xPBS/0.02% Tween-20 and horseradish peroxidase (HRP) coupled secondary antibodies were directly detected using the SuperSignal West Pico Chemiluminescent Substrate kit (Pierce, USA). Blots were exposed for 1 s to 20 min using Kodak Biomax MR films.

2.2.1.14. Co-immunoprecipitation

Mouse brains dissected from wild type and homozygous mice were homogenized in the Co-IP buffer (50 mM Tris-Cl, pH7.5, 15 mM EGTA, 100 mM NaCl, 1 mM dithiothreitol (DTT) plus complete protease inhibitor cocktail (Roche diagnostics)). The homogenate was centrifuged at 800 x g for 10 min; the supernatant was

collected and centrifuged at 20,000 x g for 1 h. The resulting pellet was resuspended in the same Co-IP buffer containing 1% (v/v) Triton X-100, then the membranes were solubilized overnight at 4 °C on a shaker. Insoluble material was removed by centrifugation, and the supernatant was stored at –80 °C after the total protein concentration was determined. For co-immunoprecipitation, the samples from wild-type mice were diluted to adjust mGluR7a concentration. The samples were precleared for 1 h at 4 °C with protein G–Sepharose beads (Amersham Bioscience). IP reaction was performed overnight at 4 °C by using 4 µg anti-PICK1 (N18) (Santa Cruz Biotechnology) antibody, followed by adsorption to protein G beads. In control experiments, non-specific goat IgG were used instead of the specific antibodies. After washing the beads, bound proteins were eluted with SDS-sample buffer and separated by SDS-PAGE and analyzed by Western blotting.

2.2.2. Cell biology methods

2.2.2.1. Culture of embryonic stem cells (ES-cells)

ES-cells were routinely grown on a monolayer of mouse embryonic fibroblasts at 37°C. Only low passages of ES-cells were used (less than 15 passages), since longer culture times adversely affect ES-cell totipotency. Cells were kept at a relatively high density and the medium was changed every 24 hours. Cells were passaged when plates reached 50% confluency. The plate was washed twice with ES-PBS, incubated with ES-Trypsin for 2 min at 37 °C in a 5% CO₂ atmosphere and cell aggregates were disrupted by pipetting with a P200 Gilson pipette five times and subsequent incubation for 1 min at 37 °C. Trypsinization was stopped by dilution with ES-medium (1:4), the cell suspension was transferred to a 15 ml Falcon tube and ES-medium were added to a final volume of 10 ml. The cells were pelleted for 5 min at 200 g at room temperature, resuspended in ES-medium and plated on ME monolayers.

2.2.2.2. Preparation of mouse embryonic fibroblasts (MEFs)

Pregnant female mice were sacrificed at E13-E14 by cervical dislocation. The embryos were removed from the uterus, and after cutting away the brain and dark red organs, washed with fresh PBS in order to remove as much blood as possible. The remaining tissue was minced with two scalpels, cells/tissue were suspended in several ml of trypsin-EDTA (about 1-2ml per embryo) and incubated under gentle shaking at 37°C for 20 min. The suspension was transferred to a Falcon tube containing a suitable volume of DMEM/10% (v/v) FCS and subjected to low speed centrifugation (5 min), the resulting cell pellet was resuspended in warm MEF medium and plated out at 1 embryo equivalent per 10 cm dish. The medium was changed on the following day, with the fibroblasts being the only cells that attached to the dishes. Plates were confluent within one to a few days. When the MEFs formed a confluent monolayer, they were trypsinized and replated in T-125 flasks. When the flasks were confluent, cells were trypsinized and either frozen in MEF-freezing medium (3x 1 ml aliquots per confluent T-125) or replated in 3xT-125 flasks. After the cells had reached confluency, the flasks were trypsinized, and the MEFs were pooled in 50 ml of MEF-medium and treated with 6000 rads of gamma irradiation to inhibit cell growth and division. The inactivated MEFs were then frozen in MEF-freezing medium (3x1 ml aliquots per confluent T-125 flask).

2.2.2.3. Freezing of cells

After trypsinization, ES cells or MEFs were pelleted for 5 min at 800 g at room temperature and resuspended in the appropriate volume of prechilled freezing medium (3 ml of MEF-freezing medium for one confluent T-125 flask; 1 ml of ES-freezing medium for one confluent well of a 6-well plate). The cell suspension was transferred to prechilled 1 ml cryovials and stored for 2 days to 2 weeks at -70 °C. For long-term storage, the cells were transferred to liquid nitrogen tanks.

2.2.2.4. Electroporation of the targeting vector into ES cells

Plasmid DNA of the targeting vector was prepared according to the Plasmid Maxi kit (Qiagen) manual, and the DNA was linearized by Not I digestion. After digestion, the targeting vector DNA was precipitated with Na-acetate/ethanol, washed twice with 70% (v/v) ethanol, and the DNA was dissolved in TE buffer for electroporation. ES-cells from a confluent T-75 flask were trypsinized and cells pelleted for 5 min at 800 g, at room temperature. The cell pellet was suspended in 800 μ l of PBS and transferred into 0.4 cm electroporation cuvette (Biorad). 15 μ g of linearized DNA were added to the cell suspension and incubated for 5 min at room temperature. The cuvette was then placed in the electroporation chamber (Biorad Gene Pulser) and electroporated using the following settings: 500 μ F, 240 V, τ = 5.7 ms. The cells were allowed to recover for 5 min at room temperature, transferred to 100 ml of prewarmed ES-medium, and then mixed, distributed into 10 cm dishes with feeder cells. After 24 h, the ES medium was replaced by selection medium containing neomycin and FIAU (5-iodo-2'-fluoro-2'-deoxy-1- β -D-arabino-furanoside). ES cells were allowed to growth in the selection medium with neomycin and FIAU for 5-7 days.

2.2.2.5. Selection of ES cell clones

One day before isolating ES-cell colonies, 24-well plates with feeder cells were prepared. The plates with transfected ES-cells were washed twice with PBS, and the cells were left in the second PBS wash during picking. All visible ES cell colonies to be picked were marked on the bottom of each plate with a marker pen by holding plate up to light. A P200 pipette set to 8 μ l and 1-200 μ l filter tips were used to pick individual colonies. First, the colonies were slightly dislodged with the pipette tip, then the drug-resistant ES cell clones were picked and transferred to a well of a 96-well plate. After picking 24 clones, 75ul trypsin/EDTA were added to each well, 10-20 pipetting cycles were used to generate single cell suspension by using a multichannel pipettor, then 75ul ES medium were added to each well and mixed. One half of the ES cell suspension were transferred into 24-well feeders and the other half were used for PCR screening. The same procedure was repeated until all clones in good shape had been isolated.

2.2.2.6. Preparation of ES cells for blastocyst injection

Three days prior to injection, the frozen ES cells were thawed in 24-well plates with feeder cells, and then the ES cells were expanded from 24-well to 6-well plates. The ES cells in 6-well with small compact colonies that were in log phase of growth were selected, the medium was removed and ES cells were washed with PBS twice; trypsin/EDTA were added and incubated at 37 °C for 2 min, then medium was added and ES cell aggregates were disrupted by pipetting 10 times. The cell suspension was transferred into 2 fresh 6-well and incubated at 37 °C for 45 min (feeder sediment). The supernatant (fraction1) was carefully collected, then the ES cells in 6-well were rinsed with 1ml medium, and the cell suspension was carefully transferred to a new Eppendorf tube (fraction2), the well was rinsed again with another 1ml medium and the ES cell suspension (fraction3) was collected. The ES cells from all three fractions were pelleted and resuspended in 100 µl injection medium (ES medium +LIF+20mM HEPES). ES cells from fraction 2 were used for blastocyst injection, ES cells from fraction1 and 3 were saved for backup.

2.2.2.7. Production of chimeric mice

Recombinant ES cell clones were microinjected into 3.5-day old blastocysts obtained from C57BL/6 female mice by the Heidelberg University Transgenic Facility. The microinjected blastocysts were transplanted to pseudo-pregnant foster females. Pups were born 17.5 days later. The coat color of pups was examined 6-10 days after birth for patches of agouti fur. Each male chimera was mated with two C57BL/6 female mice every 1-2 weeks when they were sexually mature (6-8 weeks old). One pregnant female mouse was housed per cage. Pups were weaned at 21-day old and separated from their mother.

2.2.3. Immunocytochemistry, immunohistochemistry and immunoelectron microscopy methods

2.2.3.1. Primary culture of hippocampal neurons for immunocytochemistry

Hippocampal neurons were isolated from mouse E17 embryos. Embryos were taken out of the uterus and kept in ice-cold PBS, 10 mM glucose buffer. Embryo heads were cut off and the skull opened to take out the brain. The hippocampus was separated from the cortex. Hippocampi were incubated in papain solution for 15 min at 37 °C. After digestion, the tissue was washed 2 times in plating medium (10% (v/v) FCS, DMEM). Cells were dissociated by trituration with pipettes for several times. The cell suspension was centrifuged for 5 min at 800 rpm, then the cell pellet was resuspended in Neurobasal medium supplemented with B27. Cells were plated onto glass-coverslips precoated with 1.5 µg/ml poly-ornithine. 40,000 cells /well were plated and incubated for 3-4 weeks at 37 °C. Every week, 1/3 of the culture medium was replaced by fresh medium.

2.2.3.2. Immuno-staining and confocal microscopy

For immunocytochemistry, neurons grown on coverslips were fixed with 4% PFA, 4% sucrose in PBS for 15 min at R/T, washed 3 times with PBS, then permeabilized for 15 min with ice-cold 0.1% (v/v) TX-100 in PBS at 4°C. After washing, coverslips were blocked for about 30 min at R/T or overnight at 4°C with 2% (w/v) bovine albumin and 5% (w/v) normal goat serum in PBS. After blocking, coverslips were transferred into a dark moist chamber and incubated with primary antibodies for at least 8 h at 4 °C. After three washing steps with PBS for 30 min, secondary antibodies, previously diluted in blocking solution, were added to the coverslips for 45 min at R/T in the dark. After washing, the samples were mounted in Mount media and dried at R/T. Images were acquired using a Leica TCS-SP confocal laser-scanning microscope equipped with 40x and 63x objectives.

2.2.3.3. Preembedding immunoelectron microscopy

Knock-in mice and wild-type (8-weeks-old) littermates were deeply anesthetized and sacrificed by cervical dislocation. Hippocampi were dissected out from the mouse brains and immediately immersion-fixed in a fixative containing 4% (v/v) paraformaldehyde, 0.05% (v/v) glutaraldehyde, and 0.75% (w/v) picric acid in phosphate buffer (PB, 0.1 M, pH 7.6) for 2 h. After washing with PBS, the hippocampi were embedded in agar and sectioned on a vibratome into 60 μ m section. Then the vibratome sections were cryoprotected in 10%, 20%, 30% (w/v) sucrose for 1 h each, and frozen and thawed twice in liquid nitrogen to increase the penetration of immunoreagents. For preembedding immunoelectron microscopy, the sections were blocked for 2 h in 10% (v/v) normal goat serum, 1% (w/v) BSA in PBS and then incubated with mGluR7a antibody (1:200, 1:400 and 1:1000 dilution in 2% NGS, 1% BSA, 0.05% Na-azide in PBS.) for 3 days at 4 °C. After washing with PBS, the sections were incubated for 2 h with biotinylated goat anti-rabbit IgG (1:100, Vector Labs). After rinsing with PBS, section were transferred to a solution containing avidin-biotinylated peroxidase complex (ABC, diluted 1:100 in TBS, Vector Labs) for 1 h at room temperature. After washing twice with PBS and twice with 0,05 M Tris-HCl, pH 7.4, Peroxidase was visualized with 0.05% (v/v) DAB using 0.01 % H₂O₂ as substrate for 8 min. The staining reaction was stopped by washing the sections in Tris-HCl and PBS. The sections were then postfixed in 2.5% (v/v) glutaraldehyde in cacodylate buffer, pH 7.4 (2 h at 4 °C), and washed with double-distilled water, followed by silver intensification to provide particulate appearance of peroxidase products (Sassoe-Pognetto et al., 1994). After washing, the sections were treated with 0.5% OsO₄ in cacodylate buffer for 30 min, washed in PBS and contrasted in 2% uranyl-acetate for 2 h. After dehydration in ethanol, they were embedded in Epon resin (Fluka, Taufkirchen, Germany). After polymerization of the resin, serial ultrathin section were cut and stained with uranyl acetate and lead citrate. Two brains of each genotype were used for sample preparation, and three blocks from each mouse were cut for immunoelectron microscopy.

2.2.3.4. Immunohistochemistry

Adult mice were sacrificed, and their brains were dissected out and frozen on dry

ice. The cryostat sections were immediately prepared at thickness of 15 μm . The sections were fixed in 4% (w/v) PFA/4% (w/v) sucrose for 30 min, then washed with PBS twice. Sections were permeabilized for 20 min with 4% goat serum/0.5% Triton X-100 in PBS, then blocked with PBS/10 % (w/v) goat normal serum for 3 h at R/T. Sections were incubated overnight at 4 °C with the primary antibody. After rinsing the sections with PBS, they were incubated 2 h with the secondary antibody coupled to a fluorescent chromophore (ALEXA Fluor 488 (green)). Thereafter the incubation steps after the addition of the secondary antibody were performed in dark. After rinsing in PBS, the slides were coverslipped and imaged. The specificity of labelling in all staining reactions was confirmed by the absence of mGluR7a labeling upon omission of the primary antibody.

2.2.3.5. NISSL Staining of cryostat sections

Cryostat sections were fixed in 4% (w/v) PFA and washed in PBS, and then stained for 5-8 min in cresyl violet (0.5% (w/v) in 70mM Na-acetate buffer, pH 3.9). The dye was rinsed off with demineralised water and the sections were incubated for 0.5-1 min in 70% ethanol. The sections were destained under the microscope with 90% ethanol with 1-2 drops glacial acetic acid until the brain tissue but not the nuclei were destained. After dehydration with 100% ethanol for 1 min then for 2 min with 100% Isopropanol, the sections were placed under a hood and incubated in Xylol for 2 min and covered with Permount (caution: no air bubbles). For drying, the sections were left under the hood overnight until all Xylol had evaporated.

2.2.4. Electrophysiology methods

2.2.4.1. Cerebellar granule cell culture and electrophysiological recordings

Primary cultures of cerebellar neurons were prepared from wild-type or mGluR7a knock-in mice, as previously described (Bertaso et al., 2006). Briefly, 8 day-old mice were decapitated, and the cerebella dissected and mechanically dissociated

in DMEM:F12 medium (1:1, Gibco) supplemented with 30 mM glucose, 2 mM glutamine, 13 mM sodium bicarbonate, 5 mM HEPES, pH 7.4, 10% semi-synthetic calf serum (Biowhittaker, Verviers, Belgium), antibiotics and KCl (25 mM). Cells were then plated at a density of $3\text{-}5 \times 10^5$ cells/dish on 35 mm dishes coated with poly-L-ornithine. Half volume of Petri dish was replaced by culture medium containing 5 mM KCl 48 hours before electrophysiological recordings.

Cultured cerebellar granule neurons were used at 9-10 DIV, for whole-cell recordings in the patch-clamp mode, at room temperature. The recording pipettes had a resistance of 3-5 MW when filled with the following medium: 140 mM KCl, 10 mM HEPES, 10 mM D-glucose, pH 7.2, osmolarity 300 mosm. Cerebellar neurons were continuously perfused with the following external medium: 140 mM NaCl, 2 mM CaCl_2 , 3 mM KCl, 10 mM HEPES, 10 mM D-glucose, 10 μM glycine, 10 μM bicucullin, pH 7.4; osmolarity 330 mosm. The membrane potential was held at -65mV and spontaneous EPSCs (sEPSCs) were recorded through an Axopatch 200B amplifier (Axon Instruments; Union City, CA, USA). Currents were filtered at 1 KHz, digitized at 3 KHz and continuously stored on a PC computer using the pClamp v.8 software of Axon Instruments. Data were then analyzed using the Clampfit routine of this software. Once a minimal sample of at least 120 events had been collected, the average frequency and amplitude of these events were measured on the total duration of the sample. L-AP4 was applied using a fast gravity perfusion system that allowed complete exchange of the cell environment in less than 50 ms.

2.2.4.2. Surgery and EEG recording

Mice were anaesthetized with 2 ml.kg^{-1} of a saline solution containing 40% ketamin (Imalgene 500) and 20% Xylazine (Rompun 2%) and placed in a stereotaxic frame using the David Kopf mouse adaptor. Five monopolar electrodes made of silver wires (d: 125 μm , Phymep, France) soldered on a male microconnector (Mateleco, France) were extradurally inserted in the skull, 2 on each parietal bone and one on the frontal bone as ground reference. The microconnector was fixed with dental acrylic cement. After surgery, animals were individually housed and maintained in a 12-h light/12-h dark cycle with food and water ad libitum. For the EEG recording, animals were put into individual Plexiglas boxes and their microconnectors were plugged to an EEG preamplifier box. The electrical activity recorded by deep and extradural electrodes

was filtered and recorded by a computer equipped with DasyLab software (DasyLab®). The EEG recording period was ≥ 80 min and performed in parallel with observation of the animal behaviour.

2.2.5. Animal behavioral assay methods

2.2.5.1. Open field test

The behavior of mGluR7 knock-in mice and wild-type littermates ($n = 8$ of each genotype) in the open field was examined using a brightly lit arena (50 cm \times 50 cm \times 50 cm, 200 lux). Mice were adapted to the test environment for 20 min and then placed in the center of the arena for 5 min. Movements of the mice in the arena were recorded using the VIDEOMOT video tracking system (TSE-Systems, Bad Homburg, Germany). Locomotor activity was monitored by measuring the total distance and speed of the animals during the test. The ratio of the distance traveled in the center vs. the periphery of the arena were evaluated as a measure of anxiety.

2.2.5.2. Elevated plus-maze test

The elevated plus-maze was used to further assess anxiety and the exploratory behavior of the mGluR7 knock-in mice ($n = 12$ per genotype). The arena consisted of a plus-shaped maze with two arms of 25cm that were closed by high side walls and two open arms without walls. The maze was located 40 cm above the table surface. Mice were placed on the open arm of the maze and were allowed to explore the maze freely for 10 min. Movements were analyzed using VIDEOMOT video tracking system (TSE-Systems, Bad Homburg, Germany). Mice were considered to be in the open region when all four paws were located on the open portion of the maze. The time spent in the open arms was used as a measure of anxiety.

2.2.5.3. Tail flick test

Pain sensitivity to acute thermal stimuli was assessed by tail flick test. The animal was gently constrained and the tip of its tail was placed above an infra-red heat source (TSE-Systems, Bad Homburg, Germany) that applied a heat stimulus with linear increasing intensity to the tail. The time taken by the animal to flick its tail was recorded. For each animal, the response was monitored three times at distinct positions of the tail.

2.2.5.4. Acoustic startle response and prepulse inhibition

Acoustic startle response and prepulse inhibition of startle were assessed using a standard startle chamber (TSE-Systems, Bad Homburg, Germany) and 10 different trials: acoustic startle pulse alone (100 dB), prepulse trials with 70-, 80-, 85- or 90-dB stimuli presented either alone or preceding the pulse, and one trial in which only the background noise (60 dB) was presented to measure the baseline movement. The amount of PPI in the prepulse plus pulse trials was expressed as a percentage of the startle response in the pulse alone trial.

2.2.5.5. Barnes maze task

Twenty males of the mGluR7 knock-in mouse line (mutant and wild type: n = 10 each) were assessed on the spatial version of the Barnes maze. The Barnes circular maze, a white platform (122 cm in diameter), was elevated 90 cm above the floor. Forty holes, 5 cm in diameter each, were located 5 cm from the perimeter, and a black plastic escape tunnel was placed under each of the holes, which was connected to the home cage of the animal. One training trial was performed before the first day of testing. To this end, the mouse was placed in the center of the maze and covered with a 15 cm high black start chamber for 2 min. Immediately after removing the start chamber, mouse was guided by the investigator to enter the

escape tunnel and then to the cage. One min after this training trial, the first test session started. At the beginning of each session, the mouse was placed in the center of the maze in the black start chamber for 2 min. After removing the start chamber, the mouse was allowed to explore and escape the maze. The session ended when the mouse entered the escape tunnel or if not successful, the mouse was guided after 5 min to enter the escape tunnel. When the mouse entered the escape tunnel, the mouse was allowed to reach the home cage and the trial was ended for this day. During each trial, the tunnel was always located underneath the same hole, which was randomly determined for each mouse. The mice were tested once every day until they met the defined criterion (4 out of 5 sessions with two or fewer errors). The testing ended after 32 sessions. The search strategies (serial random and spatial) were defined as described elsewhere (Bach et al., 1995) .

3. Results

3.1. Generation of mGluR7a knock-in mice

The development of gene targeting technology (Thomas and Capecchi, 1987; Melton, 1994) has made it possible to produce genetically modified mouse models for determining gene functions in the brain. Gene targeting approaches and the application of site-specific recombinase technology provide investigators with the opportunity to engineer genes in the mouse that will allow for the deletion, insertion, inversion, or exchange of chromosomal DNA with high fidelity (Branda and Dymecki, 2004). The ability to modify expression of specific genes in mice has revolutionized the field of molecular neuroscience. There are two principal types of mouse models that can be created, knock-out and knock-in mice. Knock-out mice carry a gene mutation introduced into the genome by a natural biological process called homologous recombination, in which the endogenous gene in mouse embryonic stem (ES) cells gene is replaced by DNA that disrupts gene function. The targeted ES cells will be used to produce chimeras and further knock-out mice. Using the same method, knock-in mice are generated to contain a specific mutation (deletion, substitution etc.) within the targeted gene that results in a protein with

altered gene function. For both knock-out and knock-in, a targeting vector has to be assembled that contains sequences of genomic DNA homologous to the chromosomal integration site, the mutant gene or exons, the selection cassettes for positive and/or negative selection, and a plasmid backbone. In this work presented, the “Replacement –type ” targeting vector was used to generate the knock-in mice which carry the specific mutation at the genomic locus of metabotropic glutamate receptor 7a (mGluR7a).

To generate mGluR7a knock-in mice, a mutation has to be correctly introduced into the mouse mGluR7 genomic locus; therefore the genomic organization of mGluR7 must be known and genomic clones must be obtained for constructing the targeting vector. The rapid progress of the Mouse Genome project has provided ample genome sequencing information, and many genomic BAC clones are commercially available. The mouse mGluR7a gene details can be found at the following website: <http://www.ncbi.nlm.nih.gov/genome/guide/mouse>. Briefly, the gene is located on mouse chromosome 6 near the region Chr6:110611375-111533007 bp, and the gene’s ID at Mouse Genome Informatics is MGI:1351344.

In order to identify BAC clones suitable for constructing a targeting vector, the mouse mGluR7a cDNA sequence was used to blast and search mouse genomic sequence database:

<http://www.ncbi.nlm.nih.gov/genome/seq/BlastGen/BlastGen.cgi?taxid=10090>.

Among all clones screened, one particular BAC clone RP23-391F16 was selected because it contained exon10 and its surrounding region. Exon10 encodes the PICK1 binding domain in the C-terminal region of mGluR7a, and the mutation disrupting the PICK1-mGluR7a interaction was introduced precisely into exon10.

The BAC clone RP23-391F16 was ordered from BACPAC resources center, children’s hospital oakland and its sequence can be found in the database. To confirm that this BAC clone contained sufficient genomic sequence for targeting vector construction, an initial PCR analysis was performed, which showed that exon10 and its surrounding sequence were intact within the BAC clone (data not shown). Based on the sequence of clone RP23-391F16 available in the database, the exon10 containing genomic fragment spanning 9.8 kb of genomic sequence was subcloned into pBluescript-SK by Bgl II digestion. This 9.8 kb genomic

sequence was further characterized by restriction mapping and sequencing (Figure 5) and used for the construction of the targeting vector.

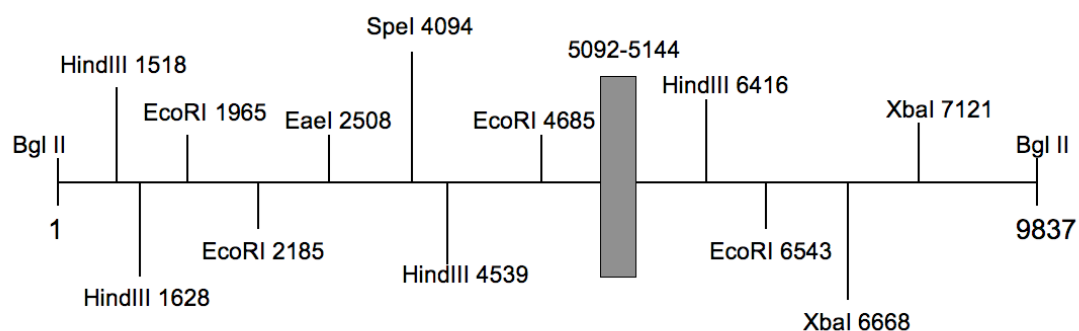


Figure 5. Restriction map of the exon10 containing 9.8 kb genomic fragment used for targeting vector construction. Several restriction sites are indicated, and the grey bar represents exon10 which encodes the PICK1 binding motif.

3.1.1. Gene targeting strategy

The mGluR7a-PICK1 interaction site has been mapped and the last three amino acids (-leucine-valine-isoleucine) of the C-terminal region of mGluR7a are crucial for the interaction with PDZ domain of PICK1(EI Far et al., 2000). Substitution or deletion of last three amino acids abolished the mGluR7a-PICK1 interaction (Boudin et al., 2000). Based on this, the strategy of the gene targeting was designed to mutate the PICK1 binding motif (-LVI) to triple alanine (-AAA). This mutation had to be introduced into embryonic stem (ES) cells and then targeted ES cells would be used to generate a knock-in mouse in which mGluR7a-PICK1 interaction should be abolished. Because the PICK1 binding motif (-LVI) is located in the exon10 of mGluR7 genomic locus, all gene targeting work was based on the surrounding regions of exon10 as illustrated in Figure 6.

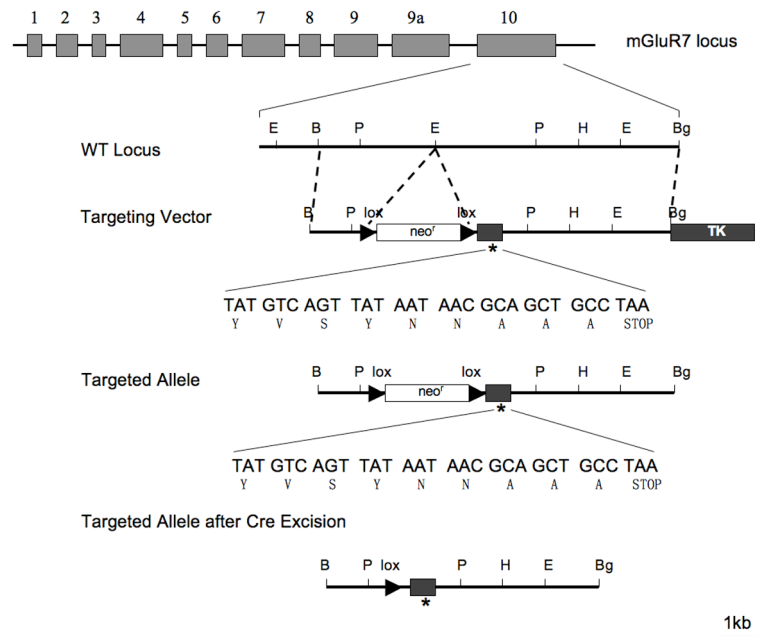


Figure 6. Strategy for the generation of mGluR7a knock-in mouse. Homologous recombination at the exon10 region of mGluR7 genomic locus. The triple alanine mutation was introduced into targeted allele, note the presence of the mutation before and after the Cre excision of the Neo cassette. E: EcoRI, B: BamHI, Bg: Bgl II, P: PvuII, H: HindIII, Lox: LoxP sequence, Neo: neomycin resistance cassette, TK: Herpes Simplex Virus Thymidine kinase cassette.

In this strategy, the gene targeting vector contained a positive selection cassette (Neo), a negative selection cassette (TK), and two homology regions (5' and 3') which were placed upstream and downstream of the positive selection cassette. The neo cassette was removed at the ES cell level. If successful, homologous recombination should introduce the triple alanine mutation into mGluR7a locus and thereby disrupt the mGluR7a-PICK1 interaction. The functional consequences of the disruption of this interaction can then be studied in detail.

3.1.2. Assembly of gene targeting vector

The plasmid backbone which was used for the construction of the targeting vector was pEasyflox. Both the neomycin cassette and the HSV-TK cassette in pEasyflox

serve as selection marker, but only the neomycin cassette is flanked by loxP sequences. A flow diagram for constructing the gene targeting vector is illustrated in Figure 7, the construct was verified by DNA sequencing before ES cells transfection.

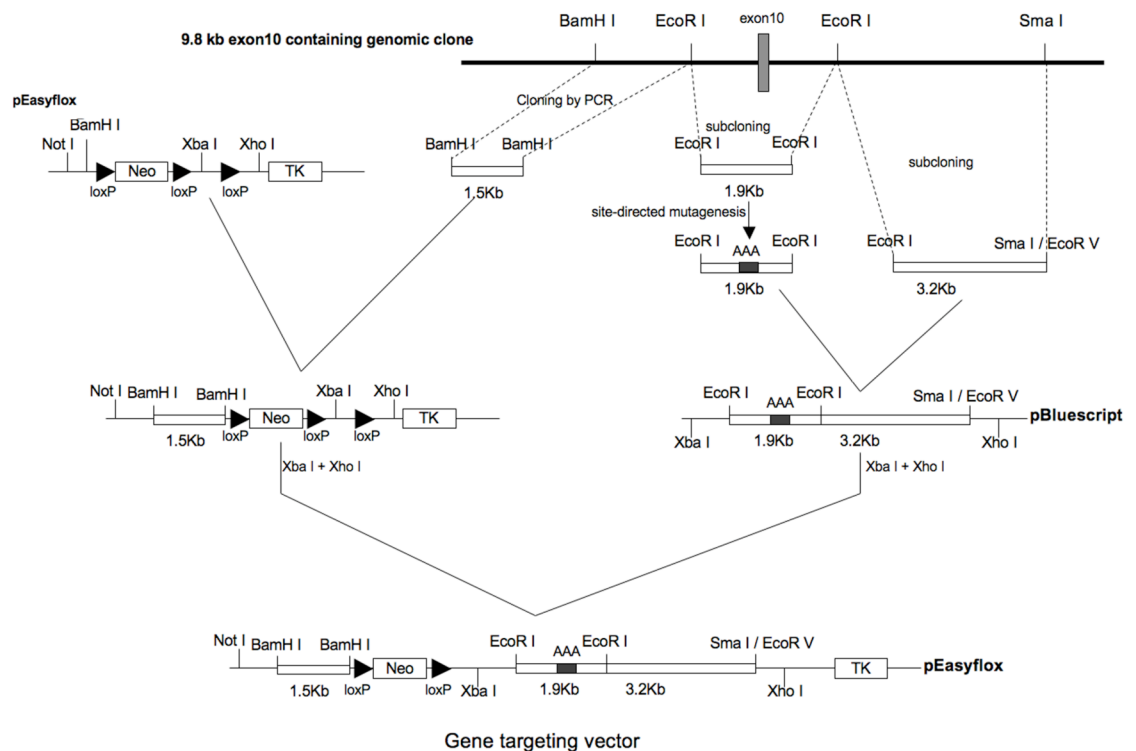


Figure 7. Construction of the gene targeting vector. In the final construct, the target mutation (three alanine codons) was introduced by site-directed mutagenesis, the Neo cassette was flanked by two loxP sequences.

Briefly, the targeting vector was constructed in the following steps:

1. Amplification of the 1.5 kb 5' short homology region from the initial 9.8 kb genomic fragment by PCR and insertion into pEasyflox by BamHI site.
2. Isolation of the 1.9 kb fragment containing the PICK1 binding motif by EcoRI digestion of the initial 9.8 kb genomic fragment followed by subcloning into pBluescript-SK, and then replacement of the last three amino acids codons (LVI) by three alanine codons via site-directed mutagenesis (Stratagene Quickchange Mutagenesis Kit). See Figure 8 for the design of the target mutation.

3. Further subcloning 3.2 kb fragment (right after the 1.9 kb fragment) by EcoRI + SmaI digestion of the initial 9.8 kb genomic fragment and ligated to pBluescript-SK (cut with EcoRI/EcoRV).
4. Isolation of the mutant 1.9 kb fragment (which carry the AAA mutation) by EcoRI cutting and ligation to a 3.2 kb fragment at the EcoRI site in pBluescript-SK, resulting in the 5.1 kb 3' long homology region.
5. Isolation of the 5.1 kb long homology region (with mutation) by cutting with XbaI and XhoI and ligated to XbaI and XhoI restriction site in pEasyfloX + short homology region.

The final construct could be linearized by Not I for gene targeting in ES cells.

Mutagenesis primers

5'-GTATGTCAGTTATAATAACGCAGCTGCCTAACCTGTTCCATCCC-3'
 5'-GGGATGGAACAGGTTAGGCAGCTGCGTTATTATAACTGACATAC-3'

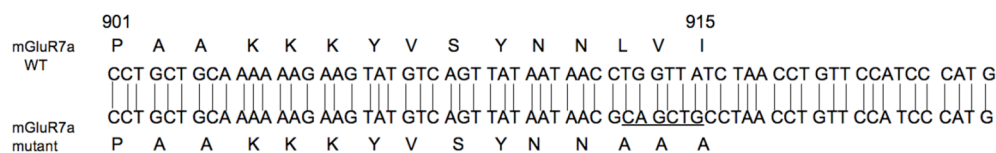


Figure 8. Introduction of the triple alanine mutation in Exon10 of mGluR7. The mutation was introduced into exon10 of mGluR7 using the mutagenesis primers indicated. As a result, in the mutant mGluR7a protein, the last three amino acids were substituted by triple alanines. Note that a new restriction site, Pvu II (underlined), occurred naturally after introduction of the mutation, which was used in the screening of the ES clones and the identification of the knock-in genotype.

3.1.3. Electroporation of ES cells and identification of homologous recombination events

For the generation of the knock-in mice, the E14 (129/OLA) embryonic cell (ES) line was used. This ES cell line can efficiently generate germline chimeras after blastocyst injection due to an increased survival rate of blastocysts in pseudopregnant mothers as compared with other types of ES cells. To maintain the ES cells in an undifferentiated state, they were cultured on the feeder layer of inactivated mouse primary fibroblasts in the presence of recombinant leukaemia inhibitory factor (LIF) in the medium. The E14 ES cells were electroporated at passage 9 with linearized targeting vector and grown for nine days under double selection of G418 and FIAU. When the surviving ES colonies were large enough for subcloning and expansion, those with undifferentiated morphology were selected for further analysis. In total, 148 clones were picked and trypsinized gently in a 96-well plate and then ES medium was added for resuspension of the cells. Half of the ES cell resuspension was plated on a 24-well feeder plate for clone expansion, the other half was collected and immediately subjected to PCR analysis in order to screen for correct homologous recombination events. The PCR- positive ES clones were expanded on the 24-well plates until confluent, trypsinized and resuspended in ES medium. 70% of the resulting cell suspension was frozen in the liquid nitrogen by adding ES cell freezing medium, and the remaining 30% of the cell resuspension was plated on gelatinized 24-well plates for the preparation of ES cell genomic DNA. This genomic DNA was later used for Southern blot analysis. For PCR screening of ES clones, primer 7 and 8 (see materials and methods) were used for the amplification of the target fragment. The primer 8 binding site was exactly located at the beginning of the neomycin cassette, while primer 7 extended to outside of the short homology region, therefore the primer 7/8 combination detected only correctly targeted ES clones. Among all the ES clones isolated, 4 clones were identified to have undergone homologous recombination correctly (Figure 9). The PCR screening of the homologous recombination events was further confirmed with Southern blot analysis. The Southern blot probe was amplified (primer 9 and 10) by using original 9.8 kb genomic fragment as PCR template. This probe was located outside of the genomic region present in the

targeting vector, and therefore could be used as an external probe. Southern blot analysis of ES cell genomic DNA using BglII digest revealed that this probe hybridized to a 9.8 kb WT, or a 5.4 kb mutant fragment (Figure 9). Thus, both PCR and southern results indicated that homologous recombination had occurred in the targeted ES clones, suggesting that the triple alanine mutation was introduced into exon10 of one of the mGluR7 alleles.

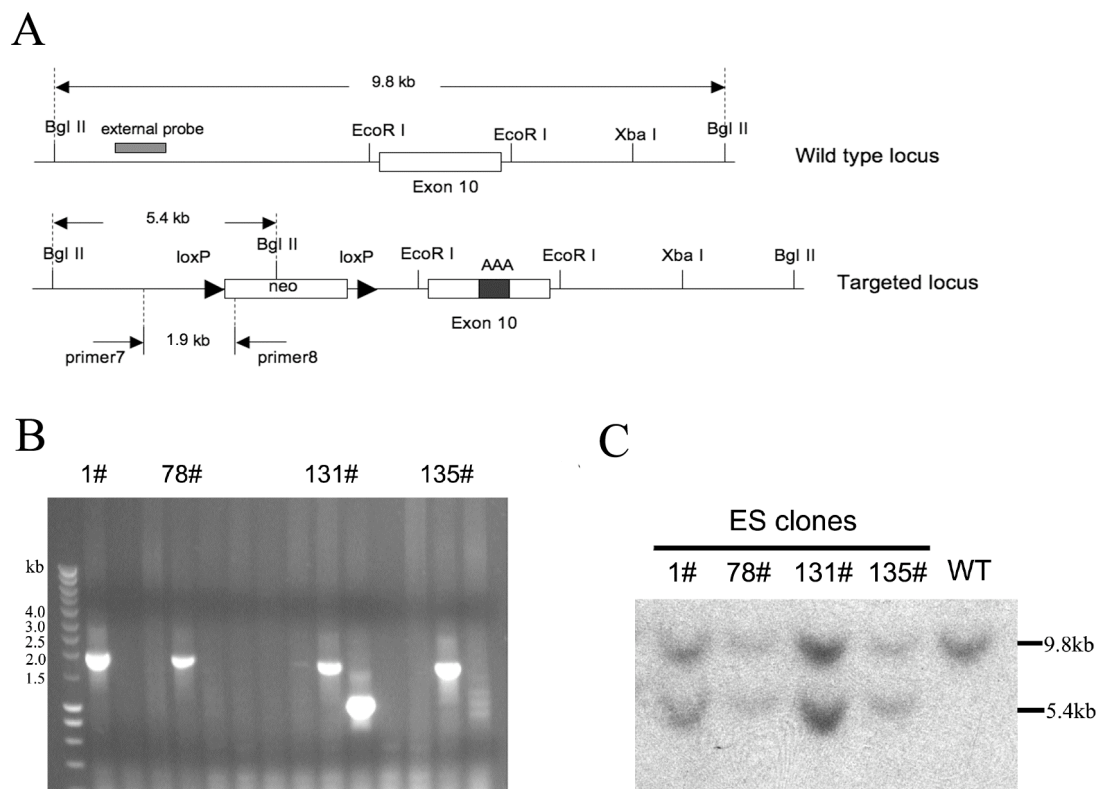


Figure 9. Identification of homologous recombination events by PCR and southern blot analysis. **A.** Strategy of PCR and Southern blot for screening of homologous recombination events. The specificity of PCR screening was determined by the position of primer8, and also note the position of 5' external probe. **B.** PCR screening of ES clones with the combination of primer 7 and 8. Correct homologous recombination yielded a 1.9 kb band which extended over the short homology region. **C.** Southern blot analysis of BglII-digested ES cell genomic DNA using the 5'-external probe. The wild-type allele gave a 9.8 kb band and the targeted mutant allele produced a 5.4 kb band.

3.1.4. Cre recombinase mediated deletion of the Neo resistance cassette in ES cells

It should be pointed out that upon introduction of the triple alanine mutation into exon10 of mGluR7 locus (described in 3.1.1), the neomycin resistance (Neo) cassette was also inserted simultaneously. It is now widely accepted that selection marker cassettes should be removed after homologous recombination (Muller, 1999). One reason is that the expression of neomycin cassette is driven by a very strong promoter (PGK-neo cassette), which may interfere with the expression of neighboring genes. Furthermore, the presence of the neomycin cassette may also influence the splicing efficiency and stability of transcripts. Hence, the mutant phenotypes may be due to effects exerted by the selection marker and not caused by the mutation itself. Here, removal of the Neo cassette was achieved by using the Cre-LoxP system. This system is frequently used for the generation of genetically modified animals. Cre is a 38 kDa recombinase protein from bacteriophage P1, which cuts at loxP-tagged sequences (Kuhn and Torres, 2002).

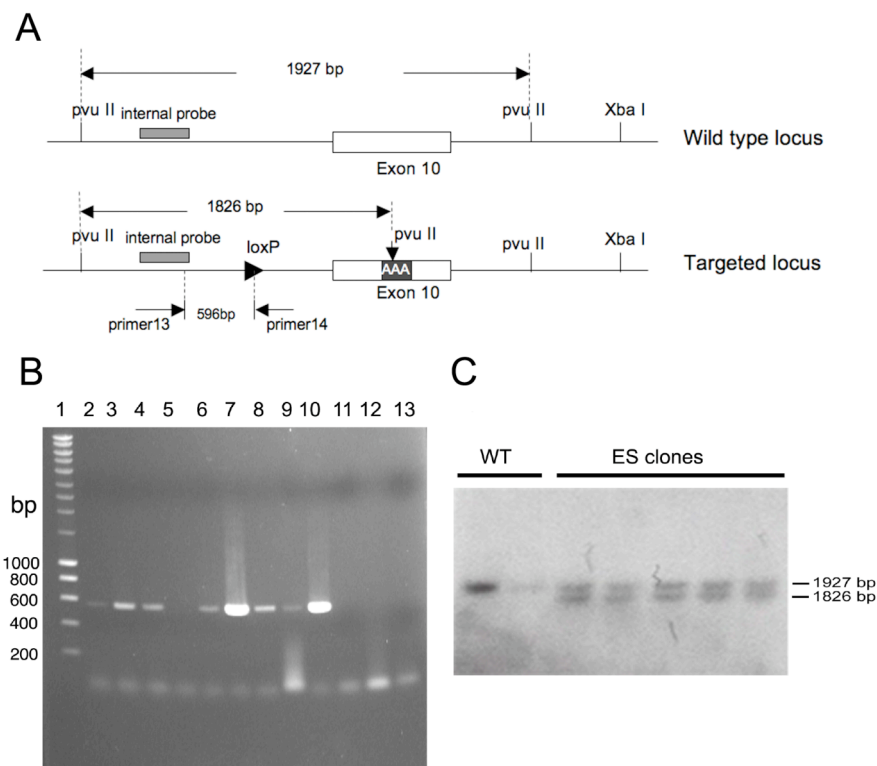


Figure 10. PCR and Southern blot analysis of Cre-recombinase mediated deletion of neomycin resistance cassette. **A.** Strategy for PCR and Southern blot confirmation of removing Neo cassette. **B.** Representative PCR screening of ES clones after excision of the neomycin cassette using the combination of primers 13 and 14. Lane 1, molecular marker; Lane 2, 3, 4, 6, 7, 8, 9, 10, PCR-positive clones (596 bp band), indicating correct deletion of neomycin cassette; Lane 5, 11, 12, 13. PCR-negative clones. **C.** Pvu II digested genomic DNA was hybridized with an internal probe. The wild-type allele gave a 1927 bp band, the targeted allele produced a shorter fragment (1827 bp) due to the introduction of an extra Pvu II restriction site within the triple alanine mutation.

To remove the neomycin resistance cassette in ES cells, one targeted ES clone with correct homologous recombination was selected for expansion and transient transfection with the Cre expression plasmid pGK-Cre. After transfection and allowing for expression of Cre recombinase in the ES cells, 24 ES clones with homogenous morphology were picked and screened by PCR and Southern blot. This showed that 14 clones had undergone correct Cre-mediated excision of the neomycin cassette. For the PCR screening, primers 13 and 14 were used. Primer 14 covers a partial region of the LoxP sequence, and if the neomycin cassette was removed correctly, the combination of primers 13 and 14 yielded a specific 596 bp band (Figure 10B). The PCR screening results were further confirmed by Southern blot analysis; here, the Southern probe was amplified by PCR using the primers 11 and 12, and the initial 9.8kb genomic fragment as template. When hybridized to Pvu II-digested genomic DNA, this internal probe detected a 1927 bp wild type band, while the new PvuII restriction site at the triple alanine mutation resulted in 1826 bp band indicative of the targeted allele (Figure 10C).

After confirming proper excision of the neomycin cassette, another PCR analysis (primer 15 and 16) was performed to check whether the targeted triple alanine mutation was detectable after two rounds of selection and screening. Sequencing of the PCR products showed that the desired mutation was indeed present (data not shown).

3.1.5. Production of chimeric mice by blastocyst injection of ES cells

Production of chimeric mice by injecting embryonic stem cells into the cavity of a mouse blastocyst is a highly critical step in the generation of mutant mouse models. Chimeric mice resulting from the injected blastocysts will be composed of tissue derived from the inner cell mass of the host blastocyst as well as from the ES cells. It is possible that ES cells contribute to all cells of the chimeric mouse, including the germline cells. Commonly, chimeric mice are produced from ES cells derived from agouti 129/SV mice and host blastocysts harvested from black C57Bl/6 mice. This was also the case here. The injection of ES cells was done by Frank Zimmermann from the Centre of Molecular Biology, University Heidelberg. Two correctly targeted ES cell clones (mgr10, mgr14) were microinjected into blastocysts derived from C57BL/6 mice. The microinjected blastocysts were transplanted into pseudopregnant female mice. For one clone (mgr10), 6-7 cells were injected into each blastocyst; in total, 33 blastocysts were injected, and 3 recipient female mice were used. For another clone (mgr14), 32 blastocysts were injected (6-7 cells per blastocyst) and 3 pseudopregnant female mice were also used for blastocyst transplantation. The production of chimeras resulting from these microinjection of ES cells is summarized in Table 2.

Table 2. Summary of chimeric mice production from ES cell injection

ES cell clone injected	Offspring born	Pups dying shortly after birth	Chimeras generated
mgr10	13	5	3
mgr14	20	0	11

The offspring was examined for coat color when mice were 10 days old. Mice displaying >70% agouti coloring were supposed to likely have ES cell contribution to the germline. The ES cells used for injection and some of the chimeric mice generated are shown in Figure 11.

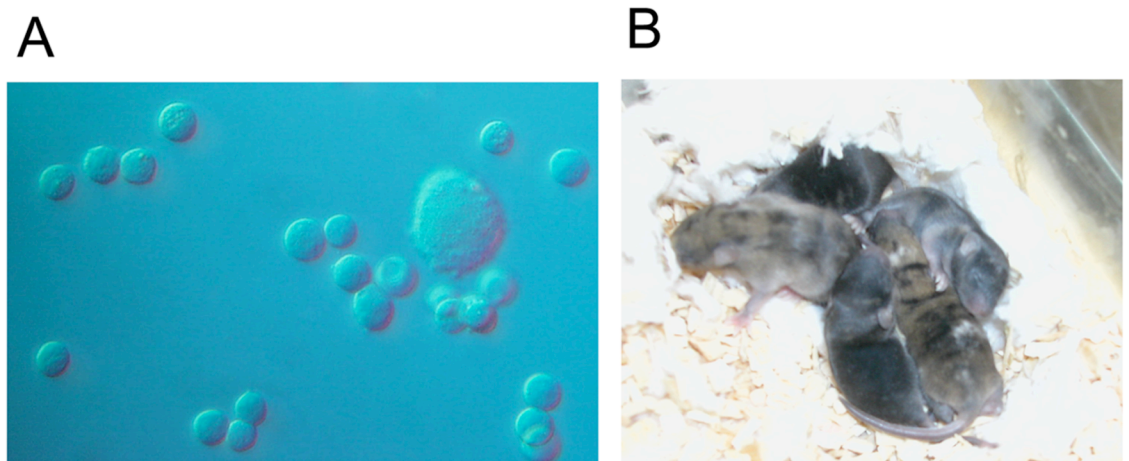


Figure 11. Production of chimeras by blastocyst injection of ES cells. **A.** Correctly targeted ES cell clones were selected for blastocyst injection; image shows representative ES cells prior to injection. **B.** Chimeric mice show the agouti coat color (light brown), indicating that chimeras have cells derived from recombinant 129/OLA ES cells.

3.1.6. Germline transmission of the mutation and generation of homozygous mutant mice

If chimeric mice carry germ cells derived from injected ES cells, Any targeted mutation introduced into the ES cells will be transmitted to the offspring. After breeding of the chimeric mice with C57BL/6 mice, if germline transmission was achieved, the offspring will have one allele from the ES cells, and its coat color will be all agouti. Non-germline transmitting mice will carry only alleles from C57BL/6 mice and will be all black. Since only one mGluR7 allele in these targeted ES cells was mutated, 50% of the agouti pups are expected to carry the mutated allele. Figure 12 shows that when the chimeric mice were bred with wild-type C57BL/6 mice, germline transmission of the PICK1 binding domain mutation (triple alanines)

was obtained in F1 generation mice, based on the agouti coat color of the offspring. To identify agouti pups carrying the mutated allele, F1 mice were genotyped by PCR (primer 15 and 16). For the PCR screening, the 3' end of the reversing primer 16 was exactly located at the triple alanine mutation, thereby yielding specific amplification products (582 bp). These PCR-positive mice should be heterozygous for the mutation (mGluR7a^{+/AAA}).

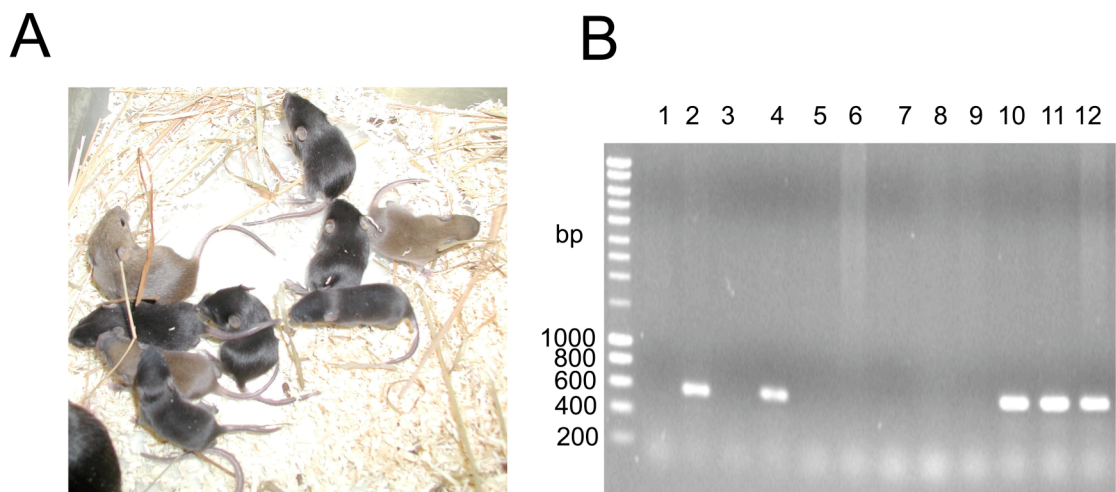


Figure 12. Generation of F1 mice with germline transmission of the triple alanine mutation. **A.** Breeding of chimeric mice with C57BL/6 mice resulted in F1 offspring with agouti coat color, indicating that germline transmission of the mutation had been obtained. **B.** PCR genotyping of F1 mice with primers 15 and 16. Lanes 2, 4, 10, 11 12 shows PCR-positive (582 bp) heterozygous mice Lanes 1, 3, 5, 6, 7, 8, 9 correspond to non-mutant mice among the F1 offspring.

The F1 heterozygous mice were then backcrossed to wild-type C57BL/6 mice for 6 generations to avoid effects of a mixed genetic background (129/OLA/C57BL/6) on phenotype analysis. The backcrossed heterozygous mice were interbred to generate homozygous mice. Offspring from breeding heterozygotes was born at Mendelian ratios, with 25% wild type (+/+), 50% heterozygotes (mGluR7a^{+/AAA}), and 25% homozygous mice (mGluR7a^{AAA/AAA}). The genotyping of the offsprings was performed by PCR (Figure 13A) with the primers 21 and 22, and also confirmed by Southern blot analysis (Figure 13B).

In order to assess whether mGluR7a^{AAA/AAA} mice expressed mGluR7a at normal level in the brain, total brain mRNA was prepared from mice brain and hybridized with a specific mGluR7a probe (generated with primers 19 and 20 from the mGluR7a cDNA). β -Actin was used as loading control. The Northern blot shown in Figure 13C indicated that the mGluR7a mRNA level in wild-type and KI mice were similar.

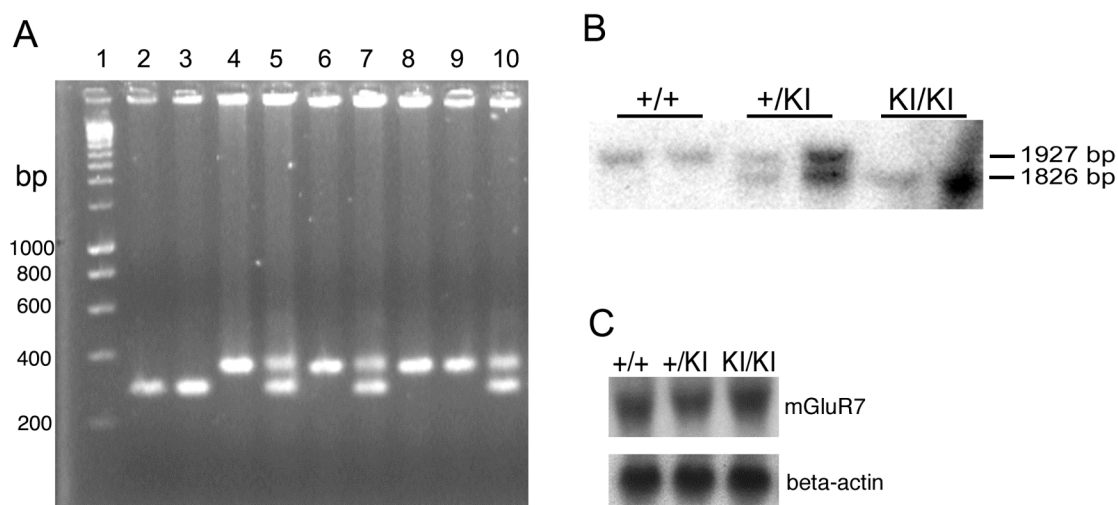


Figure 13. Generation of mGluR7a knock-in homozygous mice (mGluR7a^{AAA/AAA}) and northern-blot analysis. **A.** PCR genotyping of offspring from heterozygote breedings revealed 3 different mouse genotypes. Lane 1: molecular marker, Lanes 2, 3: wild-type (+/+); Lane 4, 6, 8, 9: heterozygous KI mice (mGluR7a^{+/AAA}); Lanes 5, 7, 10: homozygous KI mice (mGluR7a^{AAA/AAA}). **B.** Confirmation of the genotype by Southern blot analysis. The internal probe hybridized to two bands in heterozygous mice (1927 bp and 1836 bp), and only one specific band in wild-type and homozygous mice, respectively. **C.** Northern-blot analysis showed that there was no alteration in mGluR7a mRNA expression level in the KI mice.

In order to check whether the knock-in mice (mGluR7a^{AAA/AAA}) indeed express the triple alanine mutation designed to disrupt mGluR7a-PICK1 interaction, the intracellular region of the mGluR7a mRNA was amplified by RT-PCR with primer 17 and 18. Sequencing of the RT-PCR products showed that in homozygous KI mice

the PICK1 binding motif (LVI) was correctly replaced by three alanine residues, while the respective coding sequence was unchanged in the wild-type littermates (Figure 14B, C).

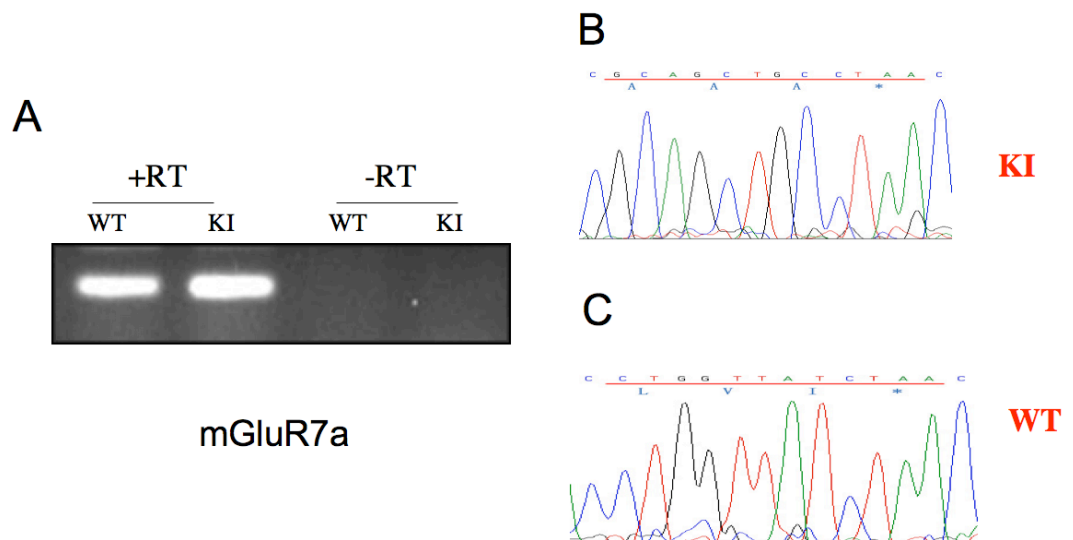


Figure 14. Confirmation of PICK1 binding domain mutation in homozygous KI mice.
A. Amplification of the intracellular domain coding region of mGluR7a mRNA by RT-PCR. Note that there is no PCR product in the control experiment without reverse transcription. **B.** Sequencing of RT-PCR products from KI mouse shows successful substitution of LVI codons by AAA codons. **C.** Normal mGluR7a sequence in the wild-type littermates.

3.2. Biochemical, anatomical and electrophysiological characterization of homozygous KI mice

It is generally thought that mGluR7 is one of the most important mGluR subtypes in regulating CNS function (Dev et al., 2001). The first mGluR7-related mutant animal model was the mGluR7 knock-out mouse (Sansig et al., 2001b). The analysis of this mouse model has suggested a primary role of mGluR7 in the negative modulation of physiological glutamate release and possibly the etiology of epilepsy. In this thesis, a new mutant mouse model was generated, in which the mGluR7a-PICK1 interaction was disrupted. The phenotypic characterization of the mutant mice was performed carefully, but it turned out that the homozygous KI mice were

born viable and showed no abnormality in size and gross appearance as compared with their wild-type littermates. The mutant mice bred normally and well groomed and a Mendelian ratio of inheritance was observed among the offspring produced by intercrossing heterozygous animals.

For further biochemical characterization of the mutant mice, mGluR7a protein expression and distribution in the brain were examined. Furthermore, the synaptic targeting and clustering of mGluR7a and mGluR7a mediated G-protein dependent signaling events were investigated in detail in the homozygous KI mice.

3.2.1. Expression of mGluR7a in homozygous KI mice

As mentioned above, the Northern blot analysis had revealed that mGluR7a gene transcription was not altered in the homozygous KI mice (Figure 13C). However, significant difference in mGluR7a expression was found at the protein level. The mGluR7a protein was detected by Western blotting in the membrane preparations from mouse brain. Quantification of the band intensities indicated that protein levels of mGluR7a in the homozygous KI mice was reduced by 40% and also slightly reduced in heterozygous mice (Figure 15A, B). In contrast, expression levels of PICK1, a strong binding partner of mGluR7a, were not different between mutant and wild-type littermates, indicating that PICK1 expression was not down-regulated by the triple alanine mutation. Since all group III mGluRs (mGluR 4, 6, 7, 8) share high sequence identity and similar pharmacological properties, it was interesting to learn whether the expression levels of other group III mGluR members was altered upon introducing triple alanine mutation. Here, mGluR4 was selected for Western blot analysis. No difference was found between KI and wild-type mice (Figure 15 A, B).

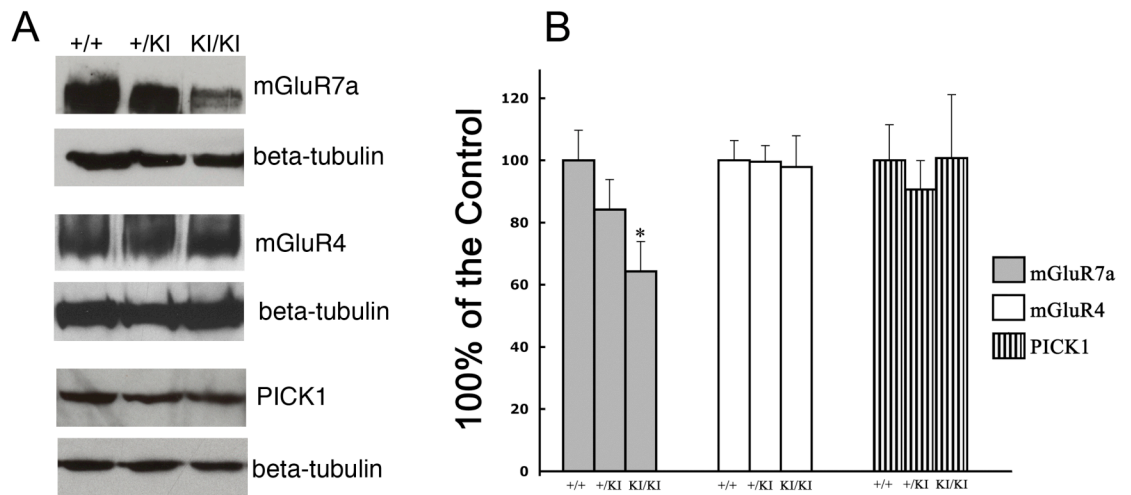


Figure 15. Expression of mGluR7a, mGluR4 and PICK1 in the brain of heterozygous and homozygous KI mice. **A.** Western blot detection of mGluR7a, mGluR4, and PICK1 in brain extracts prepared from wild-type, heterozygous and homozygous littermates, β -tubulin was used as control. Protein expression levels were normalized to the internal standard β -tubulin. **B.** Quantification of the Western blot results. Note significant reduction of mGluR7a expression in homozygous KI mice ($P < 0.05$, student's t test), while no difference was found for mGluR4 and PICK1 expression between wild-type and KI animals. The results represent means \pm SEM, $n=8$ mice for each genotype.

3.2.2. Reduced mGluR7a–PICK1 interaction in homozygous KI mice

Previous work has shown that the PICK1 PDZ-domain binding motif is located in the last three amino acids residues (LVI) of the mGluR7a C-terminal region, deletion or substitution of these residue results in abolishment of PICK1 binding to mGluR7a (El Far et al., 2000). To test whether PICK1 still interacts with mGluR7a in homozygous KI mice, a co-immunoprecipitation experiment was performed using a PICK1 antibody. The mGluR7a–PICK1 immuno-complex was robustly precipitated from wild-type brain extracts, while it was strongly reduced in mutant mice (Figure 16 A, B). This indicates that the PICK1–mGluR7a interaction is efficiently disturbed in the mutant mice.

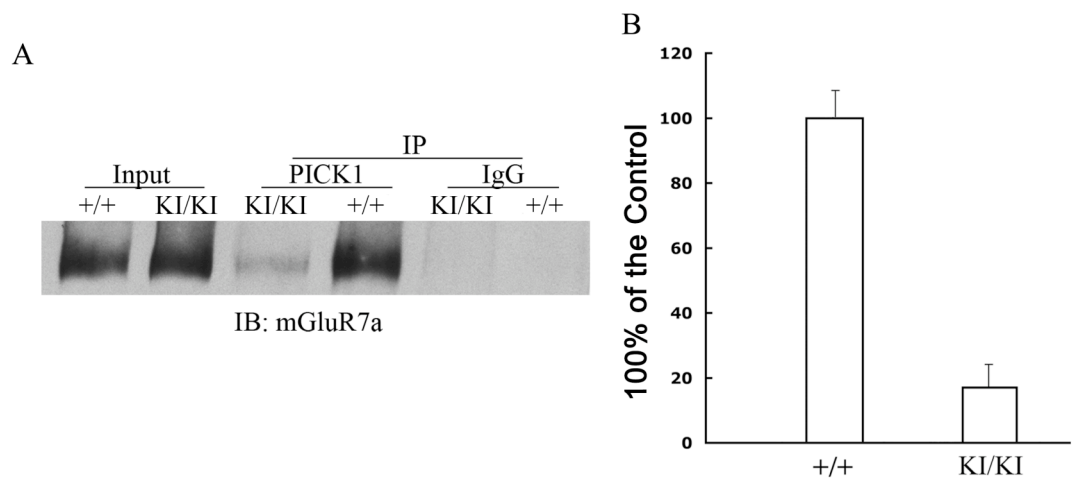


Figure 16. Co-immunoprecipitation of mGluR7a and PICK1 from brain extracts of wild-type and KI mice. **A.** PICK1 antibody and control IgG were used for co-immunoprecipitation, followed by Western blot analysis with the indicated antibodies. Note that reduced amount of mGluR7a were pulled down from KI brain extracts. **B.** Quantification of the immuno-blotting results showed that the mGluR7a-PICK1 interaction was strongly reduced in KI mice. The same experiment was repeated 4 times, and the results are shown as means \pm SEM.

3.2.3. Homozygous KI mice show normal gross brain anatomy and mGluR7a distribution

To examine whether the triple alanine mutation introduced into the mGluR7 locus may have effects on mouse brain anatomy, Nissl staining was used to analyze the morphology of the brain in sagittal sections, KI mice showed no detectable abnormalities in brain cytoarchitecture as compared with the wild-type controls (Figure 17 A, C). Similarly, immunohistochemical staining of mGluR7a with the mGluR7a antibody revealed no major difference in general distribution of mGluR7a between wild-type and mutant animals (Figure 17 B, D). For both Nissl staining and mGluR7a antibody staining, the data were obtained for the whole brain, but for the reason of simplicity, only data from representative hippocampus region was shown. To sum up, these results show that the triple alanine mutation at the C-tail of

mGluR7a produced no detectable alteration in brain anatomy and mGluR7a expression pattern.

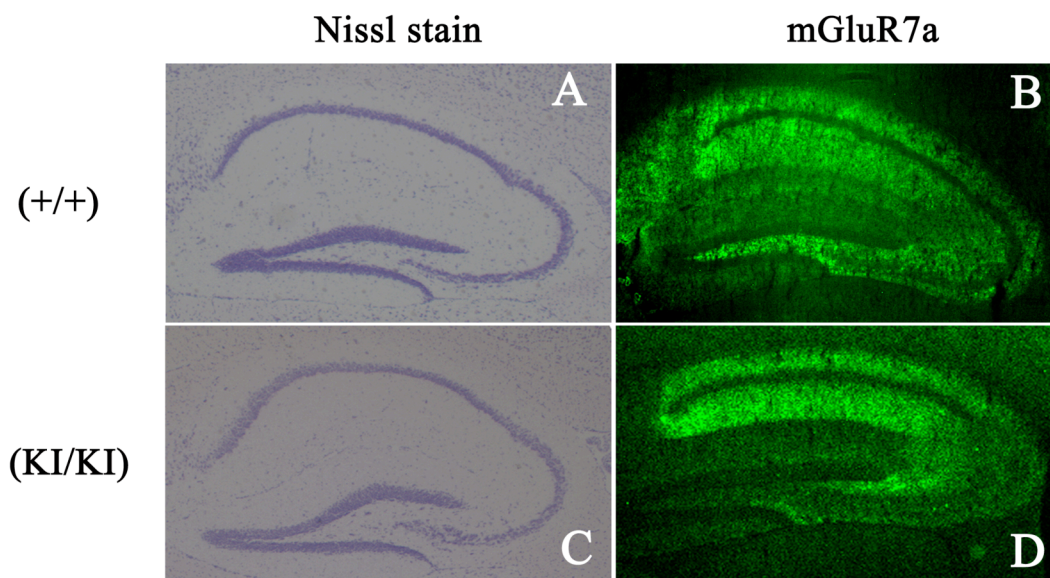


Figure 17. Normal cytoarchitecture and mGluR7a staining in the hippocampus of KI mice. (A, C). Nissl staining of sagittal brain sections showed no differences in hippocampus anatomy between wild-type and KI mice. **(B, D).** The distribution of mGluR7a was detected by immunohistochemistry. Antibody staining revealed no major differences between wild-type and KI mice .

3.2.4. Synaptic targeting and localization of mGluR7a in homozygous KI neurons

mGluR7a has been previously shown to localize presynaptically in cultured hippocampal neurons (Stowell and Craig, 1999). PICK1 is thought to serve as an adaptor protein which organizes presynaptic portions at synaptic contacts (El Far and Betz, 2002). Boudin et al. (2000) reported that a mutant mGluR7a protein which lacks the PICK1 binding domain at its C-terminal region is targeted to the axonal membrane efficiently, but not clustered at the axon terminals (Boudin et al., 2000). Here, I analyzed the synaptic localization of mGluR7a in hippocampal

neurons prepared from the homozygous KI mice. Immunofluorescence labeling showed that mGluR7a clustering was unchanged in mutant neurons. They displayed the same punctate distribution as wild-type neurons in primary cultures. Furthermore, the mGluR7a punctate staining colocalized with the presynaptic marker synapsin 1 in both wild-type and mutant neurons (Figure 18). These data indicate that PICK1 binding to the C-terminal region of mGluR7a is not essential for its membrane targeting and synaptic localization.

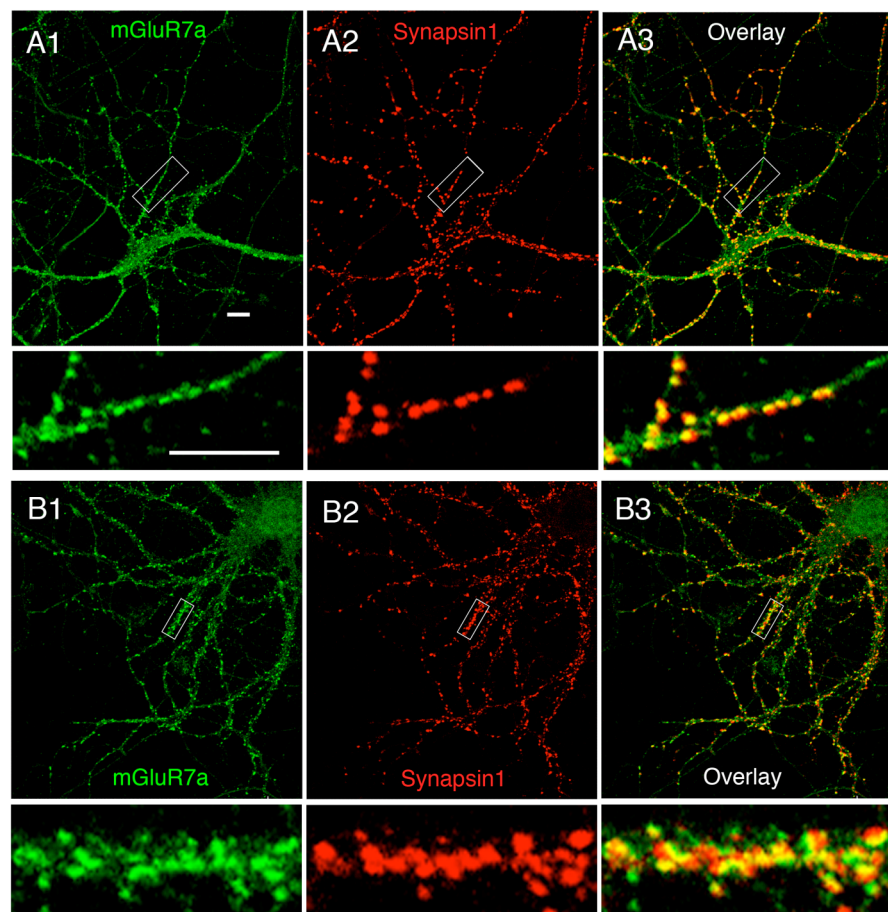


Figure 18. Immunostaining of mGluR7a in wild-type and KI hippocampal neurons. A. Immunofluorescence labeling of mGluR7a and the presynaptic marker synapsin 1 in cultured wild-type hippocampal neurons. Note that the mGluR7a and synapsin1 immunoreactivities colocalize. **B.** The colocalization of mGluR7a and synapsin1 is unchanged in hippocampal neurons KI mice. Scale bar, 10 μ M. White boxes in the upper panels (A1-A3, B1-B3) define enlargements shown in the lower panels.

3.2.5. Ultrastructural localization of mGluR7a by immunoelectron microscopy

To finally examine the localization of mGluR7a at hippocampal synapses in mGluR7a KI mice ultrastructurally, immunoelectron microscopy experiments were performed on hippocampi of 8 week-old mouse using a mGluR7a antibody raised against the C-terminal region. The detection of mGluR7a was carried out using a highly sensitive method combining peroxidase staining with silver intensification and gold toning on the CA-3 region of mouse hippocampus. Consistent with other published data (Shigemoto et al., 1996; Dalezios et al., 2002), the mGluR7a immunoreactivity in the CA-3 region of wild-type animals was mostly concentrated along the presynaptic active zone in nerve terminals (Figure 19 A, B). In addition, some immunoperoxidase reaction product was found to diffuse into the presynaptic compartment, resulting in the labeling of synaptic vesicles. An identical labeling pattern was observed in hippocampal sections prepared from mGluR7a KI mice (Figure 19 C, D). Thus, the synaptic distribution of mGluR7a was not altered by disruption of the mGluR7a-PICK1 interaction.

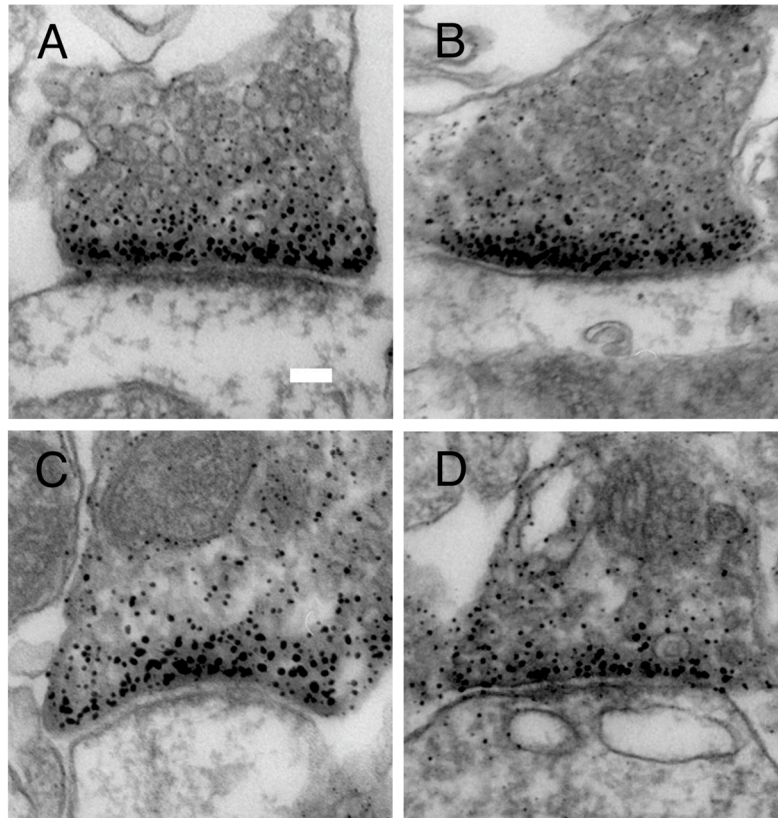


Figure 19. Immunoelectron microscopy reveals similar presynaptic localization of mGluR7a in wild-type and KI mice. A-B. mGluR7a staining signal is mainly found at the presynaptic membrane in the CA-3 hippocampus region of wild-type mice. In addition, some labeling of synaptic vesicles was seen, probably due to reaction product diffusion. C-D. Presynaptic localization of mGluR7a was not altered in KI mice. Scale bar, 0.1 μ m

3.2.6. Loss of mGluR7a mediated presynaptic inhibition in homozygous KI mice

Both the immunocytochemistry and the immunoelectron microscopy results indicate that the membrane trafficking and synaptic targeting of mGluR7a are not impaired in KI mice. To test whether mGluR7a mediated G-protein signaling and synaptic transmission are changed in KI mice, electrophysiological methods were used. It is well documented that activation of mGluR7 depresses synaptic transmission at a variety of central synapses (O'Connor et al., 1999; Perroy et al., 2002; Losonczy et al., 2003). This aspect of mGluR7 function was tested here by using cerebellar

granule cell culture as a model system. It has to be mentioned that these experiments were performed by Dr. Laurent Fagni from Institute of Functional Genomics, CNRS UMR5203, Montpellier France.

In brief, cerebellar granule cells were prepared from 7 day-old wild-type and KI mice. The cells were allowed to differentiate for 9-10 DIV. Spontaneous excitatory postsynaptic currents (sEPSCs) were then recorded at a membrane potential of -60 mV in the absence and presence of L-AP4 (Figure 20A). L-AP4 (400 μ M) was applied for 7-10 min. Quantification of the recorded events demonstrated that L-AP4 dramatically reduced the frequency, but not the amplitude of EPSCs in wild-type neurons. However, this inhibitory effect of L-AP4 on the recorded EPSCs was not observed in knock-in neurons (Figure 20B), indicating that the mGluR7a (AAA) did not respond properly to agonist stimulation. Therefore, it seems that mGluR7 mediated presynaptic inhibition requires an interaction with PICK1. Taken together, these results corroborate the previous conclusion (Perroy et al., 2002) that PICK1 has an essential role in mGluR7a G-protein dependent signaling, although it is not required for the synaptic targeting and localization of the receptor.

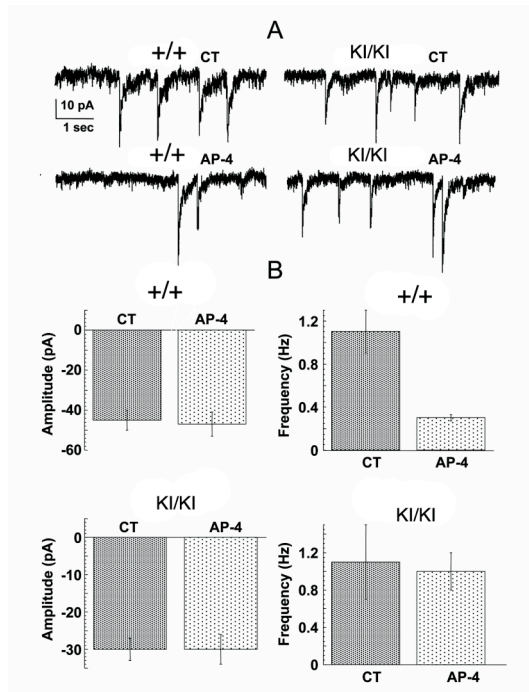


Figure 20. mGluR7 stimulation inhibits spontaneous EPSCs in wild-type but not KI cerebellar neurons. A. Recording of spontaneous EPSCs from both wild-type and knock-in cerebellar granule cells in the absence (CT, upper trace) and presence (lower trace) of L-AP4. **B.** L-AP4 treatment decreased the frequency, but not the amplitude of the recorded EPSCs in wild-type neurons, whereas inhibitory effects of L-AP4 were absent in KI neurons.

3.2.7. Increased susceptibility of the mGluR7 KI mice to convulsant drugs

It has been reported that mGluR7 knock-out mice showed the increase in threshold sensitivity for the convulsant pentetrazole (PTZ) (Sansig et al., 2001a). We wondered whether the disruption of the mGluR7-PICK1 protein complexes and the associated signalling got involved in this hypersensitivity to convulsant drugs. In order to test that, we collaborated with Drs. Federica Bertaso, Joël Bockaert, and Mireille Lerner-Natoli from Institute of Functional Genomics, CNRS UMR5203, Montpellier France. They performed the experiments using mGluR7a KI mice aged 9 weeks or more. All analysis of the data were based on the detailed description made by Weiergraber *et al.* on the different phases of the symptoms developed by mice injected with pentetrazole (Weiergraber et al., 2006). According to their grading, phase 1 corresponds to an "absence-like, non-convulsive state, with reduced motility and

typical prostrated position of the animal; phase 2 shows partial clonus of the head, vibrissae and/or forelimbs; phase 3 implies a generalized myoclonus of the four members and the tail and vocalisation; this phase can develop into typical "running fits"; phase 4 corresponds to a generalized tonic-clonic seizure with tonic extension of the four limbs; this phase is eventually followed by death of the animal, due to respiratory insufficiency. Examples of electroencephalogram (EEG) traces recorded in wild-type mice administered with 70 mg/kg PTZ are shown in Figure 21A. Different doses of pentetrazole were tested on n = 6 or 7 mice per genotype and per dose and the results are summarized in Figure 21C. At the lowest dose of PTZ (40 mg/kg) all the wild-type animals entered phase 1, with typical prostration and spindles appearing on the EEG recording. At the same dose, four KI mice showed partial myoclonus typical of phase 2, whereas two animals died as consequence of a rapidly developing tonic-clonic seizures. At 50 mg/kg PTZ all wild-type animals entered phase 2, whereas all the KI mice showed at least a generalized myoclonus (phase 3), while 4 animals died of phase 4 seizures. We tested higher doses only on wild-type animals, to ensure that they were indeed able to develop clonic seizures. Overall, wild-type mice showed a greater resistance to PTZ than KI mice, with 80 mg/kg being necessary for all the animals to develop either phase 3 or 4 seizures. Moreover and opposite to the KI mice, all the animals survived the phase 4 and recovered within 30 minutes.

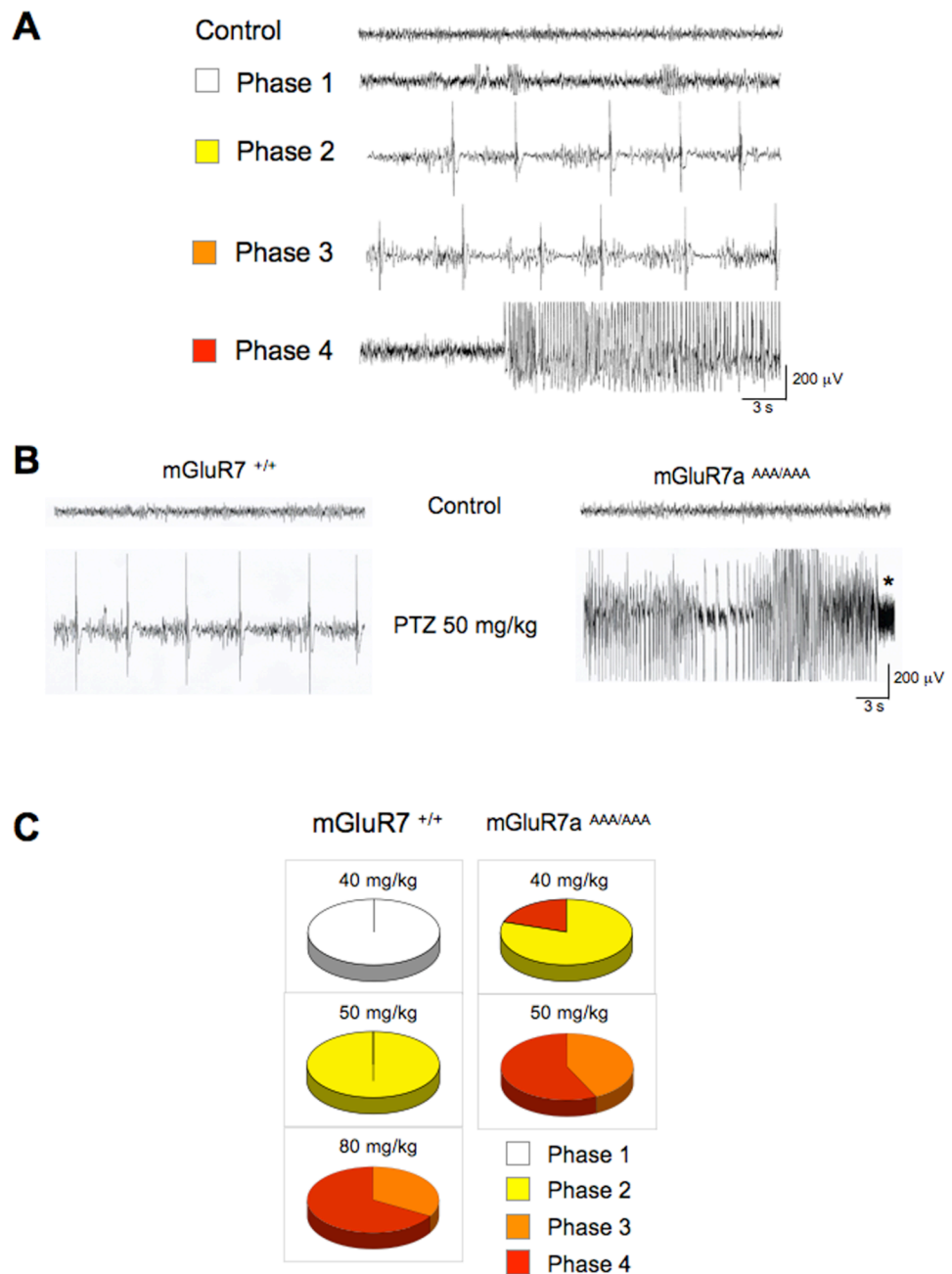


Figure 21. Increased susceptibility of mGluR7 KI mice to convulsant drugs. **A.** Example EEG recordings from wild-type mice injected with 70 mg/kg in the different PTZ-induced epileptic phases. **B.** Example EEG recordings from wild-type and KI mice treated with 50 mg/kg PTZ. Note KI mice have the greater sensitivity to PTZ. **C.** Percentage of animals in the different phases (see colour-coded legend) after intraperitoneal administration of the indicated doses of PTZ.

3.2.8. mGluR7a KI mice develop spontaneous absence-like seizures

After establishing that mGluR7a KI mice displayed hypersensitivity to convulsant drugs, we went further to check whether the KI mice develop any form of epilepsy phenotype. Dr. Federica Bertaso performed the surface electroencephalogram (EEG) recordings of the KI mice. Indeed, the mGluR7 KI mice showed spontaneous seizures that displayed similar characteristics to absence-like spike-and-wave discharges (SWD) (Figure 22A). These mice showed on average 28 ± 5 seizures over a 20 min observation period, each seizure having with a mean frequency of 7.7 ± 0.6 Hz and mean duration of 1.43 ± 0.04 s (Figure 22B, C). Notably, the KI mice displayed the behavioural arrest, associated to facial myoclonus and vibrissal twitching during the SWD. As the absence-like seizures should respond to anti- and pro-absence specific drugs (Manning et al., 2003), we tested commonly used anti-absence drug, ethosuximide, which reduces the severity of the seizures and Carbamazepine (CBZ) which is able to worsen absence epilepsy. The results showed that the seizures of KI mice have the same pharmacological profile as absence epilepsy described in human being and mouse (Figure 22 B, C). And also, the EEG recording demonstrated that the absence-like seizures appeared once the mice were adapted to a quiet and silent experimental environment. However, it is necessary to point out that no any other spontaneous epileptic events were observed for the KI mice, the absence seizures we found here are only visible on the EEG recording, therefore are well far from the classical myoclonic or tonico-clonic epileptic seizures. Nevertheless, these data indicated that alteration of the mGluR7a PDZ ligand motif is sufficient to develop absence-like seizures in the mouse.

The above experiments were carried out on mGluR7a KI mice aged more than 8 weeks. We also analysed the phenotype of younger KI animals and found that the spontaneous seizures were absent in mice younger than 5 weeks and present in the totality of the animals tested aged 9 weeks or more (Figure 22 D).

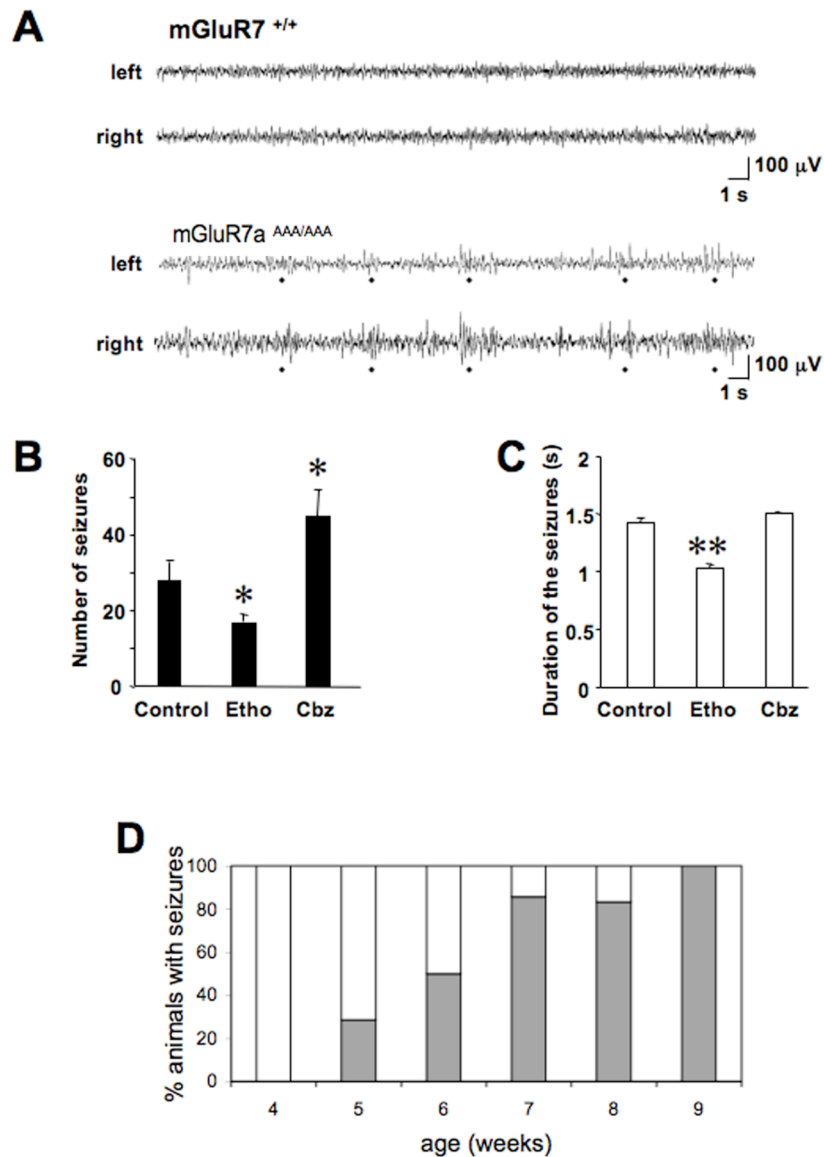


Figure 22. Absence –like seizures of mGluR7a KI mice. **A.** Comparison of cortical EEG recordings obtained from one wild-type mouse (top traces) and one mGluR7a KI mouse (bottom traces). **B-C.** Histograms of number of seizures and mean seizure duration over a 20 min period after drug treatment (* $p < 0.05$, ** $p < 0.01$, student's t test compared to control). **D.** Age-related development of the absence-like phenotype in KI mice. The plot represent the percentage of animals showing seizures for the total number of animals tested ($n = 6$ to 7 per age).

3.3. Behavioral analysis of mGluR7a KI mice

A variety of behavioral test strategies have been developed and extensively used for characterizing phenotypic changes of many different mutant mouse lines. Behavioral phenotyping is of prime importance for the analysis of targeted gene mutations. Here, different numerous commonly used mouse behavior test paradigms were used for studying the mGluR7a KI mice. The aim was to find out whether this mouse line has deficits in locomotion and emotional activity, pain sensitivity, startle response and spatial learning.

All animal experiments discussed below were subjected to institutional review and conducted in accordance with the veterinary authority of Germany. Age-matched (2-3 months old) and gender-matched (only male mice) mutant and wild-type littermates were used for all tests described below. Mice were housed individually in cages in temperature-regulated rooms with a 12-h light : 12-h dark cycle. All behavioral experiments were conducted during the light phase of the diurnal cycle.

3.3.1. Open field

The open field test is a relatively simple assay which is designed to measure several behavioral responses such as locomotor activity, hyperactivity and exploratory behavior. The open field test is also used as an assessment of anxiety-related traits (Dishman et al., 1988; Markel et al., 1989). Generally, mice tend to avoid brightly illuminated, novel and open spaces; so the open field environment acts as an anxiogenic stimulus and therefore can be used for the measurement of anxiety-induced changes in locomotor activity and exploratory behavior.

mGluR7a KI mice and wild-type littermates were subjected to the open field test at the same condition. Table 3 shows the summarized results of this test. All values are expressed as means \pm SEM. In the open field and exploration tasks, mGluR7a knock-in mice showed a tendency to cover less distance during the test. On the other hand, they spent slightly more time and traveled somewhat more distance in the center, suggesting that these mice maybe less anxious than wild-type animals.

However, these differences were not statistically significant. The anxiety-related traits were further studied using the elevated plus maze.

Table 3. Summary of open field test resultd for wild-type and mGluR7a KI mice

	mGluR7a ^{+/+} (n=8)	mGluR7a ^{AAA/AAA} (n=8)
Total distance traveled (cm)	2019 ± 333	1605 ± 280
Visits in center	19 ± 5	17 ± 2
% distance traveled in center	18 ± 3	20 ± 3
% time spent in center	12 ± 3	15 ± 3

3.3.2. Tail flick test

The tail flick test is a pain assay in which a mouse's tail is exposed to a heating device and the latency of the mouse to remove its tail from the heat is recorded. This latency is used as a measure to indicate neurological pain sensitivity (Harris et al., 1988; Hentall and Fields, 1988). mGluR7a KI mice and wild-type controls were subjected to this test, and no difference was observed between the genotypes (Figure 23). It seems that disturbance of the mGluR7a-PICK1 interaction does not interfere with the signaling pathways required for pain sensation.

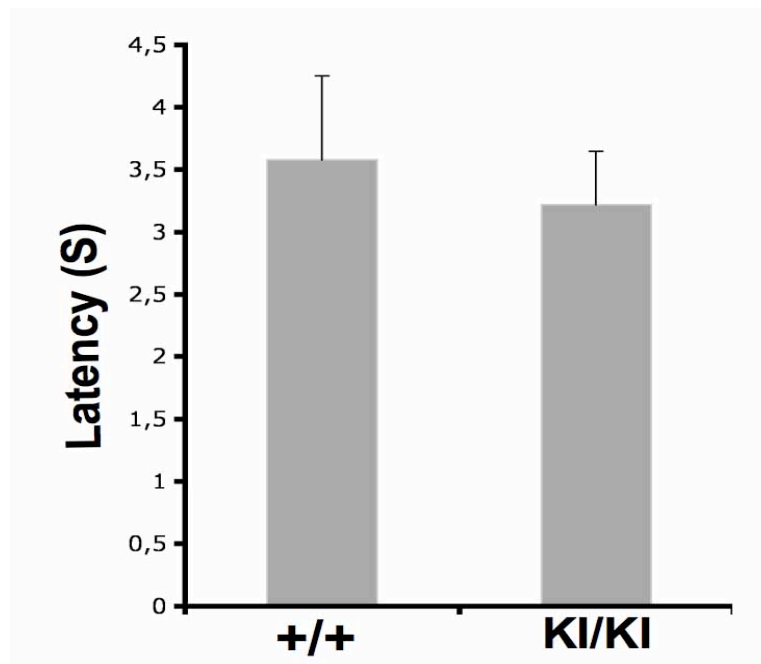


Figure 23. Tail flick test with mGluR7a KI mice and wild-type littermates. Tail flick latencies of mGluR7a knock-in mice did not differ from wild-type controls (n=8 each). Bars represent mean values \pm SEM.

3.3.3. Acoustic startle response and prepulse inhibition

The acoustic startle response (ASR) is a transient motor response to an unexpected stimulus. The response is determined by stimulus parameters such as intensity, rise time and duration. The acoustic startle reflex has been observed in many species (e.g. rats, mice and also humans). In rodents, the startle response is characterized by contractions of the major body muscles. General information about sensory-motor processing can be achieved from acoustic startle response experiments (Seaman et al., 1994; Storozeva and Pletnicov, 1994). As for prepulse inhibition (PPI), it is often used to measure sensorimotor gating in humans and animals (Arguello and Gogos, 2006). In response to a stimulus (pulse), the animal exhibits a quantifiable, reflexive startle response. If, however, a brief, low-intensity acoustic prepulse precedes the loud noise (pulse), the startle response is diminished. The magnitude of change is then expressed as percent PPI. PPI is

believed to reflect the ability to screen out (filter or gate) irrelevant environmental information. Studies have shown certain areas in the brain - the limbic system and the basal ganglia - are implicated in PPI.

The startle response experiments were performed for both mGluR7a KI and wild-type control mice. It was observed that KI and wild-type animals exhibited a stable response to the stimulus. A slightly, but not significantly, different startle amplitude, was observed between wild-type and mutants (Figure 24, A). mGluR7a KI mice showed a somewhat higher startle amplitude than the control mice. Different studies have implicated PICK1 as a susceptibility gene for schizophrenia (Hong et al., 2004; Fujii et al., 2006). Hence, there could be an association between mGluR7a-PICK1 pathway and schizophrenia. PPI is extensively used to study oversensitivity to stimuli in schizophrenic patients. Therefore, the PPI was also measured for mGluR7a KI and wild-type control mice. This revealed that no obvious defect in PPI for the mGluR7a KI mice (Figure 24, B). However, when increasing the intensity of the prepulse stimulus, the results of wild-type and mutant mice started to diverge; however, never a significant difference was reached (Figure 24, B). Taken together, the mGluR7a-PICK1 signaling pathways seem not to be significantly correlated with startle response and prepulse inhibition.

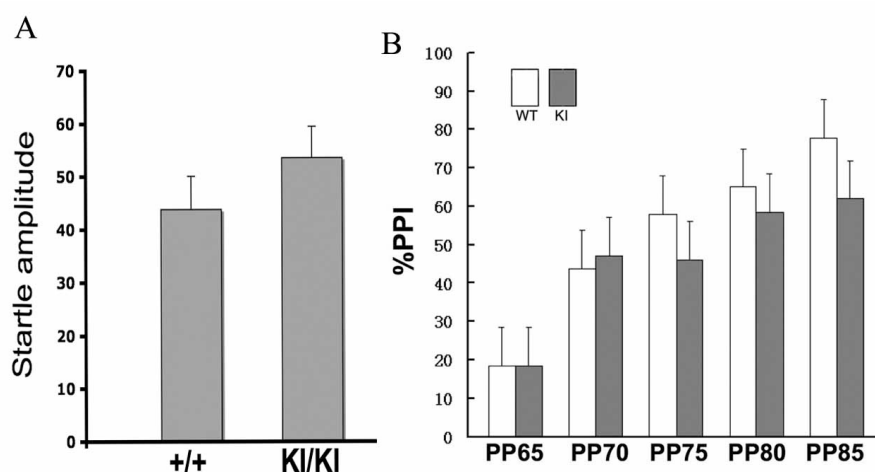


Figure 24. Startle response and PPI in wild-type and mGluR7a KI mice (n=12 per genotype). **A.** The indicated startle amplitudes were measured at the intensity of 100 dB. **B.** The PPI is measured as percent startle response to a 100-dB pulse for prepulses of the indicated intensities. Values are expressed as means \pm SEM.

3.3.4. Elevated plus-maze

The elevated plus-maze is widely used as an anxiety measurement and is based on unconditioned responses of mice to a potentially dangerous environment. A combination of maze height, luminosity and open space is assumed to induce fear or anxiety. The animal's anxious behavior is assessed by measuring the time spent in the open and closed arms. When placing mGluR7a KI mice and wild-type littermates in the elevated plus-maze, the performance of the animals revealed that the mutant mice were more active in exploring the maze than wild-type mice. Accordingly, a higher number of open arm entries were observed for the mutant mice. Notably, mGluR7a KI mice spent more time in the open arms than wild-type littermates (Figure 25A, B), suggesting that the mutation somehow is anxiolytic. Based on these observations, the mGluR7a-PICK1 interaction appears to be relevant in signaling pathways of fear and anxiety.

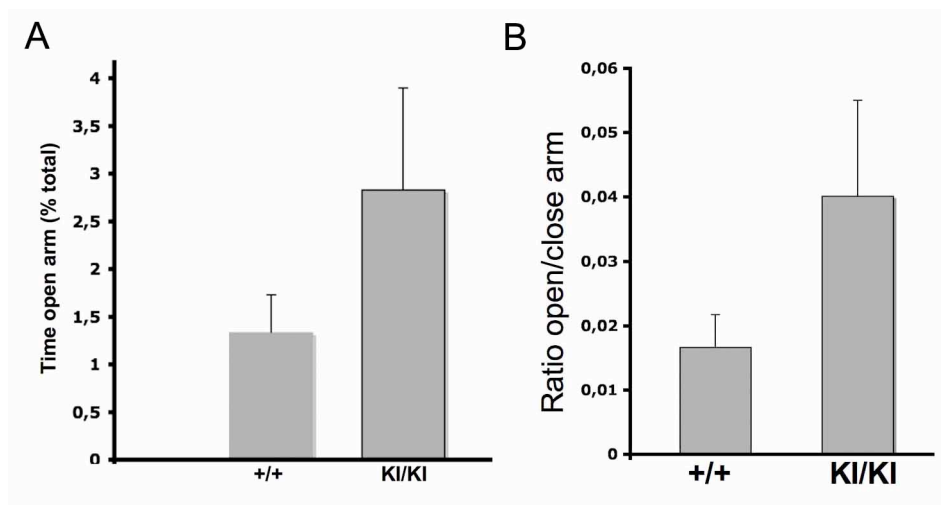


Figure 25. Elevated plus maze performance of mGluR7a KI and wild-type mice (n=12 per genotype). **A.** mGluR7a KI mice showed anxiolysis in this test, as indicated by spending more time in the open arms ($P=0.22$, student's t test). **B.** An increased ratio of open/closed arm as compared to wild-type mice ($P=0.17$, student's t test). Data are presented as means \pm SEM.

3.3.5. Barnes maze

The Barnes Maze is designed to disclose capacity of spatial learning and memory in rats and mice (Barnes, 1979; Bach et al., 1995). Upon exposure to the Barnes Maze, animals intend to escape from the brightly lit, open platform surface to a tunnel that is connected to a target box underneath the holes of the maze. During testing, the animal learns the spatial location of the particular hole which allows to escape from the surface of the maze to the target box. In general, the Barnes Maze is used to monitor the hippocampus-dependent long-term spatial memory of the animal.

When mice learn to perform in the Barnes maze, they use a fixed sequence of three search strategies: random, serial, and spatial. The strategies can be simply recognized, analyzed, and quantified. By seeing which strategies the animals use, one can determine whether an animal learns the task and thereby judge the animal's spatial memory capability.

Here, the mGluR7a KI mice and wild type littermates were tested on the spatial version of the Barnes circular maze. The results indicated that the mutant mice learned random, serial, and spatial search strategies as well as control mice (Figure 26, A, B, C). Both wild-type and mutant animals initially employed the random search strategy, spending more than half of the time using this strategy during the first 5 sessions. Upon further training, the mutant mice learned the serial, and spatial search strategies with similar speed as control mice. Finally, almost the same number of the mice acquired the task within the 32 sessions of the test (Figure 26, D). Therefore, we conclude that the mGluR7a KI mice are not defective in spatial learning. Apparently, the mGluR7a-PICK1 signaling pathways are not important for long-term learning and memory.

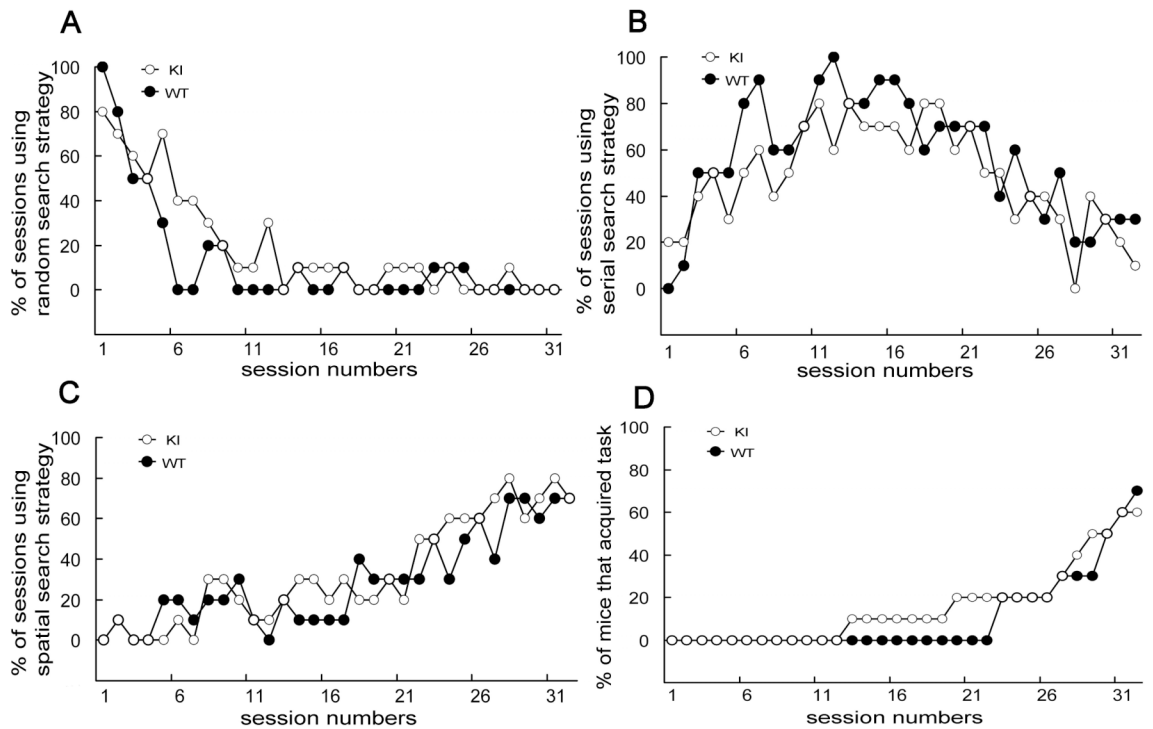


Figure 26. In the Barnes maze test, mGluR7a KI mice show a spatial learning performance similar to that of wild-type mice

Both mutant and wild-type mice employed random (A), serial (B) and spatial (C) search strategies. No learning deficiency was found for the KI mice. D. Percentage of mutant and wild-type mice acquired the task of the Barnes maze.

4. Discussion

In this thesis, the functional role of PICK1 in mGluR7 signaling and synaptic targeting was investigated by generating a knock-in mouse in which the mGluR7a-PICK1 interaction was disrupted. For gene targeting, mouse genomic DNA isolated from a BAC clone was used for the construction of a targeting vector which contained exon 10 of the mGluR7 gene. The bases encoding the three C-terminal amino acids of mGluR7a (-LVI) were mutated by site-directed mutagenesis to generate alanine codons (resulting tail sequence -AAA). The targeting vector was then introduced into mouse 129/OLA embryonic stem cells. Homologous

recombination events were confirmed by Southern blot analysis. Removal of the loxP-flanked neomycin cassette was achieved by transfection with the Cre-recombinase expression plasmid, and properly targeted clones were used for blastocyst injection to generate chimeric mice. Chimeras were backcrossed to C57BL6 mice, and the resulting heterozygous offspring was bred further to generate wild-type, heterozygous and homozygous mGluR7a knock-in mice. The presence of the mutation was confirmed by DNA sequencing, and then the mutant mice served as a model for studying the role of protein interaction at the mGluR7 C-terminus in glutamatergic signal transduction mechanisms.

4.1. Knock-in approach and the role of proteins interacting with C-terminal region of mGluR7

In this work, the PICK1 interaction site was mutated in the tail region of mGluR7a. Detailed analysis of the generated mouse line showed that the expression level of mGluR7a protein was reduced by 40%, which suggests interaction with proteins, like PICK1 might stabilize mGluR7a at the presynaptic membrane. The removal of PICK1 binding might enhance internalization of mGluR7a. Future investigations of this aspect might provide insights into the membrane recycling of mGluR7a. On the other hand, the triple alanine mutation introduced into the mGluR7a gene did not alter the brain anatomy and mGluR7a distribution. Co-immunoprecipitation confirmed the loss of mGluR7a-PICK1 interaction, this mutant mouse line therefore constitutes a reliable model for investigating mGluR-PDZ protein interaction *in vivo*.

Based on the analysis of mGluR7a knock-in mice described here, it becomes obvious that the same approach could be used to analyze the functions of other proteins interacting with C-terminal end of mGluR7. Proteins shown to interact with the C-terminus of mGluR7 can be classified into actin binding (Filamin-A, Tubulin), scaffolding (GRIP, PICK1) and signaling (syntenin, protein phosphatase 1, G_{βγ} subunits, calmodulin) proteins (O'Connor et al., 1999; El Far et al., 2000; Enz, 2002; Hirbec et al., 2002). So far, no clear function has been demonstrated for other mGluR7 interacting proteins. In fact, the generation of knock-in mice in which respective protein interactions are inactivated provides a very useful method for

studying their physiological roles, because the phenotype of the mice can be analyzed at many different levels. With additional functional studies on mGluR7 interacting proteins, the membrane trafficking of mGluR7 and the signaling cascades activated by this receptor will be understood more clearly. Respective progress should also create more options for testing new therapeutic targets, since protein interactions at mGluR7 are highly promising for drug discovery (Enz, 2007).

4.2. The role of PICK1 in the presynaptic targeting and localization of mGluR7a

PICK1 was first identified as binding partner for protein kinase α (PKC α) (Staudinger et al., 1995) and was therefore termed Protein Interacting with C-Kinase 1 (PICK1). PICK1 comprises a single PDZ domain which mediates the association with other proteins. In addition, it also contains other protein-protein interaction motifs, for instance, two coiled-coil motifs, which are involved in PICK1 dimerization. Recently, a new Bin–Amphiphysin–Rvs (BAR) domain was identified in PICK1 (Jin et al., 2006). However, little is known about the function of this BAR domain. At the C-terminal of PICK1, a glutamate-/aspartate-rich (E/D) acidic region (E/D motif) has been suggested to regulate PICK1-mediated synaptic localization and co-clustering of its interacting proteins. Besides mGluR7, PICK1 has been reported to interact with various membrane proteins, such as AMPA receptors (Xia et al., 1999), dopamine transporter (DAT) (Torres et al., 2001), and the ErbB receptors (Harrison and Owen, 2003).

As a single PDZ-domain containing protein, PICK1 is generally believed to act as a scaffolding protein, which is located at neuronal synapses and associates with many different proteins via its functional domains (Dev, 2004). Notably, PICK1 co-work with protein kinase C (PKC) and regulates the phosphorylation of many PICK1 interaction partners, thereby altering their synaptic clustering, and membrane recycling. The best-understood example of PICK1 function concerns its interaction with the AMPA receptors. Extensive work has shown that there is direct interaction between GluR2 subunit of AMPA receptors. It has been suggested that this interaction of GluR2 with PICK1 would allow to form an extrasynaptic pool of

calcium-impermeable AMPA receptors at both intracellular and extrasynaptic plasma membranes sites, which could be recruited to synapses upon stimulation (Gardner et al., 2005). Moreover, it was reported that treatments that block interactions between the carboxy-terminal PDZ binding motif of GluR2/3 and PICK1 strongly attenuate the expression of cerebellar LTD in cultured Purkinje cells (Xia et al., 2000). In case of another important PICK1 interacting partner, the DAT, Torres et al. (2001) found that PICK1 binding was important for proper targeting and surface clustering of the transporter protein, since overexpression of PICK1 together with the DAT in HEK293 cells resulted in enhanced surface expression and the formation of cluster-like structures; Furthermore, disruption of the PDZ binding site in DAT impaired transporter distribution in neurons (Torres et al., 2001).

Based on the roles of PICK1 at AMPA receptors and the DAT, one might expect that PICK1 may have a similar role in the regulation of mGluR7a surface clustering and signaling mechanism. Actually, two groups have probed the functional consequences of PICK1-mGluR7a interaction. Dev et al. (2000) reported that PICK1 may play a role for modulating PKC α dependent phosphorylation of mGluR7a, thereby influencing the mGluR7a signaling (Dev et al., 2000). Others (Boudin et al., 2000) overexpressed wild-type mGluR7a and a mutant mGluR7a, which lacked the PICK1 binding site, in cultured hippocampal neurons. They showed that wild-type mGluR7a receptor clusters were localized at synaptic sites and the receptors were targeted to axonal terminals. They could also show that the mutant mGluR7a, which does not bind to PICK1, was efficiently targeted to axons. However, contrasting with the wild-type mGluR7a, the mutant mGluR7a receptor immunoreactivity was not concentrated at synaptic sites, but exhibited rather a more diffuse pattern, distributed in large stretches along axonal processes. Moreover, double localization with the synaptic marker SV2 showed no correspondence between mutant mGluR7a-expressing axonal portions and the presence of synapses. They therefore concluded that the deletion of PICK1 binding domain prevented the synaptic aggregation of mGluR7a, but not its axonal targeting.

The data obtained here with mGluR7a knock-in mice generated in this thesis are not consistent with the results of Boudin et al. (2000). Both our

immunocytochemical data obtained with hippocampal neuron cultures and the immunoelectron microscopy results with mouse brain tissue clearly show that there was no impairment of mGluR7a synaptic membrane targeting and localization in the knock-in mice. This indicates that PICK1 is not crucial for the clustering of mGluR7a at presynaptic active zones *in vivo*. It seems that some other targeting and clustering mechanisms must exist for this receptor. The C-terminus of mGluR7a probably contains a dominant and sufficient signal for both axon targeting and synaptic clustering of mGluR7a that is independent of PICK1 and/or other PDZ-domain proteins. To sum up, the results obtained with knock-in mice here do not support the conclusions reached by Boudin et al. (2000). It should be pointed out, however, that the transfection experiments in the latter study were performed on the wild-type background; hence, the endogenous mGluR7a may have competed with the recombinant mutant mGluR7a for other binding protein. This question could be addressed by performing respective transfection experiments on hippocampal neurons from mGluR7 knockout mice.

4.3. Requirement of PICK1 in the mGluR7a receptor signaling and control of synaptic transmission

mGluR7 is one of the most important mGluR subtypes and is primarily localized on presynaptic terminals (Kinoshita et al., 1998) where it is thought to regulate neurotransmitter release. Many studies indicate that this receptor is a key player for modulating both glutamatergic and GABAergic transmission (Losonczy et al., 2003). It is well established that mGluR7 activation depresses synaptic transmission at a variety of synapses in neuronal cultures (O'Connor et al., 1999; Perroy et al., 2002). mGluR7 mediated presynaptic inhibition probably involves different mechanism; however, increasing evidence suggests that presynaptic Ca²⁺ channels are the primary target of mGluR7 (Perroy et al., 2000; Millan et al., 2002; Millan et al., 2003). Their inhibition mediates down regulation of neurotransmitter release.

To address the contribution of PICK1 in mGluR7a mediated synaptic transmission, the knock-in mice were analyzed electrophysiologically using cerebellar granule cell

cultures as model system. Spontaneous excitatory postsynaptic currents (EPSCs) were recorded with cerebellar neuron cultures in the absence and presence of L-AP4. We found that L-AP4 dramatically reduced the frequency, but not the amplitude of EPSCs in wild-type neurons. However, this inhibitory effect of L-AP4 was lost in knock-in neurons, indicating that the mutant mGluR7a, which does not bind to PICK1, did not respond properly to agonist stimulation. We therefore concluded that mGluR7 mediated presynaptic inhibition requires an interaction with PICK1. Moreover, these data corroborate the previous notion (Perroy et al., 2002) that PICK1 has an essential role for inhibition of P/Q-type Ca^{2+} channels and synaptic transmission by mGluR7. Taken together, the data collected from the knock-in mouse model strongly suggest that the PICK1-mGluR7a protein complex at the presynaptic terminal determines the signaling specificity of mGluR7a and the control of synaptic transmission by mGluR7a is PICK1 dependent.

Considering that the mGluR7a receptor has a low affinity for glutamate (Saugstad et al., 1994), this receptor is thought to be activated only when the concentration of glutamate in the synaptic cleft is highly elevated. This implies that the mGluR7a–PICK1 complex mediated signaling pathway will be operative only under enhanced presynaptic activity in cerebellar granule cells. Excessive glutamate release would activate this pathway, and thereby decrease glutamate release and reduce synaptic transmission. The data shown here corroborate that mGluR7a mediates inhibition of glutamate release.

4.4. Involvement of mGluR7a-PICK1 signaling pathway in anxiety

Anxiety disorders represent a range of conditions that include generalized anxiety, panic attacks, post-traumatic stress disorder, obsessive-compulsive syndrome and social phobias (Martin, 1998). These disorders are often resistant to current therapeutic approaches such as anxiolytic drug treatment and cognitive behavior therapy. Novel treatment strategies are required, and manipulations of the glutamatergic system through mGluRs are widely considered a promising targets (Swanson et al., 2005). Previous studies of mGluR7 knockout mice has established the notion that mGluR7 is involved in anxiety-related behavior, and that this

receptor could be exploited for the psychopharmacological and behavioral treatment of anxiety disorders (Cryan et al., 2003; Callaerts-Vegh et al., 2006).

In mGluR7a knock-in mice, the electrophysiological analysis revealed that the signaling of mGluR7a was blocked, we therefore examined whether there are some alterations in anxiety-related behavior for the KI mice. The elevated plus-maze, a widely used anxiety test, was employed to assess the mGluR7a knock-in mice. Although not statistically significant, a difference was found for the behavior of KI and control animal in elevated plus-maze test. The knock-in mice showed anxiolytic-like behavior, which is similar to the anxiety-related phenotype observed in mGluR7 knockout mice (Callaerts-Vegh et al., 2006). This provides the evidence of the significance of mGluR7 in anxiety pathways and mGluR7a-PICK1 interaction could be involved in these processes. Further investigation of mGluR7-PICK1 signaling will help to understand the details of their involvement in anxiety pathways.

4.5. mGluR7a knock-in mice – an animal model for absence epilepsy?

Epilepsy is a chronic neurological disorder characterized by seizures that are quite diverse, ranging from only electrographically detectable seizures (Petit Mal) to massive generalized seizures of the entire body musculature (Grand Mal). Among genes related to epilepsy, mGluR7 is of special interests because it may be involved in absence epilepsy (Alexander and Godwin, 2006). Typical absence seizures are characterized behaviourally by a loss of consciousness of abrupt onset and a termination process that is associated with a bilateral synchronous SWD measuring about 3 Hz in the human EEG and 5 Hz in mouse EEG (Manning et al., 2003).

The analysis of the mGluR7a knock-in mice has shown that the increase in threshold sensitivity for the convulsant pentetrazole (PTZ) was observed in the KI mice. Moreover, surface parietal cortex EEG recordings of the KI mice revealed a series of synchronous oscillation, or "spike-and-wave discharges" (SWD), and meanwhile the mutant mice displayed the behavioural arrest, associated to facial myoclonus and vibrissal twitching during the SWD. Notably, the KI mice responded to pharmacology

as human absence epilepsy. Based on this observation, we defined that the KI mice displayed the phenotype of absence-like seizures.

The question remains of what could be the mechanism of mGluR7's acting on the absence-like seizures? The classic view of the seizures pathology believes that a thalamocortical circuit, particularly the contribution of the ventrobasal thalamus (VB) and reticular thalamic nucleus (RTN), are involved in the propagation of absence seizures. Aberrant corticothalamic rhythms are believed to be the substrate of SWD (Gloor and Fariello, 1988). Studies have shown that expression of mGluR7 in the structures involved in absence seizures (RTN, VB and somatosensory cortex) (Bradley et al., 1998; Kinoshita et al., 1998; Dalezios et al., 2002). It is possible that mGluR7 could exert their action on a range of synapses at different levels in these regions. mGluR7 inhibits Ca^{2+} channel and, as a consequence, neurotransmitter release and synaptic transmission. Data of this thesis showed that the mGluR7 PDZ ligand-dependent inhibition of EPSCs was mediated by blockade of Ca^{2+} channels. Similarly the receptor inhibits Ca^{2+} entry through N-type Ca^{2+} channels in cortical synaptosomes. The dysfunction of mGluR7 in the KI mice might account for the pathophysiology of the absence-like seizures. However, it is difficult to clarify the role of PICK1 in these processes, the detailed analysis of mGluR7a-PICK1 interaction in both glutamatergic and GABAergic neurotransmission is therefore required.

Overall, our results provide an original animal model of absence epilepsy, a single identified protein-protein interaction is directly linked to this neuropathology. This model might identify mGluR7-PICK1 interaction as a novel anti-absence seizure target. Orthosteric or allosteric mGluR7 agonists or compounds reinforcing the mGluR7-PDZ interactions could be of particular interest.

4.6. The interaction of PICK1 with mGluR7a and mGluR7b

The yeast two-hybrid screens identified PICK1 as a binding partner of the C-terminus for both mGluR7a and mGluR7b (El Far et al., 2000; Enz and Croci, 2003). mGluR7a and b differ only at the C-termini. The C-terminal last 3 amino acids of mGluR7a are required to bind PICK1 via its PDZ domain, while mGluR7b interacts with PICK1 through different binding motifs (Enz and Croci, 2003). The

gene targeting strategy described in this thesis has mutated the last 3 amino acids residues of mGluR7a, suggesting that only the PICK1-mGluR7a interaction was disrupted in the knock-in mice. In principle, the PICK1-mGluR7b interaction should not be affected in the mutant mice. One remaining question is whether the PICK1 binding of mGluR7b will compensate for mutation-induced effects in the knock-in mice. However, anatomical data have shown that mGluR7a is more abundant than mGluR7b in the central nervous system of the adult rat and mouse (Kinoshita et al., 1998). Although the mGluR7b splice variant also has been reported to display PICK1 binding ability, a at least 20-fold reduced efficacy as compared to mGluR7a was found upon quantifying the binding data (El Far et al., 2000). On the other hand, little is known about the physiological function of mGluR7b, its contribution to brain function seems less apparent than that of mGluR7a. The outlined reasons above suggest that binding of PICK1 to mGluR7b should not have biased the analysis of the mGluR7a knock-in mice. The results on the role of PICK1 and/or other PDZ-domain proteins in mGluR7a mediated signaling pathways could be confidently studied in the mutant mice.

4.7. Perspectives

Disruption of the mGluR7a-PICK1 interaction in the knock-in mice resulted in normal targeting and synaptic clustering of mGluR7a, while mGluR7a mediated presynaptic inhibition was abolished, this confers that PICK1 is not essential for receptor membrane trafficking and presynaptic localization, but required for the receptor-mediated inhibition of presynaptic Ca^{2+} channels. Three major questions arise from this for future work.

First, since PDZ domain-containing proteins obviously play a central role in signaling complex assembly, it will be interesting to learn whether mGluR7 still organizes its signolosomes efficiently at presynaptic sites in mutant mice after inactivation of PICK1 binding. This question has to be investigated by further biochemical experiments. New knowledge on this will shed light on how supramolecular signaling complexes of mGluRs are formed.

Second, the analysis of knock-in mice suggested an important role of PICK1 in the control of glutamatergic synaptic transmission. However, previous work has shown that the C-terminus of mGluR7a directly interacts with Ca^{2+} -Calmodulin at a binding site that overlaps with that of G-protein $\beta\gamma$ subunits (O'Connor et al., 1999), and accordingly these interactions are mutually exclusive. It has been proposed that action potential-induced Ca^{2+} influx into synaptic terminals might activate calmodulin, which in turn would displace G-protein $\beta\gamma$ subunits from mGluR7 receptors to activate presynaptic Ca^{2+} channels, thereby causing depression of glutamatergic synaptic transmission (O'Connor et al., 1999). Notably, both mGluR7 receptor-coupled calmodulin and PICK1-dependent inhibitory pathways might act on the same presynaptic Ca^{2+} channels. It would be interesting to test whether these two pathways are complementary or exclusive. Moreover, if a functional crosstalk between these two signaling cascades could be found, this would lead to better understanding of intracellular signaling mechanism of mGluR7.

Third, the neurobiological studies of mGluR7 function have correlated mGluR7-driven intracellular signaling pathways to synaptic plasticity (Pelkey et al., 2005). The contribution of mGluR7-PICK1 interaction and downstream signaling to mGluR7-dependent synaptic plasticity could also be investigated using the knock-in mice generated in this thesis. A major focus of such studies could be whether transcription and translation are changed by disrupting mGluR7-PICK1 interaction in the mutant mice. More investigations could provide insights into the question whether mGluR7 has a role in the long-term regulation of synaptic efficacy in the central nervous system.

5. Bibliography

- Abdul-Ghani AS, Attwell PJ, Singh Kent N, Bradford HF, Croucher MJ, Jane DE (1997) Anti-epileptogenic and anticonvulsant activity of L-2-amino-4-phosphonobutyrate, a presynaptic glutamate receptor agonist. *Brain Res* 755:202-212.
- Alexander GM, Godwin DW (2006) Metabotropic glutamate receptors as a strategic target for the treatment of epilepsy. *Epilepsy Res* 71:1-22.
- Anderson CM, Swanson RA (2000) Astrocyte glutamate transport: review of properties, regulation, and physiological functions. *Glia* 32:1-14.
- Anwyl R (1999) Metabotropic glutamate receptors: electrophysiological properties and role in plasticity. *Brain Res Brain Res Rev* 29:83-120.
- Arguello PA, Gogos JA (2006) Modeling madness in mice: one piece at a time. *Neuron* 52:179-196.
- Aronica E, Gorter JA, Rozemuller AJ, Yankaya B, Troost D (2005) Activation of metabotropic glutamate receptor 3 enhances interleukin (IL)-1beta-stimulated release of IL-6 in cultured human astrocytes. *Neuroscience* 130:927-933.
- Bach ME, Hawkins RD, Osman M, Kandel ER, Mayford M (1995) Impairment of spatial but not contextual memory in CaMKII mutant mice with a selective loss of hippocampal LTP in the range of the theta frequency. *Cell* 81:905-915.
- Barnes CA (1979) Memory deficits associated with senescence: a neurophysiological and behavioral study in the rat. *J Comp Physiol Psychol* 93:74-104.
- Barton ME, Shannon HE (2005) Behavioral and convulsant effects of the (S) enantiomer of the group I metabotropic glutamate receptor agonist 3,5-DHPG in mice. *Neuropharmacology* 48:779-787.
- Baude A, Nusser Z, Roberts JD, Mulvihill E, McIlhinney RA, Somogyi P (1993) The metabotropic glutamate receptor (mGluR1 alpha) is concentrated at perisynaptic membrane of neuronal subpopulations as detected by immunogold reaction. *Neuron* 11:771-787.
- Berger ML, Rebernik P (1999) Zinc and ifenprodil allosterically inhibit two separate polyamine-sensitive sites at N-methyl-D-aspartate receptor complex. *J Pharmacol Exp Ther* 289:1584-1591.
- Bertaso F, Lill Y, Airas JM, Espeut J, Blahos J, Bockaert J, Fagni L, Betz H, El-Far O (2006) MacMARCKS interacts with the metabotropic glutamate receptor type 7 and modulates G protein-mediated constitutive inhibition of calcium channels. *J Neurochem* 99:288-298.
- Borgdorff AJ, Choquet D (2002) Regulation of AMPA receptor lateral movements. *Nature* 417:649-653.
- Boudin H, Doan A, Xia J, Shigemoto R, Haganir RL, Worley P, Craig AM (2000) Presynaptic clustering of mGluR7a requires the PICK1 PDZ domain binding site. *Neuron* 28:485-497.
- Bough KJ, Mott DD, Dingledine RJ (2004) Medial perforant path inhibition mediated by mGluR7 is reduced after status epilepticus. *J Neurophysiol* 92:1549-1557.
- Bradley SR, Rees HD, Yi H, Levey AI, Conn PJ (1998) Distribution and developmental regulation of metabotropic glutamate receptor 7a in rat brain. *J Neurochem* 71:636-645.

- Brakeman PR, Lanahan AA, O'Brien R, Roche K, Barnes CA, Huganir RL, Worley PF (1997) Homer: a protein that selectively binds metabotropic glutamate receptors. *Nature* 386:284-288.
- Branda CS, Dymecki SM (2004) Talking about a revolution: The impact of site-specific recombinases on genetic analyses in mice. *Dev Cell* 6:7-28.
- Callaerts-Vegh Z, Beckers T, Ball SM, Baeyens F, Callaerts PF, Cryan JF, Molnar E, D'Hooge R (2006) Concomitant deficits in working memory and fear extinction are functionally dissociated from reduced anxiety in metabotropic glutamate receptor 7-deficient mice. *J Neurosci* 26:6573-6582.
- Cartmell J, Schoepp DD (2000) Regulation of neurotransmitter release by metabotropic glutamate receptors. *J Neurochem* 75:889-907.
- Conn PJ (2003) Physiological roles and therapeutic potential of metabotropic glutamate receptors. *Ann N Y Acad Sci* 1003:12-21.
- Conn PJ, Pin JP (1997) Pharmacology and functions of metabotropic glutamate receptors. *Annu Rev Pharmacol Toxicol* 37:205-237.
- Cryan JF, Kelly PH, Neijt HC, Sansig G, Flor PJ, van Der Putten H (2003) Antidepressant and anxiolytic-like effects in mice lacking the group III metabotropic glutamate receptor mGluR7. *Eur J Neurosci* 17:2409-2417.
- Dalezios Y, Lujan R, Shigemoto R, Roberts JD, Somogyi P (2002) Enrichment of mGluR7a in the presynaptic active zones of GABAergic and non-GABAergic terminals on interneurons in the rat somatosensory cortex. *Cereb Cortex* 12:961-974.
- Danysz W, Parsons AC (1998) Glycine and N-methyl-D-aspartate receptors: physiological significance and possible therapeutic applications. *Pharmacol Rev* 50:597-664.
- Dev KK (2004) Making protein interactions druggable: targeting PDZ domains. *Nat Rev Drug Discov* 3:1047-1056.
- Dev KK, Nakanishi S, Henley JM (2001) Regulation of mglu(7) receptors by proteins that interact with the intracellular C-terminus. *Trends Pharmacol Sci* 22:355-361.
- Dev KK, Nakajima Y, Kitano J, Braithwaite SP, Henley JM, Nakanishi S (2000) PICK1 interacts with and regulates PKC phosphorylation of mGLUR7. *J Neurosci* 20:7252-7257.
- Dingledine R, Borges K, Bowie D, Traynelis SF (1999) The glutamate receptor ion channels. *Pharmacol Rev* 51:7-61.
- Dishman RK, Armstrong RB, Delp MD, Graham RE, Dunn AL (1988) Open-field behavior is not related to treadmill performance in exercising rats. *Physiol Behav* 43:541-546.
- Doherty J, Dingledine R (2002) The roles of metabotropic glutamate receptors in seizures and epilepsy. *Curr Drug Targets CNS Neurol Disord* 1:251-260.
- El Far O, Betz H (2002) G-protein-coupled receptors for neurotransmitter amino acids: C-terminal tails, crowded signalosomes. *Biochem J* 365:329-336.
- El Far O, Airas J, Wischmeyer E, Nehring RB, Karschin A, Betz H (2000) Interaction of the C-terminal tail region of the metabotropic glutamate receptor 7 with the protein kinase C substrate PICK1. *Eur J Neurosci* 12:4215-4221.

- Enz R (2002) The actin-binding protein Filamin-A interacts with the metabotropic glutamate receptor type 7. *FEBS Lett* 514:184-188.
- Enz R (2007) The trick of the tail: protein-protein interactions of metabotropic glutamate receptors. *Bioessays* 29:60-73.
- Enz R, Croci C (2003) Different binding motifs in metabotropic glutamate receptor type 7b for filamin A, protein phosphatase 1C, protein interacting with protein kinase C (PICK) 1 and syntenin allow the formation of multimeric protein complexes. *Biochem J* 372:183-191.
- Flor PJ, Van Der Putten H, Ruegg D, Lukic S, Leonhardt T, Bence M, Sansig G, Knopfel T, Kuhn R (1997) A novel splice variant of a metabotropic glutamate receptor, human mGluR7b. *Neuropharmacology* 36:153-159.
- Fujii K, Maeda K, Hikida T, Mustafa AK, Balkissoon R, Xia J, Yamada T, Ozeki Y, Kawahara R, Okawa M, Haganir RL, Ujike H, Snyder SH, Sawa A (2006) Serine racemase binds to PICK1: potential relevance to schizophrenia. *Mol Psychiatry* 11:150-157.
- Gardner SM, Takamiya K, Xia J, Suh JG, Johnson R, Yu S, Haganir RL (2005) Calcium-permeable AMPA receptor plasticity is mediated by subunit-specific interactions with PICK1 and NSF. *Neuron* 45:903-915.
- Gereau RWt, Conn PJ (1994) Presynaptic enhancement of excitatory synaptic transmission by beta-adrenergic receptor activation. *J Neurophysiol* 72:1438-1442.
- Ghuri M, Chapman AG, Meldrum BS (1996) Convulsant and anticonvulsant actions of agonists and antagonists of group III mGluRs. *Neuroreport* 7:1469-1474.
- Gloor P, Fariello RG (1988) Generalized epilepsy: some of its cellular mechanisms differ from those of focal epilepsy. *Trends Neurosci* 11:63-68.
- Gray EG (1959) Axo-somatic and axo-dendritic synapses of the cerebral cortex: an electron microscope study. *J Anat* 93:420-433.
- Gundelfinger ED, tom Dieck S (2000) Molecular organization of excitatory chemical synapses in the mammalian brain. *Naturwissenschaften* 87:513-523.
- Hamlyn LH (1962) The fine structure of the mossy fibre endings in the hippocampus of the rabbit. *J Anat* 96:112-120.
- Harris DP, Burton R, Sinclair JG (1988) A simple microcomputer interface for tail-flick determination. *J Pharmacol Methods* 20:103-108.
- Harrison PJ, Owen MJ (2003) Genes for schizophrenia? Recent findings and their pathophysiological implications. *Lancet* 361:417-419.
- Heinbockel T, Pape HC (2000) Input-specific long-term depression in the lateral amygdala evoked by theta frequency stimulation. *J Neurosci* 20:RC68.
- Hentall ID, Fields HL (1988) How two sites in the rat's nucleus raphe magnus interact to inhibit the tail-flick reflex. *Neurosci Lett* 90:141-146.
- Herin GA, Aizenman E (2004) Amino terminal domain regulation of NMDA receptor function. *Eur J Pharmacol* 500:101-111.
- Herrero I, Vazquez E, Miras-Portugal MT, Sanchez-Prieto J (1996) Decrease in $[Ca^{2+}]_c$ but not in cAMP Mediates L-AP4 inhibition of glutamate release: PKC-mediated suppression of this inhibitory pathway. *Eur J Neurosci* 8:700-709.

- Hertz L, Dringen R, Schousboe A, Robinson SR (1999) Astrocytes: glutamate producers for neurons. *J Neurosci Res* 57:417-428.
- Hirbec H, Perestenko O, Nishimune A, Meyer G, Nakanishi S, Henley JM, Dev KK (2002) The PDZ proteins PICK1, GRIP, and syntrophin bind multiple glutamate receptor subtypes. Analysis of PDZ binding motifs. *J Biol Chem* 277:15221-15224.
- Hollmann M, Heinemann S (1994) Cloned glutamate receptors. *Annu Rev Neurosci* 17:31-108.
- Hong CJ, Liao DL, Shih HL, Tsai SJ (2004) Association study of PICK1 rs3952 polymorphism and schizophrenia. *Neuroreport* 15:1965-1967.
- Houamed KM, Kuijper JL, Gilbert TL, Haldeman BA, O'Hara PJ, Mulvihill ER, Almers W, Hagen FS (1991) Cloning, expression, and gene structure of a G protein-coupled glutamate receptor from rat brain. *Science* 252:1318-1321.
- Jin W, Ge WP, Xu J, Cao M, Peng L, Yung W, Liao D, Duan S, Zhang M, Xia J (2006) Lipid binding regulates synaptic targeting of PICK1, AMPA receptor trafficking, and synaptic plasticity. *J Neurosci* 26:2380-2390.
- Johnson JW, Ascher P (1987) Glycine potentiates the NMDA response in cultured mouse brain neurons. *Nature* 325:529-531.
- Kahn L, Alonso G, Robbe D, Bockaert J, Manzoni OJ (2001) Group 2 metabotropic glutamate receptors induced long term depression in mouse striatal slices. *Neurosci Lett* 316:178-182.
- Kashiwagi K, Pakh AJ, Masuko T, Igarashi K, Williams K (1997) Block and modulation of N-methyl-D-aspartate receptors by polyamines and protons: role of amino acid residues in the transmembrane and pore-forming regions of NR1 and NR2 subunits. *Mol Pharmacol* 52:701-713.
- Kawasaki Y, Kohno T, Zhuang ZY, Brenner GJ, Wang H, Van Der Meer C, Befort K, Woolf CJ, Ji RR (2004) Ionotropic and metabotropic receptors, protein kinase A, protein kinase C, and Src contribute to C-fiber-induced ERK activation and cAMP response element-binding protein phosphorylation in dorsal horn neurons, leading to central sensitization. *J Neurosci* 24:8310-8321.
- Keele NB, Arvanov VL, Shinnick-Gallagher P (1997) Quisqualate-preferring metabotropic glutamate receptor activates Na(+)-Ca²⁺ exchange in rat basolateral amygdala neurones. *J Physiol* 499 (Pt 1):87-104.
- Kinoshita A, Shigemoto R, Ohishi H, van der Putten H, Mizuno N (1998) Immunohistochemical localization of metabotropic glutamate receptors, mGluR7a and mGluR7b, in the central nervous system of the adult rat and mouse: a light and electron microscopic study. *J Comp Neurol* 393:332-352.
- Kinzie JM, Shinohara MM, van den Pol AN, Westbrook GL, Segerson TP (1997) Immunolocalization of metabotropic glutamate receptor 7 in the rat olfactory bulb. *J Comp Neurol* 385:372-384.
- Klapstein GJ, Meldrum BS, Mody I (1999) Decreased sensitivity to Group III mGluR agonists in the lateral perforant path following kindling. *Neuropharmacology* 38:927-933.
- Kosinski CM, Risso Bradley S, Conn PJ, Levey AI, Landwehrmeyer GB, Penney JB, Jr., Young AB, Standaert DG (1999) Localization of metabotropic glutamate

- receptor 7 mRNA and mGluR7a protein in the rat basal ganglia. *J Comp Neurol* 415:266-284.
- Kuhn R, Torres RM (2002) Cre/loxP recombination system and gene targeting. *Methods Mol Biol* 180:175-204.
- Lee JM, Zipfel GJ, Choi DW (1999) The changing landscape of ischaemic brain injury mechanisms. *Nature* 399:A7-14.
- Lerma J (2003) Roles and rules of kainate receptors in synaptic transmission. *Nat Rev Neurosci* 4:481-495.
- Lester RA, Jahr CE (1990) Quisqualate receptor-mediated depression of calcium currents in hippocampal neurons. *Neuron* 4:741-749.
- Linden AM, Baez M, Bergeron M, Schoepp DD (2003a) Increased c-Fos expression in the centromedial nucleus of the thalamus in metabotropic glutamate 8 receptor knockout mice following the elevated plus maze test. *Neuroscience* 121:167-178.
- Linden AM, Bergeron M, Baez M, Schoepp DD (2003b) Systemic administration of the potent mGlu8 receptor agonist (S)-3,4-DCPG induces c-Fos in stress-related brain regions in wild-type, but not mGlu8 receptor knockout mice. *Neuropharmacology* 45:473-483.
- Linden AM, Johnson BG, Peters SC, Shannon HE, Tian M, Wang Y, Yu JL, Koster A, Baez M, Schoepp DD (2002) Increased anxiety-related behavior in mice deficient for metabotropic glutamate 8 (mGlu8) receptor. *Neuropharmacology* 43:251-259.
- Loscher W (1998) Pharmacology of glutamate receptor antagonists in the kindling model of epilepsy. *Prog Neurobiol* 54:721-741.
- Losonczy A, Somogyi P, Nusser Z (2003) Reduction of excitatory postsynaptic responses by persistently active metabotropic glutamate receptors in the hippocampus. *J Neurophysiol* 89:1910-1919.
- Lovinger DM, McCool BA (1995) Metabotropic glutamate receptor-mediated presynaptic depression at corticostriatal synapses involves mGluR2 or 3. *J Neurophysiol* 73:1076-1083.
- Lujan R, Roberts JD, Shigemoto R, Ohishi H, Somogyi P (1997) Differential plasma membrane distribution of metabotropic glutamate receptors mGluR1 alpha, mGluR2 and mGluR5, relative to neurotransmitter release sites. *J Chem Neuroanat* 13:219-241.
- Madden DR (2002) The structure and function of glutamate receptor ion channels. *Nat Rev Neurosci* 3:91-101.
- Manning JP, Richards DA, Bowery NG (2003) Pharmacology of absence epilepsy. *Trends Pharmacol Sci* 24:542-549.
- Markel AL, Galaktionov Yu K, Efimov VM (1989) Factor analysis of rat behavior in an open field test. *Neurosci Behav Physiol* 19:279-286.
- Martin P (1998) Animal models sensitive to anti-anxiety agents. *Acta Psychiatr Scand Suppl* 393:74-80.
- Masu M, Tanabe Y, Tsuchida K, Shigemoto R, Nakanishi S (1991) Sequence and expression of a metabotropic glutamate receptor. *Nature* 349:760-765.
- Masu M, Iwakabe H, Tagawa Y, Miyoshi T, Yamashita M, Fukuda Y, Sasaki H, Hiroi K, Nakamura Y, Shigemoto R, et al. (1995) Specific deficit of the ON

- response in visual transmission by targeted disruption of the mGluR6 gene. *Cell* 80:757-765.
- Masugi M, Yokoi M, Shigemoto R, Muguruma K, Watanabe Y, Sansig G, van der Putten H, Nakanishi S (1999) Metabotropic glutamate receptor subtype 7 ablation causes deficit in fear response and conditioned taste aversion. *J Neurosci* 19:955-963.
- Mayer ML, Westbrook GL, Guthrie PB (1984) Voltage-dependent block by Mg²⁺ of NMDA responses in spinal cord neurones. *Nature* 309:261-263.
- McBain CJ, Mayer ML (1994) N-methyl-D-aspartic acid receptor structure and function. *Physiol Rev* 74:723-760.
- McCool BA, Pin JP, Harpold MM, Brust PF, Stauderman KA, Lovinger DM (1998) Rat group I metabotropic glutamate receptors inhibit neuronal Ca²⁺ channels via multiple signal transduction pathways in HEK 293 cells. *J Neurophysiol* 79:379-391.
- Melton DW (1994) Gene targeting in the mouse. *Bioessays* 16:633-638.
- Millan C, Lujan R, Shigemoto R, Sanchez-Prieto J (2002) Subtype-specific expression of group III metabotropic glutamate receptors and Ca²⁺ channels in single nerve terminals. *J Biol Chem* 277:47796-47803.
- Millan C, Castro E, Torres M, Shigemoto R, Sanchez-Prieto J (2003) Co-expression of metabotropic glutamate receptor 7 and N-type Ca(2+) channels in single cerebrocortical nerve terminals of adult rats. *J Biol Chem* 278:23955-23962.
- Mitsukawa K, Yamamoto R, Ofner S, Nozulak J, Pescott O, Lukic S, Stoehr N, Mombereau C, Kuhn R, McAllister KH, van der Putten H, Cryan JF, Flor PJ (2005) A selective metabotropic glutamate receptor 7 agonist: activation of receptor signaling via an allosteric site modulates stress parameters in vivo. *Proc Natl Acad Sci U S A* 102:18712-18717.
- Muller U (1999) Ten years of gene targeting: targeted mouse mutants, from vector design to phenotype analysis. *Mech Dev* 82:3-21.
- Myers SJ, Dingledine R, Borges K (1999) Genetic regulation of glutamate receptor ion channels. *Annu Rev Pharmacol Toxicol* 39:221-241.
- Nishi M, Hinds H, Lu HP, Kawata M, Hayashi Y (2001) Motoneuron-specific expression of NR3B, a novel NMDA-type glutamate receptor subunit that works in a dominant-negative manner. *J Neurosci* 21:RC185.
- Nowak L, Bregestovski P, Ascher P, Herbert A, Prochiantz A (1984) Magnesium gates glutamate-activated channels in mouse central neurones. *Nature* 307:462-465.
- O'Connor V, El Far O, Bofill-Cardona E, Nanoff C, Freissmuth M, Karschin A, Airas JM, Betz H, Boehm S (1999) Calmodulin dependence of presynaptic metabotropic glutamate receptor signaling. *Science* 286:1180-1184.
- O'Hara PJ, Sheppard PO, Thogersen H, Venezia D, Haldeman BA, McGrane V, Houamed KM, Thomsen C, Gilbert TL, Mulvihill ER (1993) The ligand-binding domain in metabotropic glutamate receptors is related to bacterial periplasmic binding proteins. *Neuron* 11:41-52.
- Okamoto N, Hori S, Akazawa C, Hayashi Y, Shigemoto R, Mizuno N, Nakanishi S (1994) Molecular characterization of a new metabotropic glutamate receptor

- mGluR7 coupled to inhibitory cyclic AMP signal transduction. *J Biol Chem* 269:1231-1236.
- Otani S, Daniel H, Takita M, Crepel F (2002) Long-term depression induced by postsynaptic group II metabotropic glutamate receptors linked to phospholipase C and intracellular calcium rises in rat prefrontal cortex. *J Neurosci* 22:3434-3444.
- Panatier A, Poulain DA, Oliet SH (2004) Regulation of transmitter release by high-affinity group III mGluRs in the supraoptic nucleus of the rat hypothalamus. *Neuropharmacology* 47:333-341.
- Passafaro M, Piech V, Sheng M (2001) Subunit-specific temporal and spatial patterns of AMPA receptor exocytosis in hippocampal neurons. *Nat Neurosci* 4:917-926.
- Pekhletski R, Gerlai R, Overstreet LS, Huang XP, Agopyan N, Slater NT, Abramow-Newerly W, Roder JC, Hampson DR (1996) Impaired cerebellar synaptic plasticity and motor performance in mice lacking the mGluR4 subtype of metabotropic glutamate receptor. *J Neurosci* 16:6364-6373.
- Pelkey KA, Lavezzari G, Racca C, Roche KW, McBain CJ (2005) mGluR7 is a metaplastic switch controlling bidirectional plasticity of feedforward inhibition. *Neuron* 46:89-102.
- Perroy J, Prezeau L, De Waard M, Shigemoto R, Bockaert J, Fagni L (2000) Selective blockade of P/Q-type calcium channels by the metabotropic glutamate receptor type 7 involves a phospholipase C pathway in neurons. *J Neurosci* 20:7896-7904.
- Perroy J, El Far O, Bertaso F, Pin JP, Betz H, Bockaert J, Fagni L (2002) PICK1 is required for the control of synaptic transmission by the metabotropic glutamate receptor 7. *Embo J* 21:2990-2999.
- Pierce KL, Premont RT, Lefkowitz RJ (2002) Seven-transmembrane receptors. *Nat Rev Mol Cell Biol* 3:639-650.
- Robbe D, Kopf M, Remaury A, Bockaert J, Manzoni OJ (2002) Endogenous cannabinoids mediate long-term synaptic depression in the nucleus accumbens. *Proc Natl Acad Sci U S A* 99:8384-8388.
- Sahara Y, Westbrook GL (1993) Modulation of calcium currents by a metabotropic glutamate receptor involves fast and slow kinetic components in cultured hippocampal neurons. *J Neurosci* 13:3041-3050.
- Sansig G, Bushell TJ, Clarke VR, Rozov A, Burnashev N, Portet C, Gasparini F, Schmutz M, Klebs K, Shigemoto R, Flor PJ, Kuhn R, Knoepfel T, Schroeder M, Hampson DR, Collett VJ, Zhang C, Duvoisin RM, Collingridge GL, van Der Putten H (2001a) Increased seizure susceptibility in mice lacking metabotropic glutamate receptor 7. *J Neurosci* 21:8734-8745.
- Sansig G, Bushell TJ, Clarke VR, Rozov A, Burnashev N, Portet C, Gasparini F, Schmutz M, Klebs K, Shigemoto R, Flor PJ, Kuhn R, Knoepfel T, Schroeder M, Hampson DR, Collett VJ, Zhang C, Duvoisin RM, Collingridge GL, van Der Putten H (2001b) Increased seizure susceptibility in mice lacking metabotropic glutamate receptor 7. *J Neurosci* 21:8734-8745.

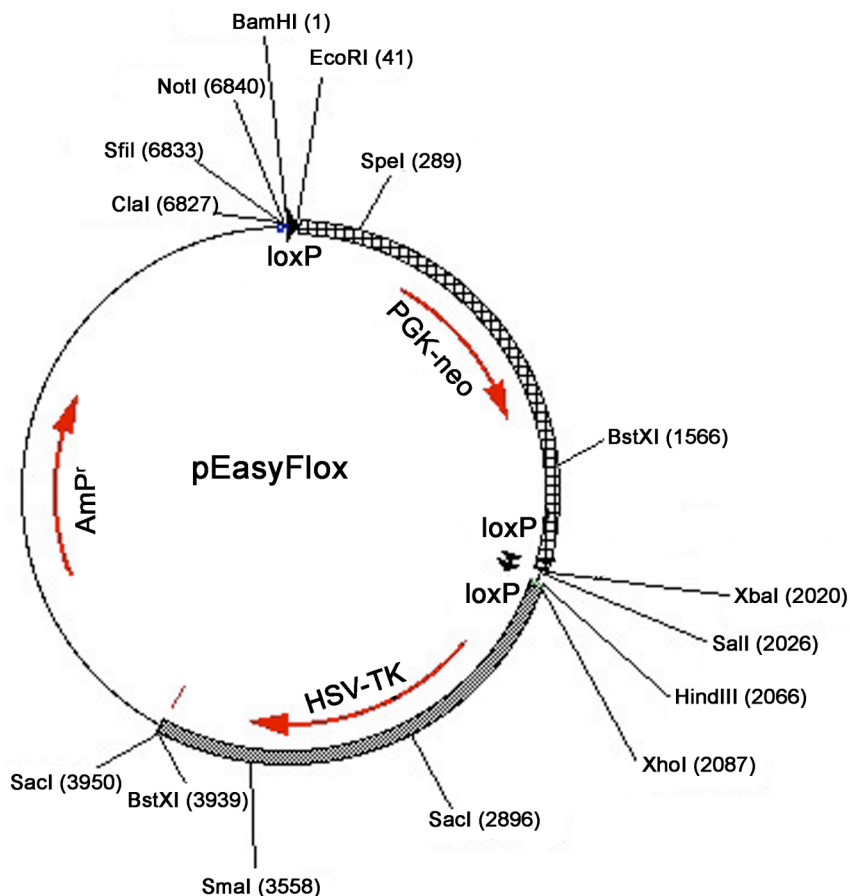
- Sassoe-Pognetto M, Wassle H, Grunert U (1994) Glycinergic synapses in the rod pathway of the rat retina: cone bipolar cells express the alpha 1 subunit of the glycine receptor. *J Neurosci* 14:5131-5146.
- Sato T, Tanaka K, Ohnishi Y, Teramoto T, Irifune M, Nishikawa T (2004) Inhibitory effects of group II mGluR-related drugs on memory performance in mice. *Physiol Behav* 80:747-758.
- Saugstad JA, Segerson TP, Westbrook GL (1996) Metabotropic glutamate receptors activate G-protein-coupled inwardly rectifying potassium channels in *Xenopus* oocytes. *J Neurosci* 16:5979-5985.
- Saugstad JA, Kinzie JM, Mulvihill ER, Segerson TP, Westbrook GL (1994) Cloning and expression of a new member of the L-2-amino-4-phosphonobutyric acid-sensitive class of metabotropic glutamate receptors. *Mol Pharmacol* 45:367-372.
- Schoppa NE, Westbrook GL (1997) Modulation of mEPSCs in olfactory bulb mitral cells by metabotropic glutamate receptors. *J Neurophysiol* 78:1468-1475.
- Schorge S, Colquhoun D (2003) Studies of NMDA receptor function and stoichiometry with truncated and tandem subunits. *J Neurosci* 23:1151-1158.
- Schrader LA, Tasker JG (1997) Modulation of multiple potassium currents by metabotropic glutamate receptors in neurons of the hypothalamic supraoptic nucleus. *J Neurophysiol* 78:3428-3437.
- Schulz HL, Stohr H, Weber BH (2002) Characterization of three novel isoforms of the metabotropic glutamate receptor 7 (GRM7). *Neurosci Lett* 326:37-40.
- Seaman RL, Beblo DA, Raslear TG (1994) Modification of acoustic and tactile startle by single microwave pulses. *Physiol Behav* 55:587-595.
- Seeburg PH (2002) A-to-I editing: new and old sites, functions and speculations. *Neuron* 35:17-20.
- Shi S, Hayashi Y, Esteban JA, Malinow R (2001) Subunit-specific rules governing AMPA receptor trafficking to synapses in hippocampal pyramidal neurons. *Cell* 105:331-343.
- Shigemoto R, Kulik A, Roberts JD, Ohishi H, Nusser Z, Kaneko T, Somogyi P (1996) Target-cell-specific concentration of a metabotropic glutamate receptor in the presynaptic active zone. *Nature* 381:523-525.
- Shigeri Y, Seal RP, Shimamoto K (2004) Molecular pharmacology of glutamate transporters, EAATs and VGLUTs. *Brain Res Brain Res Rev* 45:250-265.
- Snead OC, 3rd, Banerjee PK, Burnham M, Hampson D (2000) Modulation of absence seizures by the GABA(A) receptor: a critical role for metabotropic glutamate receptor 4 (mGluR4). *J Neurosci* 20:6218-6224.
- Sommer B, Burnashev N, Verdoorn TA, Keinänen K, Sakmann B, Seeburg PH (1992) A glutamate receptor channel with high affinity for domoate and kainate. *Embo J* 11:1651-1656.
- Songyang Z, Fanning AS, Fu C, Xu J, Marfatia SM, Chishti AH, Crompton A, Chan AC, Anderson JM, Cantley LC (1997) Recognition of unique carboxyl-terminal motifs by distinct PDZ domains. *Science* 275:73-77.
- Staudinger J, Lu J, Olson EN (1997) Specific interaction of the PDZ domain protein PICK1 with the COOH terminus of protein kinase C-alpha. *J Biol Chem* 272:32019-32024.

- Staudinger J, Zhou J, Burgess R, Elledge SJ, Olson EN (1995) PICK1: a perinuclear binding protein and substrate for protein kinase C isolated by the yeast two-hybrid system. *J Cell Biol* 128:263-271.
- Storozeva ZI, Pletnicov MV (1994) Habituation of acoustic startle in rats--a functional ablation study. *Neuroreport* 5:2065-2068.
- Stowell JN, Craig AM (1999) Axon/dendrite targeting of metabotropic glutamate receptors by their cytoplasmic carboxy-terminal domains. *Neuron* 22:525-536.
- Stricker NL, Christopherson KS, Yi BA, Schatz PJ, Raab RW, Dawes G, Bassett DE, Jr., Bredt DS, Li M (1997) PDZ domain of neuronal nitric oxide synthase recognizes novel C-terminal peptide sequences. *Nat Biotechnol* 15:336-342.
- Sugiyama H, Ito I, Hirano C (1987) A new type of glutamate receptor linked to inositol phospholipid metabolism. *Nature* 325:531-533.
- Sung KW, Choi S, Lovinger DM (2001) Activation of group I mGluRs is necessary for induction of long-term depression at striatal synapses. *J Neurophysiol* 86:2405-2412.
- Swanson CJ, Bures M, Johnson MP, Linden AM, Monn JA, Schoepp DD (2005) Metabotropic glutamate receptors as novel targets for anxiety and stress disorders. *Nat Rev Drug Discov* 4:131-144.
- Takahashi T, Forsythe ID, Tsujimoto T, Barnes-Davies M, Onodera K (1996) Presynaptic calcium current modulation by a metabotropic glutamate receptor. *Science* 274:594-597.
- Thomas KR, Capecchi MR (1987) Site-directed mutagenesis by gene targeting in mouse embryo-derived stem cells. *Cell* 51:503-512.
- Thomsen C, Dalby NO (1998) Roles of metabotropic glutamate receptor subtypes in modulation of pentylenetetrazole-induced seizure activity in mice. *Neuropharmacology* 37:1465-1473.
- Torres GE, Yao WD, Mohn AR, Quan H, Kim KM, Levey AI, Staudinger J, Caron MG (2001) Functional interaction between monoamine plasma membrane transporters and the synaptic PDZ domain-containing protein PICK1. *Neuron* 30:121-134.
- Trombley PQ, Westbrook GL (1992) L-AP4 inhibits calcium currents and synaptic transmission via a G-protein-coupled glutamate receptor. *J Neurosci* 12:2043-2050.
- Weiergraber M, Henry M, Krieger A, Kamp M, Radhakrishnan K, Hescheler J, Schneider T (2006) Altered seizure susceptibility in mice lacking the Ca(v)2.3 E-type Ca²⁺ channel. *Epilepsia* 47:839-850.
- Wisden W, Seeburg PH (1993) Mammalian ionotropic glutamate receptors. *Curr Opin Neurobiol* 3:291-298.
- Wu S, Wright RA, Rockey PK, Burgett SG, Arnold JS, Rostock PR, Jr., Johnson BG, Schoepp DD, Belagaje RM (1998) Group III human metabotropic glutamate receptors 4, 7 and 8: molecular cloning, functional expression, and comparison of pharmacological properties in RGT cells. *Brain Res Mol Brain Res* 53:88-97.
- Xia J, Zhang X, Staudinger J, Huganir RL (1999) Clustering of AMPA receptors by the synaptic PDZ domain-containing protein PICK1. *Neuron* 22:179-187.

- Xia J, Chung HJ, Wihler C, Huganir RL, Linden DJ (2000) Cerebellar long-term depression requires PKC-regulated interactions between GluR2/3 and PDZ domain-containing proteins. *Neuron* 28:499-510.
- Xiao MY, Zhou Q, Nicoll RA (2001) Metabotropic glutamate receptor activation causes a rapid redistribution of AMPA receptors. *Neuropharmacology* 41:664-671.
- Yamakura T, Askalany AR, Petrenko AB, Kohno T, Baba H, Sakimura K (2005) The NR3B subunit does not alter the anesthetic sensitivities of recombinant N-methyl-D-aspartate receptors. *Anesth Analg* 100:1687-1692.
- Yokoi M, Kobayashi K, Manabe T, Takahashi T, Sakaguchi I, Katsuura G, Shigemoto R, Ohishi H, Nomura S, Nakamura K, Nakao K, Katsuki M, Nakanishi S (1996) Impairment of hippocampal mossy fiber LTD in mice lacking mGluR2. *Science* 273:645-647.
- Zhu JJ, Esteban JA, Hayashi Y, Malinow R (2000) Postnatal synaptic potentiation: delivery of GluR4-containing AMPA receptors by spontaneous activity. *Nat Neurosci* 3:1098-1106.

6. Appendices

APPENDIX I. Plasmid Map of pEasyFloX, which is used as backbone for construction of the gene targeting vector.



APPENDIX II. Sequence of 9.8 kb genomic clone subcloned from BAC RP23-391F16, the exon 10 is highlighted.

```
AGATCTTTTTTCTTCTCTGCTTTTGGTTTTTACATTTTTTTATAGTTTCTCAATCTAGTTTGAAT
TAGCAAAAGTTTTTAAAGGCAAAAATTTGCAGAGTTGGGAGTGAGACAGCTCAGGGGTAAGGTGC
TTGCTGCCACTGTGAGCCTCTGAGTTCCATCCACACAGTGCGACACGTGGACCACCTCACTCTATCTG
TCCTCTGAGCTCCACAACATGCCACCGCAGGATCCCCCTCCTTCCACAAATCAGAGTAGTTAAAA
AGCAAATCCTGGAGAAAGTTATATTTAAAAATTAATTAATATTTAAAAATTGGCCTCCTAAGTCAATGCC
AAATTGACAGTACATTTTGACAAAATGAGAATGAATTGGATGTCTAATATTTACTAATAAGAAAATG
TGTATTAATAATGTATTTAGAAAATCAATGTCCTTAAGACTTTTTTCATTGAAAACCTCAGGTCTTTTA
AATACCTGAGTTTGAGAAAATGTAATAGGAACAATACAATCTACTCTTGTCTTTCTCGATGTAAT
```


CAGATTATTCGGTTCCTTAAAAGCACTCGCTGTTCTTGGAGAACGCCAGCTTCAGCTCCTAGCACCTA
CATCATGTGCGACAGTCATCCATAACTCCTGTTTCAGGGCATCTGACACCCTCTTCTGAGCTCTGTAA
GCAACGGGAACCCATATGGTACATATTCATACATGTAGGCAAACATGCACACACATGAAATACAT
ATTTTTAATTTCAATTCGACACACATTCTTAAAAATAAAATGAAAAACTCCAGCTTCTGAGGGAAAGA
AATTTCCAGCCTTTCAACATAAAAGGCATATCTCTTAAACAACCATTTTTTCTGGACAACCTATTTTGA
GCTAGGCAATTCTTCTCTGACCATAAACTACATTGCTATTCAAATAAATAGAAATTATCAGCCCTG
TAGGCACTTCTTTATTTACTCATAAGGCCAGGATGGTTTAAAAATAAACTATAATACTAGGACT
TTACTGTGATAAAGGGCAGAAATGCCGTTTCGAGGGGCTGCATAAACTTCATTATAACCTTGCTGCA
ACGCTCAAAGCAATTCTGCAAAGAAAGCAGATACTGAGGCTTATCCTTTGTAGAGAAGTTTGTAA
CTAAAAATACATTTATATGTTTTATTCCCAGCGAGAGACTGGGATAAATTCTGACATCTGTGCTATCA
ACAGTCTCAGGGTCTGAATTACTGTCTCATTTTAAAGCCTCCACAAAATTCAGCCTTATGGTAGAG
GGCTGGGCTCATCTCATGTAAGTGATGGAGCACAACAGAACCCAGGCAGGTGAGTCCCAGGCAGC
AGTTTCTTCCCATGATGGCTTGCAGGGGAAAAAAGAGAGACTCATGGGTCTATAGCATGTTTTCT
CAAATGCTGGTCCCTCTGTGTCCATGTCCCTCCCAACTATAAAGGGGAATAAAAAATTATGTGTCTCA
TTTTCTGAAAATACAAGAAGATAATGCCACAAGCTTCAGGGAGCCTTGCCGTGTTCTCCAAAACA
TAATTTTCTAATTTTCATTTGTTTCATTGTTTTCTTGTGCTAACTTGGGGTTTACCTAGACCAGGCT
GGCTCAAAGCTGTTGTGAAACTGAAAATGAACCTTGCCCAACCCCACTTGTGCTGCTGCTGCTGCT
CTGCTATGTAAGGATGAGAGGCATGTAACACCACGCCTTACTCACCCAGTGTGTTGGGGTGGAGCT
CAGGGCTCTGTGCACACTAAGCAAGTACTCTCAACTGAGTTCTATTCCCATCCCCACTCTCCAAGT
TTGTCTTATTCATTCTATGTATATGTTTGTCTGTATGTTAGCTGTGGTCCCGAGACACATGGGAGGA
AGTCACAGGATAACTCGTGGGAATCAGTTTACTCTTCCCCTACGTTTATTGCACTCAAGTCTTTACA
TGCAGAAATCTCCCGCTGCCCCAAGTATCTAATTGTTAAAAAGCATAGCTAGATTTTGATTCCAATT
AATCCAAAACAGTCTTCACTACAGCATAGGAACAGGGTTTTTCTGAGCTACAATTTCTTTAGTAAAA
AAAAAAATCTTTATTGACTGCTATTATATAGTAACCTATTTGAGGAAATTTAATTATTCCTTTTCCA
CTAGACAATTTCTGCTTGACAGAAATTCGGCATTAAATTAGCCACACCATGGAGGTGTCTGAGATATTT
ACGTCAGTTCAGGCTTCTGGGGTTTTTGTGTTTTCTTTCCCTTTGGTCTGGAGGGTAATTAGCTCCT
TGGCATTGACAAGGGTACTGTTTTTTTTTCTTTCCATTTTTTATTAGGTATTTAGCTCATTACATT
TCCAATGCTATACAAAAGTCCCCCATACCCACCCACCCCACTCCCCTACCCGCCACTCCCCCTT
TTGGCCCTGGCGTTCCCTGTTCTGGGGCATATAAAGTTTGTGTGTCCAATGGGCCTCTCTTTCCAGT
GATGCCGACTAGGCCATCTTTTGATACATATGCAGCTAGAGTCAAGAGCTCTGGGGTACTGGTTAG
TTCATAAGTGTGATCCTGGCGTTCTCAGAAAATGGACATAGTACTACCGGAGGATCCAGCAATA
CCTCTCTGGGCATATATCCAGAAGATGCCCAACTGGTAAGAAGGACACATGCTCCACTATGTTCA
TAGCAGCCTTATTTATAATAGCCAGAAGCTGGAAAGATGCCCTCAACAGAGGAATGGATACAGAA
AATGTGGTACATCTACACAATGGAGTACTACTCAGCTATTAAGAAGAATGAATTTATGAAATTCCTA
GCCAAATGGATGGACCTGGAGGGCATCATCTGAGTGAGGTAACACATTCACAAAGGAACTCACAC
AATATGTACTCACTGATAAGTGGATATTAGCCAAAAACCTAGGATACCCAAGATATAAGATACAATT
TCCTAAACACATGAAACTCAAGAAAAATGAAGACTGAAGTGTGGACACTATGCCCTCCTTAGAAGT
GGGAACAAAACACCCTTGAAGGAGTTACAGAGACAAAAGTTTGGAGCTGAGATGAAAGGATGGACC
ATGTAGAGACTGCCTTATCCAGGGATCCACCCATAAATCAGCATCCAAACGCTGACACCATTGCATA
CACTAGCAAGATTTTATCGAAAGGACCCAGATGTAGCTGTCTCTTGTGAGACTATGCCGGGGCCTAG
CAAACACAGAAGTGGATGCCACAGTCAGCTAATTGATAGATTACAGGGCTCCAATGGAGGAGCT
AGAGAAAGTACCCAAGGAGCTAAAGGGATCGACAAGGGTACTGTTACAATGACTCTGTCTGTGTC
AGCTGAGGTTGGCTGACTGTGACACTGTAATAAAGTGTGGAGTCAAGCATCTTTAGAAAGTTTCCC
CCTGAAGAGCTGGGGAGGGAGCCTAACTGGCAGAGAGCTTGCTTAGCAAGTCCACCTCCCGGGT
CAATTCTCACCTTGCATTAAGGATGTGATGATATGTACCTGTAATCTCAGCACTTTGGAGGTGCAG
ACAAGTGGATCAGAAGTTCAAAGCCCTGCTTGGACATATAAAGGGTTTGGGGCAGCCTAGAATAC
AAGATACCCTATCTTAAAAAAAATCCTATAAAGAAGCTTCTTTATCTTCTTATACCCCAAAAGAAG
AAAGATGCTGAAGGCAAAGACACTGGAAGAGCCAAAGGAATGTTCTTGGGGGCTTGGAGTCTCTG
AGGCTTAGTCCATGTGTTATCAAGCGCAATGCATCATGATTAAGTTCAGGAGACGCTCACTTTC
ATGCAATTTAGTTTCTTTAATTTTATCTACTGAACACAATACTCTGTAACAGAGATATAAGTCTTC
CATTACAGAAATGCCAGAGGGTATATCTGAATTTCTCCATAAAATGAGATTCAACTTTGTAGTCTGTGC
AGAATATGTGGGGAAAAATGATGTTTTGTGTGTAATAGAATGTAGCACATAGACTATCCAGAGGC
TAGTTATAAGTACTTAGCACACTAATGCAGTGGCTTGGCCTCCAAATCCACACTAGTCCCTGCTTAA
GAGTTCTGGAACGATTCATTTTTACTTTGCTGTGCCCATGAACATCTCTATTGAGAATCTAAAAAGA
ATAAAGAAGTAAGCCATTGTCAAGTACACATGACAAAGAGTCTATACTAATAGAAATTGATGCAA
CATGACTAAAACCGAATTGAGTCAAGAACCATAAATTACAGACTCAGTGTACATACAGAACTGAG
AACAGAACCTAGGGATACTATAAATACCTTGAAGTGTGTTCCATCTCAAGCACAGAGAAAGGGCC
GCCTTTTGGCTCAGTGTGTAGTCTGTGCTACCATGGGAGAACCAGTAGGTGAGTATTTACTGGAA
ACCTGACTAGAGGAAAGAGTCCCAGGACTGAATAAAAAAGTGTGTTCTGCTTCTGAGGAAACA
AAGTCCAGTGTGATTGTTTACAGACATCGAAAGCTTCAAGGTGTGCTTTTAAAGCTAAATGGAATA
CCAAGAAGATTGTGATGTACAGTTGCTGACGAGATTGGAAAGGGGACGCTAGCCATTTGATATTA
GGAATGCTAACCTGTAGATGCACTCAGCCAGACAAAATAAATGAATTCATGACACAGGACATCC

TCCTCCAGGCAGTAGGCATTCCCTTTTGAACCGTTTCAGGAAATGGTCCACAGGATAAACATCTCTGAT
AAAAACCAGATCACCTTTGCAGCTTAGGGCTGGTTAATAAGAAAGCATGGTGGTCAATAATAAATCT
GATGATCTTATTGACCCCAAATGGGTGAGGTTGGGGACATATCAAAGAAGTGAATGAAGGTGAGTG
TGTACTACTGGCACATCAATCTTAGATTGGAATAAGCCTATAGATAAACGCAAAAATGCCAAAAGTGT
ATGTGATTCTCAATGATGTCTCATTGTGTCTTGACTTGGTCTGGAAATCATCCACGCTCTATCTTT
GAAAACAGGGTCATTGCCACAATTGACTTTTCCCTCTCTTTCTCTTCAGGC

CCTGCTGCAA

P A A

AAAAGAAGTATGTCAGTTATAATAACCTGGTTATCTAA

K K K Y V S Y N N L V I STOP

CCTGTTCCATCCCATGGAACACAGAGGAGGAAGACCTTGAATTATTCTGTCCACCCAGCCTGGCGTA
GGACTCTTTTGGTCTGCCTGCTTCCCTATCTCTGGAGGAGCTTCCCACGCGGGAGAGCAATGGCAG
AGGATCCACACATCCTGAACAGCTGCTTTATGAGACACCTTACTTTATCTTGGCTTAAGAAGTCATT
GGCATCAGCACTGCCATCTTGGCTGCAATTCTGGACTCCCTACAGCAAAGGGAGAGTTGAGATTCAA
GTCCCACCCGGCTCTTTGGATGAACCGCTGAGAGCCTCAGGACTGTTTTTGGGGGGTACTTGTCT
TTCTACGTACTTCCAGGCTGCAAGGTTTGAATTTTCTGTACAGTGTGAGGACATTTGCAAT
TTTGCCACTCAATGTCGTACCTCGGTTCACTGTTTGTGTTTTTGAATGCCCTGTTTTTCATAGAATCCTATC
CTCTCAGATGGTGGAATCTTTGGGGAAACTTTAAAGTAACTAATTTTTATTTAAAAAATACTCG
GCAGACATAAGAGAACAACACACCCCCCATGCACATCTGTAATGACTGTATGGTTATGATTATAGTAC
CACGAAAAATCATGTTATTTTTTTTAAAGACACACAAAAAGATACTTAAAGACAAAAACTGTGC
TGGGAAGATATGCCCCACCTATCTTTGGTACATGGTAGGTGTTGTGATGGAAATGGAAAGCATTGGT
TAAATGGAATAGAGGTCTTGATCTTTGGAATGCATGCCGGTAATGTATTTTACAGTACATGTTAATA
ATTTATGTTAATATTTGTATTTGTCTCTTTTGTATTTTACTTAGGGTATATGGATATTTTGTCAAT
AATTTAATGATTCTTAAAGCTATTTGAAGGAAAGAATATGGATTTCTCATGTCTTGAGGTTTTGTTC
TGCCCTATGACTGACCAATGTGATAAGGACTTTAAAAAGAAGCATGTATGTTTTTACTGTTTGT
AGAAGTACTTTCGTTAATCTTGCTGCTTATGTGTCAATTTAGTGAAAAGAAATCCCTTGCTGAAAA
AAAAATCCCTTCCATTCTCTCCAGTTCTGTGGTATTGTCCAAGATGTATCAATAAAATACTTTGG
TTAACTTTTTTATTTCTGTAGTAAGTGCTTTAGTTGTTCTCCCAGCCACCTACCTCCACTTGT
ACAGCTTATTTGAAACCCTGGGCTACAGAACAATAAGGACAGCTCAGGTCCTAAGCTTCCAATAACA
GTGCGTGTGAATGCACAGCAAAAACCTAGAGGCACTGGTGAGTTCTCTAGAAAAGGGACAATGAC
AAAAACCAAGCGTTCTTCCATTATAACTGAAAGTTCAATCCTTAAAGAATTCATGTCTCAGATGCTAAC
CAAGTTGTCTATCAAAAACAATAACAAGAAAGATAAGACAAAAGAAATATTTGCTTACAGAAACAG
TACTCTGCAAAAAGAATCATTAAAAAGTTAAACATTTCTAGAAAAGTAACTGAAAGGATGTAGG
GCTCAGGAACAGACAACGGAGACAATGGGCTTGGTTCTGCATACACATGTGGCATTGAGGTTTGTAG
AACCAAGATTAATAATGCAGTACTCCATGGTCTGTAGAAAACAAAACAAAATAAGACAAACAATAAG
CAAAAAGTAACTACTCACAGCAACATACTCCAGGAACATACTATCATCTCCTTATACAGG
GTAGCAGTGGTCTTAGCACTCCAAGTGGGCCCCCAAGTCCAATATTTGAAATATCCCTGGCTG
AACAGGGGGATAGCTCAGATGAAATTGCAACTGCCACACAAGCAAGAACCAAGTTGATCC
CAGAAATCCATATTAATAAAAAGCAAGACTCAGTGTGTGGACTTATAATTCCTGAAGTGGAGAGGTA
AAGCCTGGCAGATCCCTGGAACATTCTAGAAGGTGACCAACCTATTAGGTGACTCCACACCAGCA
GGAACCCCTGTGTCAGAAAATAGGAACATCACTCATGTTGACTTCTGCCCCCCCCACACACACACA
CATACAAACAGAGATGACAGAGACAGACAGAGAAAAAGAGAAGAGAAAAGACAGAGAAATACCCAC
ACATATTTACATAGAACAGATTGGGTTAACAGATAGATTGGATGATGATAGACAGATACATACATAC
ATACATACATACATACATACATACATCAATAGATGATAGATAGATAGATAGATAGATAGATAGATA
ATAGATAGATAGATAGATAATTGATAGAGAGAGAGAGAGATGATAGATAATTGGTAAAGGGATAAA
TACATAGATACAAAGACACATAGATACATAGATAGCTACATAGACAGAGATAGATGGAACACAGAC
AAATGATAGATGATAGATAGATAGATAGATAGATAGATAGATAGATAGATAGATAGATAGACAGAC
AGACAGTAGACAGATACATAGATGTGCAATCAATATTCCTTTGTCAACAATGTTTCCACAGTGCCAG
GTAACCCCTCATATTTTCTACTTTTGGTCTCTGTTGAGTTTTTCTATAGTCCCTTGTGAACAATG
CTTTCACAGAGACTCCAAAACCTATTTTAGTATCAGACTGCAGAAAAATAAATTGCTTTTCCCAATTC
TTCTATCCCTTCAACATCTCAAACATAAGACCATGGAGAAATCCAAATCAAAGAAGAAACACAT
TTAAATCATTGACATTTTTTCTCAAGCTGTAGAGTCAAACCCTGTATAGAAAGTCTGCCCTTCT
GCTGACTTGTAAATCAGGTTGGTTATATAAACATTCTCCATGTCGTTAGCTAGAAAATGATTTGGATA
AATCTACCTCATTAGAAAGAAAGGATGAAGAGAGAAATTTGACAAATGACTACTCAGCATGGCAGC
TCTCAGGAGCATGGCTTTTGTGACGACTAGCACCATATTAGTCATTATATACTTTTTTCTTTTCTTT
TTTTTAAATTAATCATTCCACTATTTACATCTAAAATAATATCCCACTTCCCAGTTACCCAGTTGCC
CTTCCACAATCCCCATCCACATCTGCCCTTATTTCCCTCCTTTGCCTCTATGACAGTGGCTCCCAT
CCACCCACCTCTTAACCTACCAACCCTCTCCCAACCCACCTTCTAGCATCCCCCTACACTGGGGC
ATCAAACCTTCTCGGGACCAAAAACCTCCTTCTGTTGATGTCTGGCAAGACCATCCTCTGCTACAT
ATTTATCTGGAGCCATGGATCCCTCCCTATATACTCCTTGGTTGGTGGTCTAGTCTGTGGGAACACTG

GGTCAGCTGATATTGTTTTTCTATGGGGTTGCAATCTCCCTCTGCTCGTCCTGTCCTTCTTCCAGCTC
CCCAACTGGGGTTCCTGAGCTCAGTATGAAGGTTAGTTCCAAGCATAGACATTTGCATTGGTCAGTT
GCTCACTGAACCTCCCAAGGAACAGCCACATCAGGTTCCCTGTCAGCAAGCACCTCTTGGCAATGGCA
ACAGTGTCAAGGTTTAGAGTCTGTAGAAAGGATGGATCCCCAGGTGGGCCCCCGATGACTGTTCCCTT
CAGTCTCTGCCCCATGTTTTGTCCCTGTTCTTAAAGCAAACCTTAATCTTGCAGTATCGTCACCTCTAG
GTGGGGAAACAGTTTATAATATACTATGTGAATAGCTCAGAGTGTGTTGTGGCCCTATTGTAAAGTC
ACTTTCATTAATAAATAATACAAAAGATTTTCTTTTCATTTTTTCAGATGTTCAACCAAGAGTACTA
AGAAGCTGAAGTCATATGCATATGGTACTAAGACTAGGACAGGGCTCCTTCTGAAAAACACCCTGTTT
TATGTATTCATCTTACAGTACAACCTGAGCTAATAGTGATCAGTAATGAGGATGAAGGGGACGATAT
AGAAGTATAGGAAATTATGAAATATATTATGTAGTTTATATAGGCTATGCATGTTATATACATTGAA
ATGTACATTTATATACATTGCACGCTCCTCAAATCCACTTCTAACACCTTGCACCACGTGCACCTCTT
ACAAAGTATTTGGGATTAAGATTGTCTATAGACATAGAGCAAATGCATCAGAAAAATACTATTATCG
TCTGATCTCTAACTTGTATCTGGCGTATCCTCCTCAAGGTCCTTTGTATGCTGAATGCATGGCTCCAG
ATTAACACGGTTGGAAAGTGGTAGAACTATGAGCAGTGAGACCTAGGAAGAAGTGATCAGATCAT
TAGGGGTGTTGCCTAGAACAGTTCCCCCTAATAGTCTTCATTCCTCTCCAGTATTTTGTGATCATTAT
CATGTCTGGTCTTTGCTGATACTGTTTAAAAGGACAGTCTTTGACCAGTAGCCCAGGGAAGCAATTT
ACTTGTTTTGCTTTTTTCTTATAACGTATGATGCTCATCTGACTTTATAGATTTCTTTTGCTGCTTT
TGCTGCCCCTTTTCAGTATTCTGTTTAAAGAAGGTCAGATACTTTTACCTTTGCTCCTAGTAATTTCTT
AACAGACTTGCTCAACAGGTAGCAGATTATCCTATAGATATTTGCCTATGTTTCAGAGAAAAAAGG
AGTGGATAAATGAAGTGCAAAACTGAAGGAACATGGCTAGAGATCT

7. Zusammenfassung

Die Aminosäure Glutamat ist nicht nur ein Schlüsselmolekül im Stoffwechsel jeder Zelle, sondern sie fungiert auch als primärer exzitatorischer Neurotransmitter im zentralen Nervensystem von Säugetieren. Erregende Nervensignale, die durch Glutamat vermittelt werden, spielen bei vielen Prozessen im Gehirn eine Rolle, einschließlich kognitiver Leistungen wie zum Beispiel Lernen und Gedächtnisbildung. Glutamat bindet nach Sekretion in den synaptischen Spalt an Glutamat-Rezeptoren, wodurch eine Reihe von Signalkaskaden im nachgeschalteten Neuron aktiviert werden. Es werden zwei Klassen von Glutamat-Rezeptoren unterschieden: ionotrope Glutamatrezeptoren, zu denen die nach ihren jeweiligen Agonisten benannten NMDA-, AMPA- und Kainat-Rezeptoren zählen, und metabotrope Glutamat-Rezeptoren (mGluR). Bei letzteren handelt es sich um G-Protein gekoppelte Rezeptoren, welche über GTP-bindende Proteine die Aktivierung intrazellulärer Signalkaskaden vermitteln. Diesen Rezeptoren werden Aufgaben bei der Regulation verschiedener Formen neuronaler Plastizität zugeschrieben. Es sind gegenwärtig acht Subtypen bekannt (mGluR1-8), die anhand von Sequenzhomologien und pharmakologischen Eigenschaften in drei Gruppen (I-III) eingeteilt werden. Von besonderem Interesse für diese Doktorarbeit war die Untersuchung des zur Gruppe III zählenden, präsynaptisch lokalisierten Rezeptors mGluR7a. Es handelt sich dabei um einen sogenannten Autorezeptor, welcher nach Aktivierung durch Glutamat zu einer Verringerung der Transmitterfreisetzung in der Präsynapse führt. Die molekularen Mechanismen dieser Form von präsynaptischer Inhibition sind erst teilweise verstanden. Es wurde bereits gezeigt, daß die Reduktion der Transmitterausschüttung mit einer Hemmung spannungsabhängiger Kalzium-Kanäle in der Präsynapse einhergeht. Allerdings ist noch unklar, ob diese Effekte direkt durch G-Proteine vermittelt werden oder weitere Signalmoleküle involviert sind. Zur Analyse der funktionellen Regulation von mGluRs der Gruppe III wurde weltweit in verschiedenen Arbeitsgruppen gezielt nach Interaktionspartnern für die einzelnen Rezeptoren gesucht. Es konnten einige Proteine identifiziert werden, welche mit mGluR7a interagieren, wie z.B. die G-Protein-Untereinheit β , Calmodulin, MacMARCKS, Filamin-A u.a. Im Rahmen der vorliegenden Doktorarbeit soll die Interaktion des PKC-bindenden Proteins PICK1 mit dem Rezeptor-C-Terminus genauer untersucht werden.

Das Protein PICK1 verfügt über eine PDZ Domäne, welche die Assoziation mit anderen Proteinen, auch die mit mGluR7a, mediiert. Weitere Motive sind zwei *coiled-coil* Motive, welche für die Dimerisierung von PICK1 verantwortlich sind; eine azide Glutamat-Aspartat-reiche Region (E/D Motiv), die möglicherweise in Interaktionen mit weiteren Proteinen eine Rolle spielt, welche die synaptische Lokalisation des Rezeptors regulieren; sowie eine BAR Domäne, die an Membranlipide binden kann. Vorangegangene Untersuchungen zur Interaktion von PICK1 mit mGluR7a legten die Vermutung nahe, dass PICK1 entweder eine entscheidende Rolle bei der gezielten Anhäufung von mGluR7a am Ort der Transmitterausschüttung spielt und/oder regulierend auf die PKC-vermittelte Signaltransduktion einwirkt. Jedoch konnte weder die eine noch für die andere Hypothese aufgrund des Fehlens geeigneter *in vivo* Modelle experimentell belegt werden. Vor diesem Hintergrund ist die Generation einer geeigneten Mausmutante, in welcher die Interaktion der Rezeptor-C-Terminus von mGluR7a mit PICK1 gestört ist, das vornehmliche Ziel dieser Doktorarbeit.

Es wurde eine *knock-in* Maus generiert, in welcher die drei C-terminalen Aminosäuren LVI des Rezeptors mGluR7a zu Alaninresten mutiert wurden. Vorausgehende Studien hatten gezeigt, dass diese Mutationen ausreichend sind, um die PICK1-Interaktion mit dem Rezeptor zu verhindern. Ein entsprechendes Targeting-Konstrukt wurde in murine embryonale Stammzellen 129/OLA transfiziert und homologe Rekombinationsereignisse mittels Southern Blot analysiert. Durch Transfektion eines Cre-Rekombinase Expressionsvektors wurde die gefloxt Neomycin-Kassette entfernt und die Mutation tragenden Klone wurden für die Injektionen von Blastocysten verwendet. Chimäre Mäuse wurden in C57BL6 Mäuse zurückgekreuzt, deren heterozygote Nachkommen für die Züchtung von homozygoten mGluR7a *knock-in* (mGluR7a^{AAA/AAA}) Mäusen verwendet wurden. Die initiale Charakterisierung der *knock-in* Mäuse erfolgte mittels Northern Blot. Es konnte gezeigt werden, dass die mGluR7a mRNA sowohl in der Mutante als auch im Wildtyp etwa gleich stark exprimiert wird. Zum exakten Nachweis der Tripel-Alanin-Mutation des Rezeptor-C-Terminus in *knock-in*-Tieren, wurde die intrazelluläre Region von mGluR7a mittels RT-PCR amplifiziert. Die Sequenzanalyse des RT-PCR-Produktes bewies, dass das PICK-Bindungsmotiv durch drei Alaninreste ersetzt worden war. Zusätzlich wurde auch die Höhe des mutierten Rezeptorproteins in den *knock-in*-Tieren mit dem des Wildtyprezeptors in Kontrolltieren vermittels

Western blotting verglichen. Die Quantifizierung der Ergebnisse ergab, dass die Proteinexpression in heterozygoten Tieren in geringem Maße und in homozygoten Mäusen um 40% im Vergleich zu Wildtyp-Tieren reduziert ist. Dieses Ergebnis lässt vermuten, dass PICK einen stabilisierenden Effekt auf mGluR7a ausübt, der, wenn die Bindung zwischen den beiden Proteinen unterbunden wird, fehlt und somit eventuell zur schnelleren Degradation des Rezeptors führt.

Um die fehlende Interaktion der Proteine PICK1 und mGluR7a^{AAA/AAA} *in vivo* nachzuweisen, wurde eine Koimmunopräzipitation mit einem Antikörper, der spezifisch das PICK-Protein erkennt, aus Hirnhomogenaten durchgeführt. Hierbei ließ sich aus dem Lysat von Kontrolltieren neben PICK1 auch mGluR7a isolieren, während aus dem Hirnlysat von *knock-in*-Tieren nur PICK1 präzipitiert werden konnte. Zusammengefasst zeigt dies, dass in den mutierten Mäusen die Bindung zwischen PICK1 und mGluR7a nicht zustande kommt. Jedoch scheint die Verhinderung der Wechselwirkung der beiden Interaktionspartner keine Auswirkung auf die generelle Lokalisation des Rezeptors im Gehirn und auf die Gehirnmorphologie zu haben, wie histologische Färbungen des Gehirns von *knock-in*-Mäusen zeigten.

Da PICK1 vermutlich als eine Art Adaptorprotein fungiert, welches für die Organisation der Präsynapse ist, wurde die Lokalisation des präsynaptisch lokalisierten mGluR7a Rezeptors in kultivierten hippocampalen Neuronen untersucht. Immunfärbungen ergaben sowohl für Nervenzellen aus Wildtyp- als auch aus *knock-in*-Mäusen die gleiche Verteilung des Rezeptors: in beiden Fällen konnten die für mGluR7a typischen punktförmigen Anhäufungen gezeigt werden, die mit dem präsynaptischen Markerprotein Synapsin kolokalisierten. Auch bei ultrastrukturellen Untersuchungen der subzellulären Lokalisation des Rezeptors in hippocampalen Synapsen mittels Immunoelektronenmikroskopie fanden sich keine Unterschiede zwischen Wildtyp und mutierten Mäusen: in der CA3 Region des Hippokampus konnten konzentrierte Ansammlungen von mGluR7a in den aktiven Zonen der präsynaptischen Endigungen nachgewiesen werden. Diese Ergebnisse widerlegen also die Annahme, dass die Interaktion zwischen PICK1 und mGluR7a ein entscheidender Faktor für den zielgerichteten Transport des Rezeptors zur Membran und dessen synaptische Lokalisation sein soll.

Um die Effekte der eingefügten Mutation funktionell zu untersuchen, wurde vermittlelelektrophysiologischer Analysen untersucht, ob die synaptische Transmission in

kultivierten zerebellären Körnerzellen von mGluR7a^{AAA/AAA} verändert ist. Es wurden spontane EPSCs bei einem Membranpotential von -60mV in An- und Abwesenheit des Agonisten L-AP4 gemessen. L-AP4 reduzierte die Frequenz der EPSCs in Wildtyp-Neuronen, jedoch nicht in denen von mGluR7a^{AAA/AAA} Mäusen. Somit scheint für die durch mGluR7 vermittelte präsynaptische Inhibition die Interaktion mit PICK1 erforderlich zu sein.

Schließlich wurden die mutierten Mäuse auf eine Änderung des Phänotyps untersucht. Verschiedene Verhaltenstests ergaben, daß Lokomotion, emotionale Aktivität, Schmerzempfindlichkeit, Schreckreaktion und räumliches Lernen bei den mutierten Tieren ungestört ist. Bei Analyse der Ängstlichkeit und des Schreckreflexes wiesen die *knock-in*-Tiere eine Tendenz zu einer erhöhten Amplitude der Schreckreaktion auf, wobei jedoch kein statistisch signifikanter Wert erreicht wurde. Zusätzlich wurde die räumliche Erinnerungsfähigkeit der mutierten Mäuse untersucht, die bei mGluR7-defizienten Tieren verändert ist, wobei die mGluR7a^{AAA/AAA} Mäuse jedoch keine Defizite zeigten.

In weiteren Experimenten wurden die Vulnerabilität der *knock-in* Tiere für Pentetrazol (PTZ)-induzierte epileptische Anfälle hin untersucht. Wildtyp- und *knock-in* Mäuse wurden im Alter von 9 Wochen verschiedene Mengen PTZ injiziert und die Gehirnströme in einem Elektroenzephalogramm über mehrere Stunden aufgezeichnet. Die *knock-in* Tiere zeigten eine größere Neigung zu PTZ-induzierten epileptischen Anfällen. Weiterhin konnte nachgewiesen werden, daß die *knock-in* Tiere spontane Anfälle hatten, welche den *spike-and-wave* Entladungen des Absence-Phänotyps ähnelten. Begleitet waren diese Anfälle von motorischen Entäusserungen wie z.B. Zuckungen der fazialen Muskulatur. Zusammenfassend weisen diese Experimente darauf hin, daß eine Veränderung der mGluR7a-PDZ-Interaktion ausreichend ist, um den Phänotyp einer spontanen oder pharmakologisch induzierten Absence- Epilepsie herbeizuführen.

Zukünftig könnte die *knock-in* Mauslinie, die in dieser Arbeit generiert wurde, als Modellsystem für pharmakologische Studien zur Absence-Epilepsie dienen. Ferner könnten weitere Interaktionspartner von mGluR7a in Analogie zu dem beschriebenen Mausmodell untersucht werden. Solche weiterführenden Experimente könnten weitere Aufschlüsse über die Relevanz von mGluR7a bei der Regulation unterschiedlicher Funktionen im zentralen Nervensystem ergeben.

ACKNOWLEDGEMENTS

As time goes by, it is time to finish my Ph.D. thesis. When looking backward, I have experienced unforgettable 4 years of life in Frankfurt am Main, Germany. Certainly I have to give my special thanks to all the people who helped me during my training as a Ph.D. student in the Max-Planck Institute for Brain Research. I would first like to thank my advisor, Heinrich Betz. I have been very fortunate to have Professor Heinrich Betz as my advisor. His enthusiasm and dedication toward science are an inspiration in my life, and his personal support has meant much to me. I would also like to thank Professor Ernst Bamberg for agreeing to be my doctor father and taking me as an external student. I will forever be grateful for his guidance as a scientist.

To the “mGluR” lab members, past and present, I surely give thanks for discussions, guidance, and friendship. A special thanks to Dr. Astrid Scheschonka, who has helped me to develop my work into a story, and also who has helped excite my interest in science. Thanks to Liane Bauer, Anne Nehring, Zhongshu Tang, Anina Moritz and Dr. Greta Ann Herin, with whom I have had the joy of sharing a room, and who know my hobby for talking and singing while I work. I have gotten wonderful technical support from Anja Arends and Nicole Fürst. Each of you has a place in my heart.

Special thanks should go to Dr. Laurent Fagni and Dr. Federica Bertaso for conducting the electrophysiology work presented in this work and Dr. Richard Huganir for providing the PICK1 antibody. I particularly would like to acknowledge Dr. Volker Eulenburg and Dr. Gregory O'Sullivan for their time and guidance and also for teaching me how to perform animal behavioral test. I would also like to thank Dr. Bertram Schmitt and Ms. Maren Baier for helping me to live in Frankfurt and making my time in Frankfurt more easy-going. In the department of neurochemistry, I owe thanks to those people for their patience, and support.

Outside of the lab, I would like to thank my family. My wonderful wife has supported me and always understands me. My son, Weifan, his arrival makes my life amazing, he smiles whenever I need it. And finally I would like to thank my parents for their love, encouragement and support however far away from home I end up!

CURRICULUM VITAE

Personal Information

Name: Chuansheng Zhang
Date of Birth: September 10, 1973
Place of Birth: Huaibei City, Anhui Province, China
Nationality: Chinese
Marital Status: Married since March 2002

Education and Working Experience

2002, 9-present: Doctor of Philosophy
Department of Neurochemistry, Max-Planck Institute
for Brain Research, Frankfurt am Main, Germany
Advisor: Prof. Heinrich Betz

1999,9-2001. Institute of Genetics and Developmental Biology,
Chinese Academy of Sciences (CAS), Beijing, China
Position: Research Assistant

1996, 9-1999, 7 Master of Science
Institute of Genetics and Developmental Biology,
Chinese Academy of Sciences (CAS), Beijing, China
Advisor: Prof. Weide Lao

1992, 9-1996, 7 Bachelor of Science
Department of Biology
Anhui Normal University
Wuhu, China